UNIVERSIDAD DE LA RIOJA

TESIS DOCTORAL

Título
Artificial Intelligence in Digital Agriculture. Towards In-Field Grapevine Monitoring using Non-invasive Sensors
Autor/es
Salvador Gutiérrez Salcedo
Director/es
Javier Tardáguila Laso y María Paz Diago Santamaría
Facultad
Facultad de Ciencia y Tecnología
Titulación
Departamento
Agricultura y Alimentación
Curso Académico

Tesis presentada como compendio de publicaciones. La edición en abierto de la misma NO incluye las partes afectadas por cesión de derechos

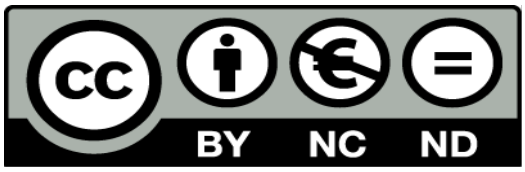

Artificial Intelligence in Digital Agriculture. Towards In-Field Grapevine Monitoring using Non-invasive Sensors

PhD Thesis

Salvador Gutiérrez Salcedo

2019

Artificial Intelligence in Digital Agriculture. Towards In-Field Grapevine Monitoring using Non-invasive Sensors

PhD Thesis

Salvador Gutiérrez Salcedo

Supervised by
Prof. Dr. Javier Tardáguila Laso
Dr. María Paz Diago Santamaría

Programa de Doctorado en Enología, Viticultura y Sostenibilidad por la Universidad de Castilla-La Mancha, la Universidad de La Rioja, la Universidad de Murcia, la Universidad de Salamanca y la Universidad de Valladolid

2019

The work leading to these results has received funding from the University of La Rioja FPI grant 299/2016, the European Union under grant agreement no 610953 (VineRobot project) and under grant agreement no 737669 (VineScout project). It has also been funded by the national project RTC-2014-3058-2 from the Ministry of Economy and Competitiveness of the Spanish Government titled "INNGRAPE: Monitorización de viñedo mediante RPAS".

PhD Thesis by published works following the normative by the University of La Rioja, comprising the following works:

1. GUTIÉRREZ, S., TARDAGUILA, J., FERNÁNDEZ-NOVALES, J., DIAGO, M.P. (2015) Support vector machine and artificial neural network models for the classification of grapevine varieties using a portable NIR spectrophotometer. PLOS One 10(11), e0143197.
   DOI: 10.1371/journal.pone.0143197. Impact Factor: 3.057 (Q1).

2. GUTIÉRREZ, S., TARDAGUILA, J., FERNÁNDEZ-NOVALES, J., DIAGO, M.P. (2016) Data mining and NIR spectroscopy in viticulture: applications for plant phenotyping under field conditions. Sensors 16(2), 236.
   DOI: 10.3390/s16020236. Impact Factor: 2.677 (Q1).

3. GUTIÉRREZ, S., DIAGO, M.P., FERNÁNDEZ-NOVALES, J., TARDAGUILA, J. (2018) Vineyard water status assessment using on-the-go thermal imaging and machine learning. PLOS One 13(2), e0192037.
   DOI: 10.1371/journal.pone.0192037. Impact Factor: 2.766 (Q1).

4. GUTIÉRREZ, S., FERNÁNDEZ-NOVALES, J., DIAGO, M.P., TARDAGUILA, J. (2018) On-the-go hyperspectral imaging under field conditions and machine learning for the classification of grapevine varieties. Frontiers in Plant Science 9, 1102.
   DOI: 10.3389/fpls.2018.01102. Impact Factor: 3.678 (Q1).

5. GUTIÉRREZ, S., TARDAGUILA, J., FERNÁNDEZ-NOVALES, J., DIAGO, M.P. (2018) On-the-go hyperspectral imaging for the in-field estimation of grape composition. Australian Journal of Grape and Wine Research 25 (1), 127-133.
   DOI: 10.1111/ajgw.12376. Impact Factor: 1.913 (Q1).

6. GUTIÉRREZ, S., WENDEL, A., UNDERWOOD, J. (2018) Ground based hyperspectral imaging for extensive mango yield estimation. Computers and Electronics in Agriculture 157, 126-135.
   DOI: 10.1016/j.compag.2018.12.041. Impact Factor: 2.427 (Q1).

A mi madre, Lola

Agradecimientos

Agradezco profundamente a mis directores de tesis de la Universidad de La Rioja. Al Catedrático de Viticultura de Precisión Javier Tardáguila y a la Doctora María Paz Diago, por su inmensa guia, apoyo y confianza, además de la ayuda y la atención, tanto en lo profesional como en lo personal, durante todo el tiempo que hemos podido trabajar juntos.

También me gustaría agradecer a todos mis compañeros del grupo de investigación Televitis, especialmente al Doctor Juan Fernández, del que he podido aprender tanto, pero sin olvidarme de Fernando Palacios, Ignacio Barrio, Eugenio Moreda, Arturo Aquino, Borja Millán y Clara Rey. Soy afortunado de haber podido trabajar a su lado todo este tiempo.

No quisiera olvidarme de agradecer al Dr. James Underwood, del Australian Centre for Field Robotics, The University of Sydney, por la acogedora estancia que me ofreció allí en Australia y su inestimable ayuda y consejo. También agradezco al Dr. Alexander Wendel por sus consejos y su ayuda durante mi tiempo allí.

Por último, pero no menos importante, me gustaría agradecer todo su apoyo a mi familia. A mi mujer, Rocío, porque sin ella no sería quien soy. A mi hermana María y a Manolo, por su ayuda y consejo. Y a mi padre, por ser un ejemplo de esfuerzo y sacrificio.

¡Gracias!

Acknowledgements

I am deeply grateful to my supervisors from the University of La Rioja. To the Professor of Precision Viticulture Javier Tardáguila and Doctor María Paz Diago, for their huge guidance, support and trust, and also for their help and interest, both in professional and personal matters, during all this time of work together.

I would also like to express thanks to all my partners from Televitis research group, especially to Doctor Juan Fernández, from whom I have learned so much. I do not want to forget Fernando Palacios, Ignacio Barrio, Eugenio Moreda, Arturo Aquino, Borja Millán and Clara Rey. I am fortunate to have been able to work with you all this time.

I could not forget to show my gratitude to Doctor James Underwood, from the Australian Centre for Field Robotics, The University of Sydney, for the warming welcome he gave me there in Australia, and for his inestimable help and advice. I am also grateful to Doctor Alexander Wendel for his advice and help during my time there.

Last but not least, I would like to thank my family for all their support. To my wife, Rocío, because I would not be the man I am without her. To my sister María and Manolo, for their help and advice. And to my father, because he is a model of effort and sacrifice.

Thank you!

Abstract

Agriculture seeks for a reduction of costs and environmental impact, better sustainability and to increase crop yield and quality. It is necessary to deliver useful applications for farmers and industries, to help for greater efficiency and sustainability. To achieve this in digital viticulture, useful information about the vineyard is necessary so better decisions can be taken. Advances in non-invasive sensing technologies allow the acquisition of high amounts of data from the vineyard, but these data alone are not enough to be used when decisions need to be made, it needs to be transformed into information. Artificial intelligence is a revolution at different social, work and industrial levels to deal with data. Within artificial intelligence, machine learning has evolved greatly during the last decades providing tools to make computers learn, and these algorithms are used in many different fields due to their high versatility for many data-related tasks, generating knowledge and information, and improving the decision-making process. Therefore, the combination of non-invasive sensors and artificial intelligence needs to be explored to meet the requirements needed to apply digital agriculture, the data-driven agriculture.

The main objective of this PhD Thesis is the combination of machine learning and non-invasive sensing technologies for the assessment of relevant agronomical, physiological and qualitative traits in digital agriculture and viticulture. Specifically, the following objectives have been pursued: i) to make use of different machine learning algorithms on data from spectroscopy for in-field grapevine phenotyping and monitoring; ii) the application of ensemble data analysis techniques for vineyard water status assessment with thermal imaging; and iii) to deploy hyperspectral imaging in the field, supported by intensive machine learning combinations, for the monitoring of different crop traits.

The first objective, covered in Chapter 3, was the combination of machine learning algorithms and near-infrared spectroscopy for vineyard monitoring and phenotyping. A handheld spectrometer was used for two goals: the classification of grapevine varieties, from several vineyard plots and vintages; and water status assessment, using the same spectral signal. Accurate models were developed for both goals. The results allow to open new ways in digital

viticulture for the quick grapevine phenotyping under field conditions, an useful tool for several actors in the wine industry.

The application of ensemble machine learning algorithms to in-field thermal images acquired on-the-go for vineyard water status monitoring, the second objective, is addressed in Chapter 4. A thermal camera was mounted on an all-terrain vehicle for continuous acquisition. A combination of rotation forests and decision trees was used for the training of prediction models. The outcomes provided by the machine learning algorithms support the use of thermal imaging for fast, reliable estimation of a vineyard water status, even suppressing the necessity of supervised acquisition of reference temperatures. The new developed on-the-go method can be very useful in the grape and wine industry for assessing and mapping vineyard water status.

The last objective was the use of on-the-go hyperspectral imaging under field conditions, modelled with machine learning techniques, and it is discussed in Chapter 5. Hyperspectral imaging is a powerful technology, but it has been classically used under laboratory conditions. Very few attempts on in-field hyperspectral imaging have been reported in the literature, due to the difficulties, like natural, irregular illumination or unknown *a priori* sample positioning in the recorded scene, that it is necessary to face. For this reason, a considerable amount of the work developed in this PhD Thesis has been focused on surpassing the challenges that come from deploying a hyperspectral camera in the field for the on-the-go vineyard monitoring. Also, as hyperspectral imaging involves the management of a high amount of data, advanced machine learning algorithms become appealing to be applied in this scenario. Three different applications were developed: varietal classification, grape composition assessment and yield estimation. In all of them, it was designed a mechanism for the automated identification of the different grapevine organs. Potent models were obtained for the monitoring of different key viticulture and agriculture parameters. The results suggest that machine learning and hyperspectral imaging can be used to accurately estimate several traits in vineyards and other crops, becoming a powerful and accurate tool in the decision making process.

The results from the research work carried out in this PhD Thesis, also published in several scientific articles, demonstrated that artificial intelligence techniques are able to exploit the potential of data acquired using non-invasive sensing technologies for the monitoring and phenotyping of key crop traits. This can be of utmost importance in digital agriculture and viticulture as new solutions can be developed as decision support tools.

Resumen

En la agricultura se busca una reducción de costes y de impacto ambiental, mejor sostenibilidad y un incremento de la calidad y el rendimiento del cultivo. Es necesario desarrollar aplicaciones útiles para agricultores que ayuden en esta mejora de eficiencia y sostenibilidad. Para lograr este objetivo en el ámbito de la viticultura, se necesita información sobre el viñedo que puede utilizarse para tomar mejores decisiones. Los nuevos avances en tecnologías de sensórica no invasiva permiten la adquisición de grandes cantidades de datos del viñedo. Sin embargo, los datos por sí solos no sirven cuando se tienen que tomar decisiones, ya que tienen que ser convertidos en información. La inteligencia artificial supone una revolución a distintos niveles sociales, de trabajo e industriales. Dentro de la inteligencia artificial, el aprendizaje automático ha evolucionado ampliamente durante las últimas décadas para proveer de herramientas que permitan a los ordenadores aprender. Por su gran versatilidad, estos algoritmos se utilizan en muchos campos distintos donde es necesario trabajar con datos, generando conocimiento e información, y mejorando el proceso de toma de decisiones. Por estos motivos, se debe explorar la combinación de sensores no invasivos con inteligencia artificial para alcanzar los requisitos exigidos en agricultura digital.

El objetivo principal de esta tesis doctoral es lograr la combinación de aprendizaje automático y tecnologías de sensórica no invasiva para la estimación de importantes características agronómicas, fisiológicas y cuantitativas en agricultura y viticultura digital. En concreto, se plantearon los siguientes objetivos específicos: i) utilizar diferentes algoritmos de aprendizaje automático sobre datos espectrales para la monitorización y fenotipado en campo de la vid; ii) la aplicación de métodos combinados de análisis de datos para la estimación del estado hídrico del viñedo con termografía; y iii) utilizar imagen hiperespectral en condiciones de campo, junto con la aplicación intensiva de aprendizaje automático, para la monitorización de distintos aspectos del cultivo.

El primer objetivo, cubierto en el Capítulo 3, fue la combinación de algoritmos de aprendizaje automático y espectroscopia de infrarrojo cercano para la monitorización y fenotipado de la vid. Se usó un espectrómetro portátil con dos fines: la clasificación de variedades de vid, con datos de

distintos viñedos y campañas; y la estimación del estado hídrico, utilizando la misma señal espectral. Se desarrollaron modelos con gran precisión para ambos objetivos. Los resultados abren nuevas vías en viticultura digital para el fenotipado rápido de la vid bajo condiciones de campo, una herramienta muy útil para varios actores en la industria vitivinícola.

El segundo objetivo fue la aplicación de métodos combinados de aprendizaje automático sobre imágenes térmicas adquiridas bajo condiciones de campo para la monitorización en continuo del estado hídrico del viñedo, que se trata en el Capítulo 4. Se instaló una cámara térmica en un quad para realizar captura de datos en continuo. El entrenamiento de los modelos de predicción se llevó a cabo mediante una combinación de rotation forests y árboles de decisión. Los resultados evidencian el uso de termografía para la estimación rápida y fiable del estado hídrico de un viñedo, incluso prescindiendo de la necesidad de medir temperaturas de referencia. El nuevo método desarrollado en continuo puede ser muy útil en la industria vitivinícola para medir el estado hídrico de un viñedo y generar mapas de variabilidad espacial.

El último objetivo, discutido en el Capítulo 5, fue el uso de imagen hiperespectral en continuo en condiciones de campo y modelada con técnicas de aprendizaje automático. Se pueden encontrar muy pocos trabajos que traten sobre el uso de imagen hiperespectral en campo, debido a las dificultades que esta configuración puede presentar, como una iluminación natural e irregular, o la localización *a priori* desconocida de las muestras en la escena. Por esta razón, gran parte de los esfuerzos dedicados en el período de investigación y desarrollo de esta tesis se han dedicado superar el reto de llevar una cámara hiperespectral a campo para la medición en continuo del viñedo, superando los inconvenientes a los que hay que enfrentarse en el nuevo escenario y diseñando aplicaciones útiles para viticultura digital. Se desarrollaron tres aplicaciones distintas: la clasificación de variedades, la evaluación de la composición de los frutos y la estimación del rendimiento. Se obtuvieron modelos precisos para la estimación de estas características del cultivo. Estos resultados sugieren que la imagen hiperespectral puede emplearse para estimar distintos aspectos del viñedo y otros frutales, convirtiéndose en una herramienta potente y precisa para la toma de decisiones.

Los resultados del trabajo de investigación llevado a cabo en esta tesis doctoral, publicados en varios artículos científicos, demuestran que las técnicas de inteligencia artificial pueden sacar provecho de datos vegetativos capturados a través de tecnologías de sensórica no invasiva, para caracterizar parámetros clave del cultivo. Estos resultados pueden ser de gran importancia en agricultura y viticultura digital, dado que permiten el desarrollo de nuevas soluciones y herramientas de apoyo a decisiones en la industria agrícola.

Contents

List of Acronyms

AI ..... Artificial Intelligence

ANNs ..... Artificial Neural Networks

ATV ..... All-Terrain Vehicle

CNN ..... Convolutional Neural Network

CNNs ..... Convolutional Neural Networks

CV ..... Cross Validation

CWSI ..... Crop Water Stress Index

DA ..... Digital Agriculture

DV ..... Digital Viticulture

GAs ..... Genetic Algorithms

HSI ..... Hyperspectral Imaging

I_g ..... Conductance Index

IR ..... Infrared

LIDAR ..... Light Detection and Ranging

ML ..... Machine Learning

MLPs ..... Multilayer Perceptrons

MSI ..... Multispectral Imaging

NDVI ..... Normalised Difference Vegetation Index

NIR ..... Near-Infrared

PLS ..... Partial Least Squares

PLS-DA ..... Partial Least Squares Discriminant Analysis

RPAS ..... Remotely Piloted Aerial Systems

SVMs ..... Support Vector Machines

UAV ..... Unmanned Aerial Vehicle

List of Figures

Chapter 1

Introduction

1.1 Digital agriculture

The majority of the decisions taken by today's farmers are based on a combination of own experience, visual inspection and recommendations. Nevertheless, a higher efficiency in agricultural outcomes is not achievable via those current practices, in a sustainable and consistent manner (Bergerman et al., 2016). In the last years, the fast development and adoption of new technologies has disrupted the way that people interact with the reality at many levels: in social relationships, work environments or entertainment. Nowadays, almost every person has a small device in his pocket that, within seconds, allows to connect with any other, seek for an answer to any question on the Internet through voice, or even use a camera to identify an object or translate a sign. All this is based on the amalgamation of different input/output technologies (wireless connections, cameras, microphones, visual interfaces), worldwide communication (mobile Internet connections, access to private servers, cloud solutions) and, what truly entailed the current revolution, new intelligent and deep data analysis (voice and image recognition, information indexing and retrieval, prediction and recommendation systems). Therefore, this amalgamation opens new windows in today's agriculture, in which more efficiency and sustainability is required. This is especially important as, because world population will reach nine billion in 2050, food production should increase approximately 25% – 70% (Hunter et al., 2017). Current trends in agriculture demand for the precise management to obtain benefits not only in the economical sense, but also in environment, logistic and security. It is necessary to deliver useful applications for farmers and industries, to increase efficiency and sustainability.

New digital technologies have indeed been adopted in current agricultural practices. A recent report from the European Commission's science and knowledge service (Barnes et al., 2019) studied the determinants of the uptake of new technologies in agriculture within a European cross-country

setting. The results showed that, although some barriers are still found in adoption, younger farmers are significantly more prone to use new technologies, potentially linked to the knowledge required to correctly operate information intensive technologies. Given the appearance of new digital devices and more intelligent data analysis tools year by year, it is thus clear that the development of technological advances applied to agriculture—the Digital Agriculture—needs to keep growing in favour of providing a broader collection of solutions to gain in efficiency and sustainability.

Digital agriculture address the use of sensing technologies for the acquisition of high resolution crop data and their transformation into information useful to the farmer in the decision-making process using trending Artificial Intelligence (AI) advances. The fact that spatial and temporal variability of soil and plant factors is present in virtually every crop is undeniable, and has been reported in the last decades (Zhang et al., 2002). Although farm management has been traditionally performed homogeneously, due to small, manageable sizes, the enlargement of crop fields made the conventional operation an outdated solution if efficiency is sought. Crop necessities can largely vary within the same field, and, for example, fertiliser treatments applied to the plants in a certain zone could be insufficient or excessive in a different area from the same crop field. This is how current practices could take advantages of digital technology to address this. Technology currently allows to scan large areas of a crop (from static ground sensors, air platforms or mobile ground vehicles), acquiring physiological data from the plants or the soil and providing useful information from it about plant nutritional status, water management, fruit ripening, etc. Digital Agriculture (DA), defined as the management of spatial and temporal variations in the fields (Pedersen, 2003; Fountas et al., 2005; Zarco-Tejada et al., 2014), put in numbers the status of a crop field to apply individual solutions to each zone.

Applying digital technologies in agriculture has advantages for farmers in terms of crop production and cost reduction, as it implies giving only the necessary resources (*e.g.*, water, chemical treatments, etc.) that each plant requires, leading to better decision making (Zarco-Tejada et al., 2014). Additionally, a precise measurement of specific plant parameters, such as yield and ripening assessment or fruit composition monitoring, could help to take better decisions about when and where to harvest. A report from the Departments of Agricultural Economics and Agronomy, Purdue University (Erickson et al., 2017) showed that, in 2017, compared to previous years, there has been an increasing rate of adoption of precision, digital technologies in digital agriculture in the United States of America, with a positive growing trend in the last years (Figure 1.1).

Still, the benefits of applying digital technologies to agriculture are not limited only to the farmer, but also positive to the environment. A scientific foresight study from the European Parliamentary Research Service (Schrijver

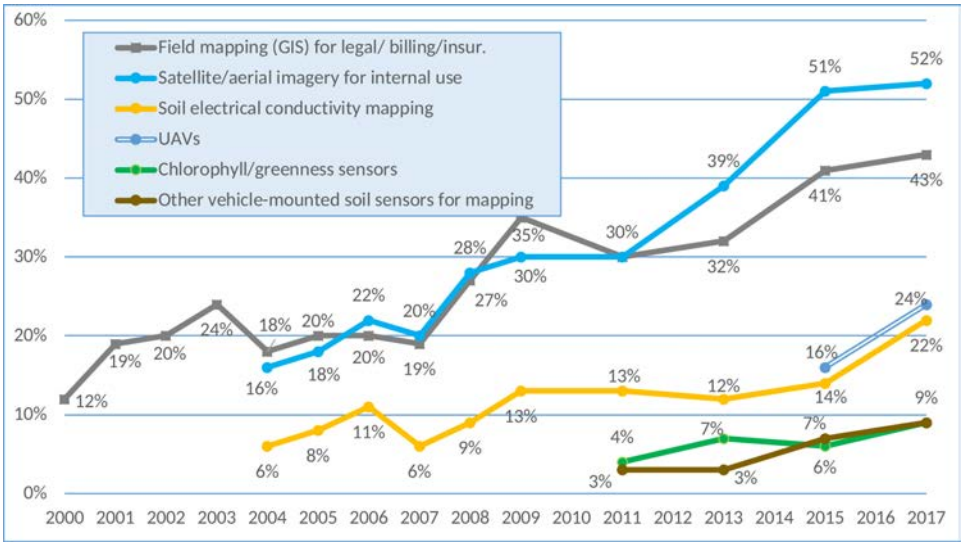

Figure 1.1: Use over time of precision digital technology in agriculture in the United States of America. Source: Erickson et al. (2017).

et al., 2016) asserted that applying techniques for a precision management in agriculture will have a positive impact in the environment in terms of soil erosion and fuel consumption, due to automated machine guidance; reduction of chemical in soil and water, due the control of pesticide sprayers, etc (Zarco-Tejada et al., 2014).

1.2 Digital viticulture

Digital viticulture is a branch of DA that applies the methodologies from the latter to vineyard management. Although grapegrowers have well acknowledged the variability that exists within a vineyard, operations have been typically carried out on them homogeneously (Bramley, 2010). Nevertheless, this approach does not help to obtain higher quality from grapes and increases management costs (Proffitt et al., 2006). DV pursues taking decisions about vineyard management based on the precise characterisation of the vines (using the advantages of new technology), with results at three different levels.

Grapevine is a very important crop in the world. In the European Union, 80% of the grapes are produced for quality wine making from a total of around 3 million hectares (Eurostat, 2017). Grape berry attributes—including relative proportions of skin, seed and flesh, and chemical composition—are altered by weather, being their main source of variation. Therefore, wine quality, derived from these attributes, is strongly affected by the weather on each season (Gladstones, 1992; Soar et al., 2008). Climate change is bringing

an increasing rate of irregular precipitations and higher temperatures. This may have positive or negative impacts on practices in viticulture, but it is undeniable the necessity of adapting the vineyard management strategies in this changing climate to preserve wine quality while maintaining good resource control (van Leeuwen and Darriet, 2016). Perpetual changes in climate conditions may drive the decision of where to start a new vineyard plantation to save production costs, moving to more favourable zones or using more resistant grapevine rootstock or varieties (Webb et al., 2008). Still, this is a decision only available to new plantations, and changes in the vineyard layout or plant material is virtually unfeasible once it has been established. For this reason, advances on digital technologies should drive the development of new tools for the precise monitoring of vineyards, allowing to detect necessities, assess costs and manage resources that are more demanded but, at the same time, more scarce if all demands are to be fulfilled.

It is of particular interest to both grapegrowers and winemakers the possibility that DV provides of identifying parcels of fruit with the same quality, so they can be taken to wineries in batches as uniform as possible (Bramley and Hamilton, 2004). This "selective harvesting" takes advantage of the observed variability in the vineyard monitored by sensing technologies, and allows to achieve the desired specifications in winemaking for the intended end product (Bramley and Proffitt, 1999; Bramley et al., 2003). The second level involves cost reductions in vineyard management. The application of new technologies for the precise monitoring in viticulture aims at the reduction of costs compared to traditional management, an increase in profitability from better quality in grape harvesting, or—ideally—both outcomes (Schrijver et al., 2016). Finally, the last level refers to environmental sustainability and optimisation. DV can be used as a tool, for example, to help to decide how much chemical products have to be used or the precise amount of water that needs to be applied depending on plant status on each area (Matese and Di Gennaro, 2015). This helps reducing chemical waste, water misuse and other environmental hazards.

The adoption of DV is a three-step cyclical process (Bramley, 2001) that starts with data acquisition from the vineyard, continues with the analysis and evaluation of the information inferred from the data, and ends with the development and implementation of a targeted management plan based on the previous analysis (Figure 1.2) The first step should involve the acquisition of large amounts of data from the vineyard that gathers all the components of interest (Figure 1.2a).

As spatial variability needs to be characterised, it is mandatory to apply some kind of georeferencing via global navigation satellite systems (Proffitt et al., 2006). The second step involves the transformation of the acquired data into understandable information (Figure 1.2b). Many sensors are available for vineyard monitoring capable of making measurements of several

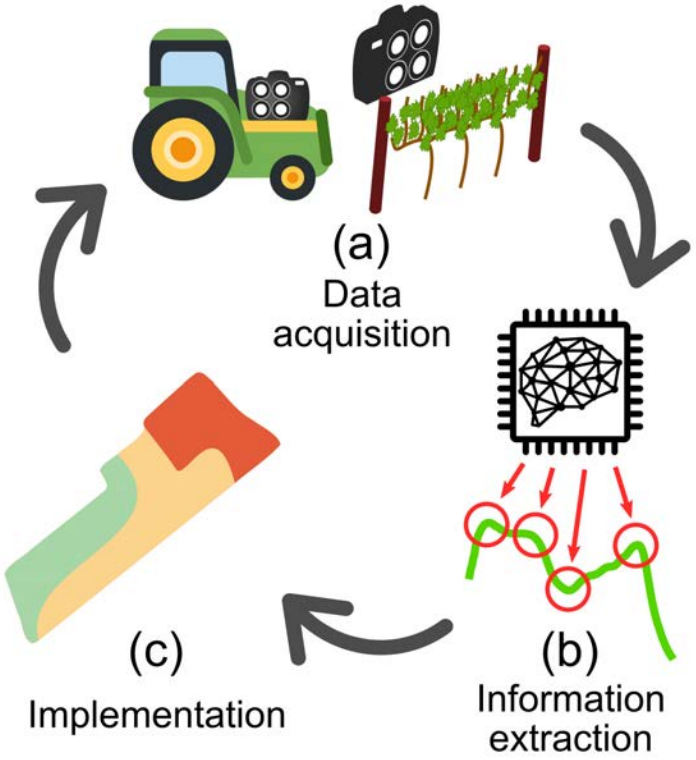

Figure 1.2: The three-step cyclical process in the adoption of DV. (a) Data acquisition from the vineyard; (b) information extraction from the acquired data; (c) development and implementation of a targeted management plan based on the previous analysis.

physiological elements in the canopy, but raw data alone are rarely useful for the determination of key traits in the plants. For example, information about grape ripeness could be present in the reflectance spectrum of the skin. Nonetheless, the raw data acquired by a spectrometer cannot be directly used for ripeness assessment. To overcome this, statistical approaches have traditionally been applied, but new advances on AI and Machine Learning (ML) have led to versatile, powerful algorithms for the training of prediction models for classification (estimation, given an input, of a categorical value) or regression (estimation of a numerical value). Further information about ML algorithms is presented in Section 1.6. In this step, the aforementioned data georeferencing lets, within the vineyard plot, for the delimitation of zones to apply ad-hoc management approaches (Bramley, 2010). The third step should involve the analysis, from a experienced manager, of the variability read in the vineyard, and taking the necessary decisions and strategies for the different plot sub-areas depending on their status (Figure 1.2c). It was said that these steps are part of a cyclical process. It is here where

the iteration restarts, evaluating the response by new measurements and new variability characterisation. Also, the cyclical procedure, if performed over several years, helps in the building of a background that can contribute in the decision-making process at the manager's end (Proffitt et al., 2006; Arnó Satorra et al., 2009).

Combining digital technologies, ML and adequate methodologies will allow winegrowers to implement DV solutions to improve and optimise production systems (Tisseyre et al., 2007). But, the question arises, how can we make use of ML in a DV application? Figure 1.3 displays an scheme for ML modelling (Section 1.6) from non-invasive sensing technologies (Section 1.3) in an agricultural application.

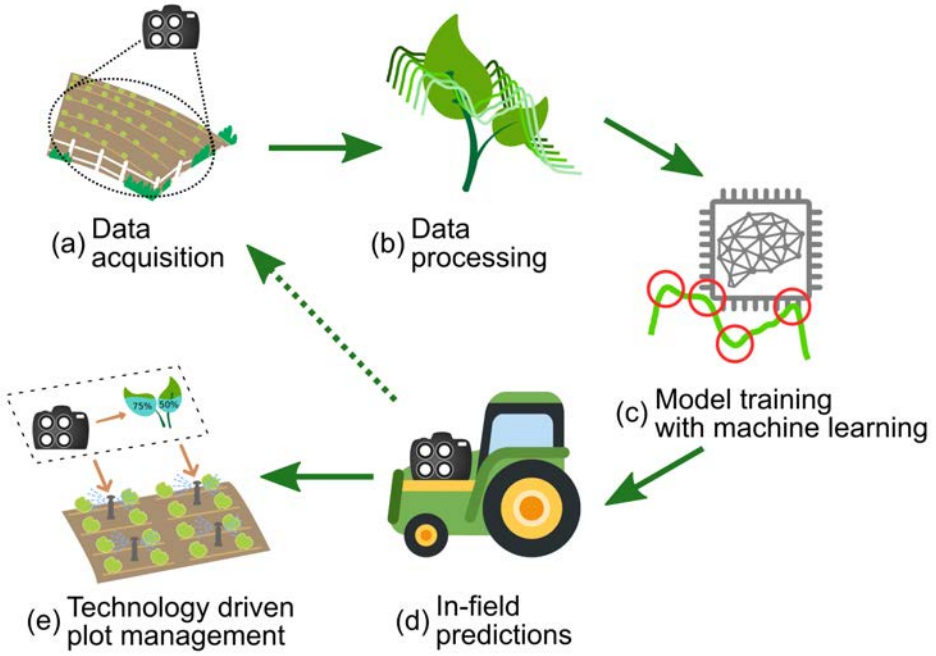

Figure 1.3: Machine learning in digital agriculture: It starts with data acquisition using sensing technologies (a). After data gathering and processing (b), the next step is the proper model training using ML algorithms (c). The knowledge acquired by the models can thus be used to perform in-field predictions (d) that would help in plot management (e). New data acquired in (d) could potentially be used to restart the process for model improvement.

The process starts with the acquisition of data for the development of prediction models (Figure 1.3a), and followed by data processing, in which all acquisitions are gathered, cleaned and sorted into datasets (Figure 1.3). The next step is the training of the models (Figure 1.3c). This step should also include the computation of validation results for performance assessment. Once a full model is trained, it can be used for in-field predictions (Figure

1.3d) to aid in the management of the plot (Figure 1.3e). The data collected in the in-field predictions step can be used for restart the process (going back to Figure 1.3a) and improve the models with new data. Further on this is discussed in Section 1.6.

The next sections discuss some available options in sensing technologies, monitoring platforms and ML techniques for their application in DV, examining characteristics and exposing examples already published in the literature.

1.3 Non-invasive sensing technologies

The accurate knowledge about different statuses of plants in the field would be very valuable for the characterisation of a vineyard plot. Some relevant plant traits are: the nutritional status, disease incidence, plant water status, ripening monitoring or yield estimation. The most adequate approach to assess the plant status is making measurements directly from the individual, as the plant physiology becomes the best target to tell its status. Sensing technology has been rapidly developed in the last years, and its use has allowed the development of many different solutions in digital agriculture and viticulture (Lee et al., 2010). Although this technology has been mainly developed for other industries, agro-food has taken advantage of it for agricultural and food-related implementations. While classical plant status monitoring has been carried out by destructive methods, like chemical or physical analysis, sensing technologies applied to agriculture focused on plant data acquisition in a faster, non-destructive way.

Different kinds of sensors are available to be used.

- **Electromechanical.** These sensors register physical measurements into digital values. Some examples are dendrometers, sap flow meters, etc.
- **Electrochemical.** Sensors that gather data about the chemical composition of the target. Some soil devices use electrodes for detecting specific ions and give readings about soil pH or nutrient levels.
- **Optical.** Optical sensors make use of the electromagnetic spectrum to read data from the targets. Some examples are common cameras, thermal imaging or spectral devices. These are probably among the most suitable kind of sensors that can be used for non-invasive monitoring, very necessary in DA, as data acquisition can be performed without even touching the samples.

In theory, applying DV solutions using different kinds of sensors is not a difficult task, but an actual implementation for industrial use is far from

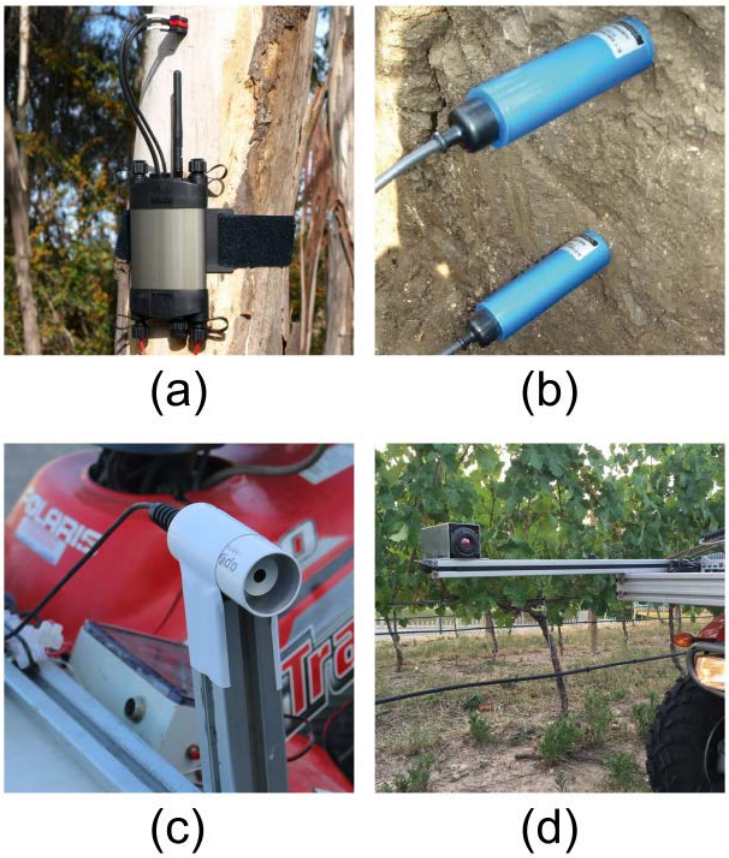

Figure 1.4: Examples of different kinds of sensors: (a) dendrometer (electromechanical sensor); (b) soil moisture detector (electrochemical sensor); (c) infra-red radiometer (optical sensor); (d) infra-red thermal camera (optical sensor) mounted on an moving ground vehicle. Copyright: *ICT International* and *University of La Rioja*.

direct and easy. There must be a procedure to bring together both plant and sensor, and this has evolved in the last years. As in destructive methodologies, like chemical analysis, the target has been taken usually indoor, in where the equipment lies. Here, tests are carried out under controlled conditions of light, temperature, humidity, etc. This approach brings some limitations, mainly that sampling is still necessary. This is not a problem if the sensing system is installed on a production line, for example at the winery, in which targets are automatically scanned in-line. In a vineyard, nonetheless, if samples need to be picked, it is infeasible to select all individuals in a plot for measurements, thus the characterisation of large areas (high-resolution monitoring) is jeopardised.

The non-destructive nature of sensing technologies should still be put into

context. For example, optical sensing devices do not need to spoil the sample for data acquisition, as they only gather the light that has bounced on the surface. However, if complex systems designed for indoor set-ups are used (*e.g.*, Hyperspectral Imaging, more in Section 1.3.3), the non-destructive trait is completely discarded when samples like leaves or branches need to be taken from the field to the system. This consequence, along with the previously mentioned low sampling capability, has been addressed from research and development in remote sensing (more in Section 1.4).

The following subsections provide further details on non-invasive sensing technologies (spectroscopy, multispectral imaging, thermal sensing, hyperspectral imaging and chlorophyll fluorescence) that can be found applied in viticulture.

1.3.1 Spectroscopy

Spectroscopy is the study of physical systems by the electromagnetic radiation with which they interact or that they produce (Herrmann and Onkelinx, 1986). In any medium that contains matter, propagation of radiation is slowed, and it is caused by the interaction between the electromagnetic field of the radiation and the bounds of the atoms in the matter (Skoog et al., 2017). This light-matter interaction can be used in favour if the light reflected by a target is captured by a detector in a certain spectral range. The analysis of this reflected light would allow the characterisation of physical properties of the target, thus inferring further information about the trait of interest. The typical spectrometric laboratory equipment comprises five elements (Skoog et al., 2017): a stable source of light (Figure 1.5a), a container for holding the sample (Figure 1.5b), a mechanism for the isolation of specific ranges of the spectrum of the light (usually involving a mono or polychromator, Figure 1.5c), a radiation detector for the translation of the radiation into electrical signal (Figure 1.5d), and an electronic signal processor (Figure 1.5e). The usual output of a spectral signal measurement given by spectrometers is a digitalised response of radiance (acquired light) in a sequential data of n bands at regular intervals. These bands lie within a defined range of wavelengths in the electromagnetic spectrum. Typically, the ranges cover the visible range (from 300 to 700 nm, approximately) or the NIR range (starting from 700 nm to higher values, depending on the device). Molecules absorb light of specific wavelengths, based on their chemical bonds (Ninfa et al., 2010), hence different spectral ranges can be useful for the determination of different compounds (molecules).

Traditional spectral analysis has been performed under laboratory conditions, using fixed equipment—also called "laboratory analysers"—controlled by trained personnel. These have been widely used in quality or process control as well as research and development in food and agriculture. Laboratory analysers share many of the advantages of spectroscopy: they are simple to

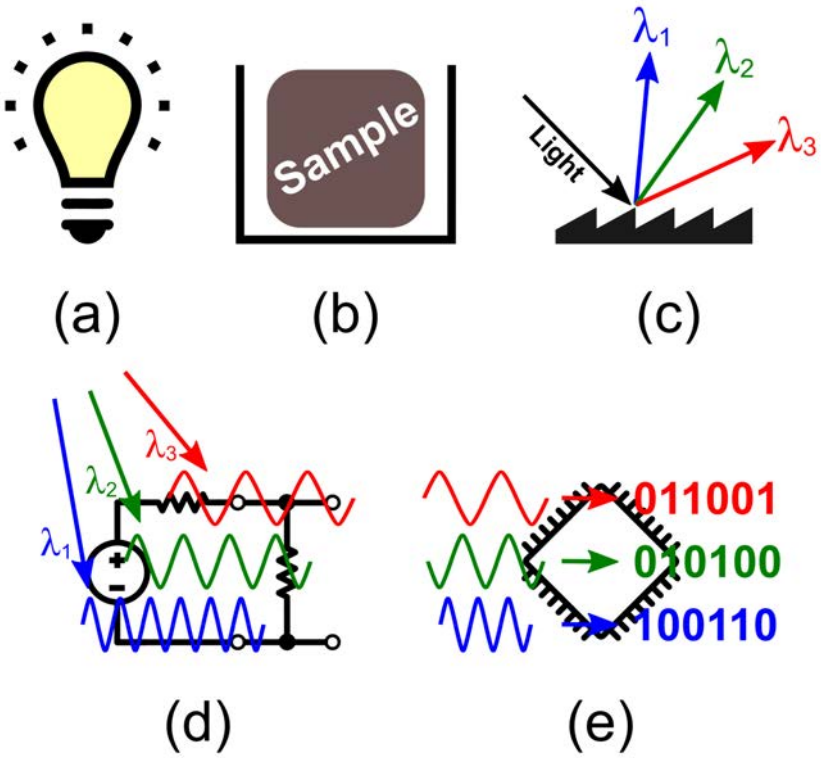

Figure 1.5: Five elements of a typical spectrometric laboratory equipment (Skoog et al., 2017): (a) source of light; (b) container for holding the sample; (c) mechanism for the isolation of specific ranges of the spectrum of the light; (d) radiation detector for the translation of the radiation into electrical signal; (e) electronic signal processor.

use, quick in analysis and require little or no sample preparation Sun (2009). Still, as they are heavy, voluminous and designed to be installed in fixed scenarios, it is a requirement for samples to be carried to the laboratory, so non-invasive analysis is not possible. Additionally, for example in agricultural applications, sampling is also necessary because it is not possible to pick all samples from the field (fruits, leaves, etc.), therefore the capability of detail characterisation of large zones is limited.

In the last years, electronic miniaturisation has allowed the design of similar spectrometer configurations in handheld devices. Nevertheless, the installation of a light source is not always present. Portable spectral sensors can be divided, among other criteria, in spectrometers with (active) or without (passive) source of light. In both cases, the sensor acquires light reflected off the surface of the target, splitting the beam into specific wavelengths and converting the signal electronically into a spectrum. The only difference is that some sensors can have an assembled light source, so the

acquired signal is calibrated to that light (Figure 1.6a), while others need of an external light source, requiring of a signal correction depending on the external light's intensity (Figure 1.6b). Portable spectrometers have critical differences compared to laboratory analysers. Handheld devices allow for a quicker, non-destructive monitoring of the crop, thus increasing the capability of obtaining a more accurate reading of plants' status. Also, they are usually easier to handle than laboratory spectrometers. However, the usage of these devices still demands a certain level of sampling, as each measurement is manually performed, and covering large areas would take considerable amounts of time to complete.

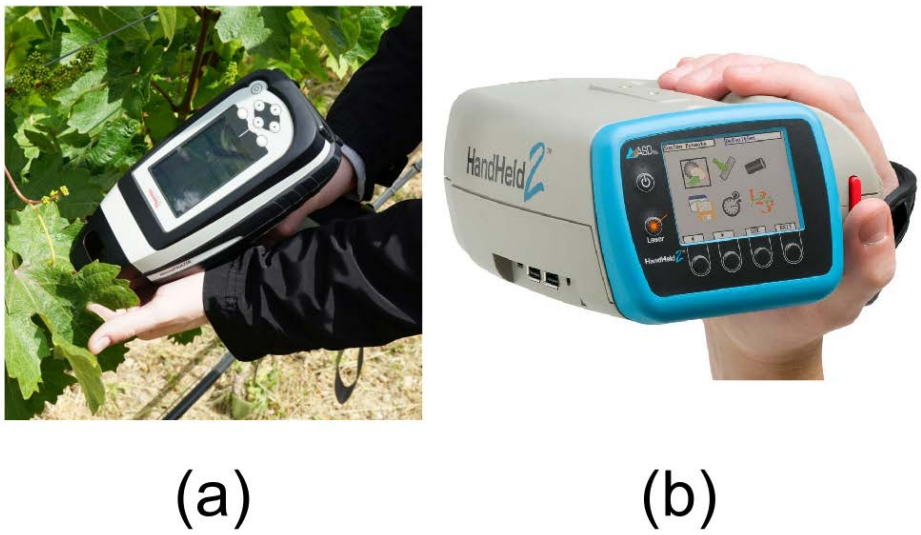

Figure 1.6: Handheld spectrometers with (a) and without light source (b). Source: *Televitis research group, University of La Rioja* and *Malvern Panalytical*.

Handheld spectral devices have been previously used in food and agriculture applications. In Sánchez et al. (2012), the authors used a portable spectrometer with an embedded light source for the non-destructive quality control of strawberries (physical and chemical analysis measuring firmness, skin colour, sugar, acidity, etc.), using Partial Least Squares (PLS) and Partial Least Squares Discriminant Analysis (PLS-DA) for the development of regression and classification models. The results demonstrated the usefulness of portable spectroscopy for quality control in strawberries, also capable of performing varietal classification on the fruit. A similar instrument was used for the estimation of physical-chemical quality parameters in plums (Pérez-Marín et al., 2010). The experiments were design to estimate the fruit's firmness and soluble solid content. The device showed a decent performance for the prediction of soluble solid content. Another example can

be found in Toledo-Martín et al. (2016), in which peppers were analysed for the successful determination of internal (sugar, pH, etc.) and external (colour, thickness, etc.) quality variables. Portable spectrometers without light source have been used for the outdoor monitoring of sugar beets in Laudien et al. (2003). Spectral signals from leaves were acquired by the device attached to a pole at a high of 2 m. The experiments resulted in significant differences between healthy and diseased plants for two different spectral indices. These devices have also demonstrated to be useful for the selection of spectral narrow bands and bandwidths for plant and soil assessment in different crops, like rice, maize or wheat (Ray et al., 2010).

Handheld spectral sensors have been proven to be useful for several objectives in agriculture. Still, new spectral solutions exist for industrial applications that can be used for on-the-go monitoring of the vineyard. Recently, a new kind of spectrometers has been released. These are designed for the non-contact monitoring at approximately 30-50 cm from the target. These devices comprise a processing unit embedded in a housing box, and a sensor head, in which light is emitted to the target and captured from the reflection (Figure 1.7). Both parts are connected by optical fibre. The spectrometer allows for acquisitions up to 120 Hz, and this, together with the possibility of proximal, non-invasive monitoring, makes it easier testing the effectiveness of mounting the devices on a mobile ground platform. The continuous spectral acquisition brings clear advantages for crop monitoring. For example, whole agricultural plots can be monitored if the system is mounted on a moving vehicle, due to the high data-acquisition rate. Additionally, as spectral measurement is not manual, but automated, these devices are very prone to be installed on autonomous monitoring platforms, like agricultural robots. This configuration has been proven successful for the in-field, on-the-go assessment of grapevine water status, mounting a spectrometer on a moving vehicle (Fernández-Novales et al., 2018; Diago et al., 2018).

1.3.2 Multispectral imaging

In agriculture, specific compounds or plant-related physiological parameters are related to some wavelengths in the electromagnetic spectrum. Therefore, these bands are more relevant than other for the prediction of certain features of interest. Normalised Difference Vegetation Index (NDVI), for example, is an index used for the quality and quantity estimation of vegetation development (Tucker, 1979; Goward et al., 1991), based on the ratio between energy emission spectral regions (reflectance) around the red and the NIR bands. For this reason, devices for spectral acquisition of specific wavelengths have been developed and used in agricultural applications, not only for NDVI computation, but for many other vegetation indices (Rodríguez-Pérez et al., 2007). While most spectral devices acquire a full spectrum (typically hundreds of bands) from a reduced spot or reduced region, Multi-

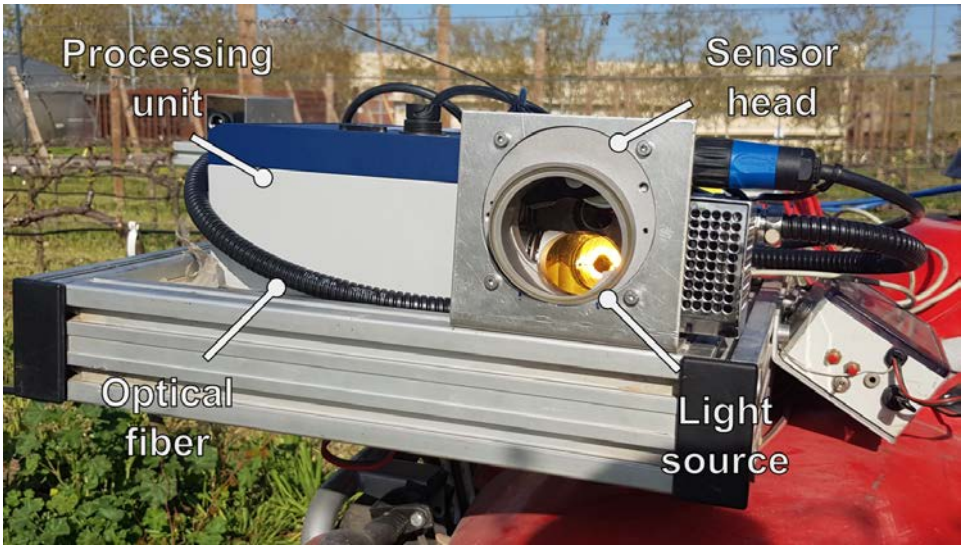

Figure 1.7: A non-contact NIR spectrometer mounted on an ATV, the "Televitis mobile lab" used by this research group. The device comprises a processing unit, and, connected with an optical fiber cable, a sensor head with a light source in it, and it is able to work under uncontrolled illumination conditions. Source: *Televitis research group, University of La Rioja.*

spectral Imaging (MSI) is based on the opposite principle: acquiring image data of wider areas but in a reduced number of bands (typically from three to no more than 10), as displayed in Figure 1.8.

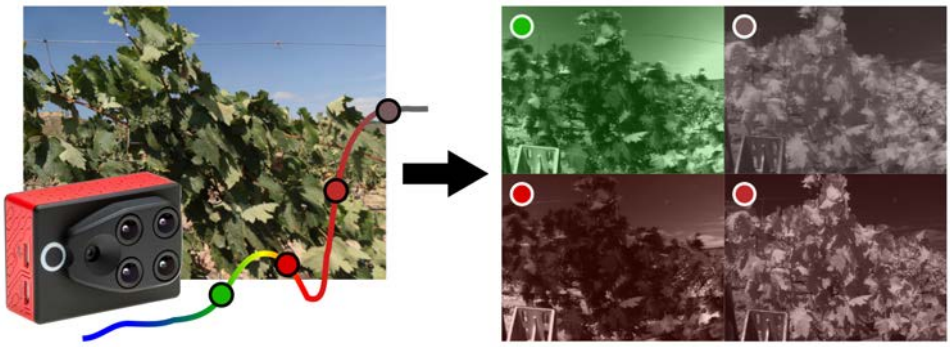

Figure 1.8: In multispectral imaging, images from a same scene are captured at different wavelengths within the electromagnetic spectrum.

MSI is often performed using multispectral cameras, that are designed to acquire a small number of bands and to provide one image for each one of them. Actually, standard cameras (like a reflex one or the cameras embedded in smartphones) are but multispectral cameras that capture the light in the red, green and blue colour wavelengths (approximately around 650, 530

and 460 nm, respectively). These are commonly known as RGB cameras. Multispectral cameras have the advantage of adding a new dimension to the acquired data (the spatial dimension), that could help when extracting information from data acquisition. Also, they do not need to be manually operated and this, along with their light construction, allow them to be installed on moving and automated platforms. The main feature of this technology is that the number of channels is definitely limited, so the modelling of the traits of interest is simpler than when the full spectrum is available.

MSI from satellites or aircraft has been employed in viticulture for several plant status monitoring applications (Hall et al., 2002). In the last years, the combination of miniaturisation—allowing the building of very light, low-consuming multispectral cameras—and evolution in the use and decrease of cost of Remotely Piloted Aerial Systems (RPAS) (Section 1.4.1) has also led to the publication of several on vineyard monitoring using MSI from these kinds of aerial platforms (Rey-Caramés et al., 2015).

1.3.3 Hyperspectral imaging

Hyperspectral Imaging (HSI) combines the potential of spectroscopy and the additional information that a two-dimensional space provides, like an image. With HSI, a whole image is provided and, in each pixel, instead of colour or multispectral information, a whole spectrum in a specific electromagnetic range is provided (hundreds of wavelengths). In previous sections, spectroscopy and MSI have been presented. As discussed, the differences between both technologies lie in that spectrometers provide high spectral resolution (hundreds of bands) in a relatively reduced spatial area, while multispectral cameras capture high resolution images but only in a reduced number of wavelengths (typically less than 10). HSI gathers the best features from spectroscopy and MSI.

It has been demonstrated that HSI is a very powerful tool for agricultural and food applications, and that the combination of high-resolution spatial and spectral dimensions provides a monitoring alternative that should be exploited in the field. But this brings a big burden, and this is the massive amount of data that HSI is able to generate. Extracting useful information from hyperspectral images is a very suitable task for ML, for the training of prediction models. Still, further work is necessary if automated systems need to be developed for the fast, in-field monitoring of plants. The design of automated hyperspectral images pre-processing steps (like segmentation, target identification, sample classification, etc.) is a requirement for that goal.

HSI is a complex technology, hence its high cost, and different hyperspectral cameras exist depending on its image acquisition mechanism and spectral range. There are four different modes of hyperspectral image acquisition (Wu and Sun, 2013): whiskbroom, pushbroom, area scanning and

snapshot (Figure1.9). In the whiskbroom (also known as point scanning), the detector acquires only the full spectrum of a single point, and either the sample or the detector should be moved along two spatial dimensions if a image wants to be acquired, making this methodology time-consuming alternative. The pushbroom scanning (or line scanning) is the most common option found on commercial hardware. It records all the spectra in a whole line in one spatial dimension. To obtain an image, either the sample or the camera needs to be moved along the other spatial dimension. Image composition needs to be done with caution, as irregular acquisition speeds result in warped images. For this reason, this method is very suitable for monitoring in conveyor belt systems. Another option could be, if both target and camera need to be fixed, the use of a rotating mirror in the scanning. The third mechanism, area scanning (also known as wavelength scanning), is just the opposite than the point whiskbroom one: a full image is capture for a single wavelength, and this is repeated for all the bands covered in the range of the camera. This has the advantage that, as the detector only acquires one wavelength at a time, it is possible to set a suitable exposure time for that wavelength. The main disadvantage of this method is that the target needs to be completely still during data acquisition. Finally, technology has brought in the last years devices with the capability of acquiring hyperspectral in a snapshot mode, *i.e.*, all pixels and spectra are captured from a single shot (Hagen and Kudenov, 2013). Nevertheless, this hardware does not offer high spatial resolutions yet, but opens a promising future in the usage of HSI in many fields.

With the exception of satellite imagery, HSI has been traditionally deployed in indoor configurations. In Figure 1.10, a typical HSI acquisition procedure is displayed. A hyperspectral camera is set up and focused to a target that is manually presented with controlled artificial illumination, needed to maximise the signal-to-noise ratio.

Many studies exist using HSI for DA and food control under laboratory conditions. This technology has been used for the determination of fruit composition parameters like soluble solid content—in apples (Ma et al., 2018; Tian et al., 2018), bananitos (Pu et al., 2018), peaches (Li and Chen, 2017), tomatoes (Rahman et al., 2017) or mangoes (Rungpichayapichet et al., 2017)—or anthocyanin content—in raspberries (Rodríguez-Pulido et al., 2017) or mulberries (Huang et al., 2017). Fruit physicochemical properties have also been modelled from hyperspectral data (Zhu et al., 2017; Sun et al., 2017a,b). Plant disease detection has been a topic in which HSI is intensively used (Thomas et al., 2018b; Lowe et al., 2017). In Moghadam et al. (2017), the authors trained machine learning models for disease detection testing three sources: the full spectrum, spectral indices and features generated ad-hoc. A HSI automated phenotyping platform in a greenhouse was set up for plant disease monitoring in Thomas et al. (2018a). State-of-the-art

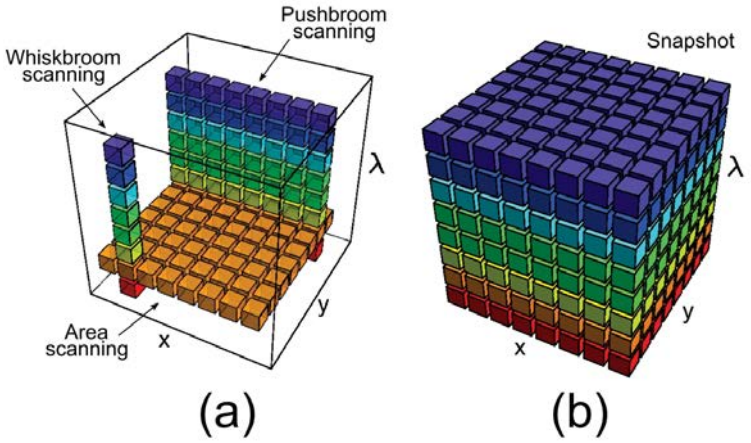

Figure 1.9: Different types of hyperspectral image acquisition mechanisms. Whiskbroom, pushbroom and area scanning (a) captures the data from the target in sequential steps (single pixel, one spatial dimension or one spectral dimension, respectively), while the snapshot method (b) records all the data from a single shot. The letters x and y refer to spatial dimensions, while λ is the spectral dimension (wavelenghts). Source: Hagen and Kudenov (2013).

portable hyperspectral cameras have also been tested for this goal in a recent study (Behmann et al., 2018). In DV, hyperspectral cameras have been used for grapevine varietal and clone classification (Diago et al., 2013; Fernandes et al., 2015), assessment of grape (**SSC!**) (Gomes et al., 2017; Piazzolla et al., 2017) or anthocyanin content (Diago et al., 2016a; Martínez-Sandoval et al., 2016; Zhang et al., 2017). These are but a small collection of examples of HSI potential in agriculture.

The translation of hyperspectral imagers from the laboratory to the field is a very significant step in DA, but it also carries very serious challenges that need to be taken into account. First, it is not assured for light conditions to be either optimal or stable, and this can profoundly affect to spectral acquisitions that, like in-field HSI, require of an external light source. Second, the composition of the hyperspectral image, is also affected by the platform the camera is mounted on, how it manages terrain irregularities, geometrical corrections depending on the position of the camera, etc. Third, in a controlled scenario like in-lab HSI, the position of the sample is both constant and known, and the segmentation and extraction of sample spectra makes it very easy to automatically process a great set of images. Nevertheless, in-field HSI acquisitions are complex, and many other targets (like sky, soil, non-plant elements, etc.) are capture by the sensor, and should be ignored in the processing. A very recent thesis has evidenced the complexity of HSI acquired on-the-go under field conditions (Wendel, 2018), leading to publications about illumination compensation (Wendel and Underwood, 2017b)

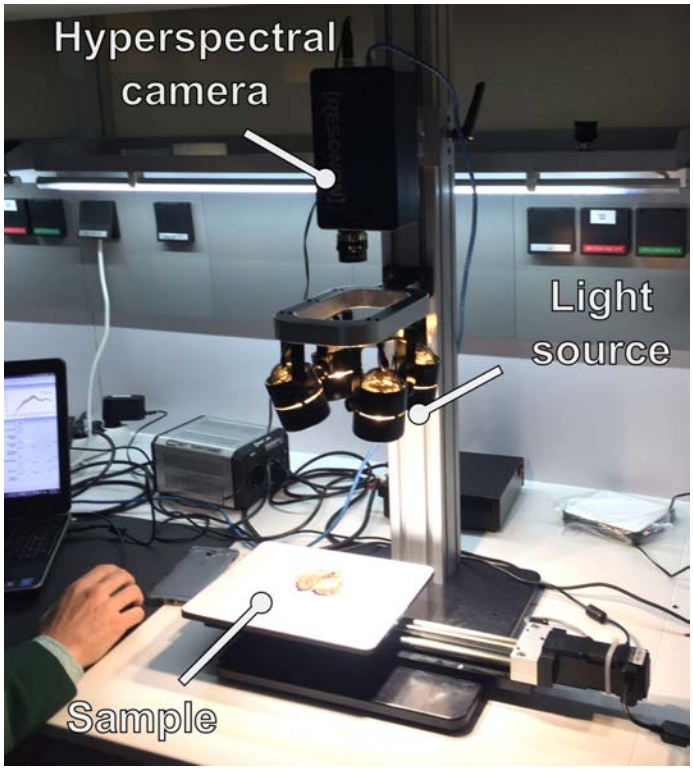

Figure 1.10: A typical configuration for hyperspectral measurements in laboratory. A hyperspectral camera is placed for image acquisition of a sample at a constant distance and using artificial and controlled light conditions. Source: *Televitis research group, University of La Rioja.*

and extrinsic parameter calibration (Wendel and Underwood, 2017a).

Although reports on HSI under field conditions in agriculture are numerous, few works exist testing hyperspectral cameras in the field. In the last years, manual, in-field HSI has been reported in Williams et al. (2017). In that paper, the authors performed hyperspectral acquisition for the segmentation of raspberry plants, using a portable platform, along with a scene background, manually operated. Advances in the research and development of mobile phenotyping vehicles—like buggies (Williams et al., 2017)—or autonomous platforms—such as agricultural robots (Underwood et al., 2017)—have driven new attempts on testing with hyperspectral sensors in the field. Nevertheless, deeper research on specific applications of in-field HSI is necessary, given the richness of this technology.

1.3.4 Thermal sensing

Non-contact thermal measurement is based on sensing thermal radiation. Matter, by the fact that has a temperature above absolute zero, emits a electromagnetic radiation generated by the thermal motion of the particles (Lloyd, 2013). If, from a target, the infrared energy emitted is known, as well as its emissivity (an object's ability to emit infrared energy), the temperature of the target can be derived with high precision by detecting radiation in the long-infrared range (from 9 to 14 µm), operating in narrow bands of the electromagnetic spectrum to avoid contamination in measurements due to water vapour, carbon dioxide, etc.

IR radiometers have been widely employed in several industrial and domestic applications. Using these sensors, the surface temperature of an object can be measured contactless. In order to minimise distortion caused by air between the target and the sensor, or temperatures from surrounding elements, the device should be relatively close to the object. There are several types of IR radiometers, from sensing guns (Figure 1.11a), that demand manual measurements, to passive sensors (Figure 1.11b), capable of a continuous thermal monitoring. IR radiometers have many advantages, as they are cheap, fast to use and process, and able to provide non-destructive measurements that have great importance in agriculture, like plant temperature. Nevertheless, they are not completely suitable when the different elements in a scene need to be individually analysed, as all the readings in the measured area are averaged to a single value.

More sophisticated technology, like IR thermography, has risen in the last decades for applications in agriculture (Ishimwe et al., 2014), specially considering the fact that the prices have lowered year by year. Thermal cameras acquire digital images (or videos), in where each pixel represents a temperature of the scene, in a fast way (Kruse, 2001). Figure 1.12 shows an example of a thermal image of a grapevine in a vertical trellis system. The scale bar indicates which colour in the image represents the temperatures in the scene (each pixel). Thermal cameras can be portable, for manual readings (Figure 1.11c), or compact, for the automated imaging (Figure 1.11d). Thermal cameras, due to their capability of providing two-dimensional images, have the advantage of allowing for deeper analyses of the scene, like object detection, temperature gradient inspection or segmentation. On the other hand, thermal imaging requires of complex processing, so its analysis is not as trivial as using IR radiometers.

Handheld thermal imaging devices are applied in agriculture for the assessment of plant water status. In particular, for DV, thermal imaging solutions, due to their capability of measuring the canopy surface, have been studied for the monitoring of grapevine water status. Leaves interact with their environment by processes involving energy-exchanges. When leaf transpires, water is lost through stomata, and leaf temperature decreases. How-

Figure 1.11: Different examples of devices for IR thermal sensing. (a) A thermal IR gun that requires manual operation. (b) A IR radiometer, capable of carry out automatic, continuous temperature monitoring. (c) A handheld thermal camera. (d) A compact thermal camera for automated imaging. Source: *FLIR Systems* and *Televitis research group, University of La Rioja*.

ever, if transpiration stops, leaf temperature increases as no heat dissipation is occurring. For this reason, thermal monitoring of plant canopies could help to infer water deficit or stress in grapevines (Costa et al., 2010; Jones and Vaughan, 2010).

In a recent study, a handheld thermal camera was employed to characterise the spatial and temporal variability of water status in three different vineyard plots (Grant et al., 2016). Temperature acquisitions were carried out on both sides of the canopies during three different dates on September 2010 at different times each day. The researchers also made acquisitions of minimum and maximum reference surface temperatures from artificial leaves—named T_{wet} and T_{dry}–for the computation of two thermal indices:

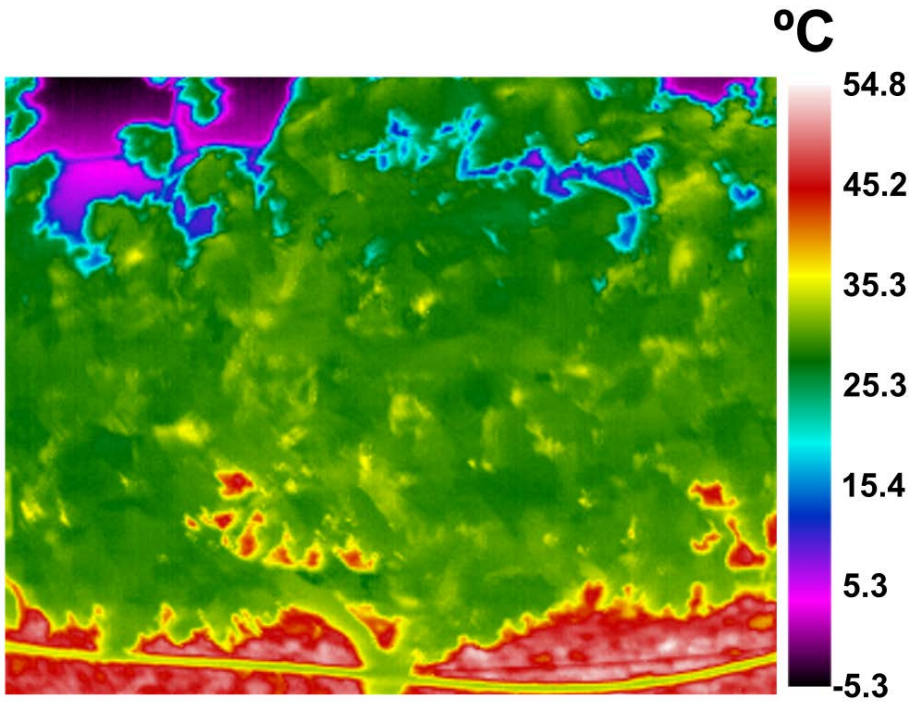

Figure 1.12: Example of a thermal image of a grapevine canopy acquired on-the-go from a moving vehicle under field conditions. The scale bar indicates which colour in the image represent the temperatures the scene (each pixel).

Crop Water Stress Index (CWSI) and Conductance Index (I_g). These indices are calculated, accordingly to Idso (1982) and Jones (1992), respectively, as:

$$\mathrm{CWSI} = \frac{T_{canopy} - T_{wet}}{T_{dry} - T_{wet}} \tag{1.1}$$

$$I_g = \frac{T_{dry} - T_{canopy}}{T_{canopy} - T_{wet}}, \tag{1.2}$$

where T_{canopy} is the temperature of the canopy. Stress indices have been developed in order to mitigate the impact of environmental fluctuations, that have a direct effect on the canopy thermal response. Good correlations were found between indices and reference parameters. Another study also explored the validation of thermal indices for water status identification in grapevine (Pou et al., 2014). A manual thermal camera was also used for the computation of CWSI and I_g thermal indices. The authors reported significant correlations between the indices and the physiological parameters.

Thermal systems have also benefited from electronic miniaturisation, and lighter, low-cost thermal cameras are available for agricultural applications.

Furthermore, airborne thermal imagery has been studied for the monitoring of grapevine water status. In one of the first articles published on this topic (Baluja et al., 2012), the authors reported the use of thermal imaging from an Unmanned Aerial Vehicle (UAV). The experiments resulted in high correlations corresponding to one measurement date, and to a direct correlation between thermal indices and reference method (no modelling performed). These features still carry some limitations, as no actual model can be used for prediction, and intra-season variability is not considered. Although UAVs and thermal imaging have been proven to be useful for the fast water status monitoring in a whole vineyard plot, it is still limited by the spatial pixel resolution of the camera. A recent study indicated that, in grapevine, because of the narrow canopy width, it is necessary to obtain high resolution thermal imagery having at least 0.30 m pixel size (Bellvert et al., 2014). This suggests that ground-based, on-the-go thermography could bring improvements in DV, mainly for water status assessment.

1.3.5 Chlorophyll fluorescence

Chlorophyll fluorescence refers to the emission of fluorescence produced when the chlorophyll molecule is excited by light. Sensors based on this mechanism have been developed, as chlorophyll fluorescence is one of the most commonly employed indicators of plant status (Bilger et al., 1997; Cerovic et al., 2002; Agati et al., 2005; Cerovic et al., 2012). In viticulture, handheld fluorescence sensors have been used for several application (Figure 1.13).

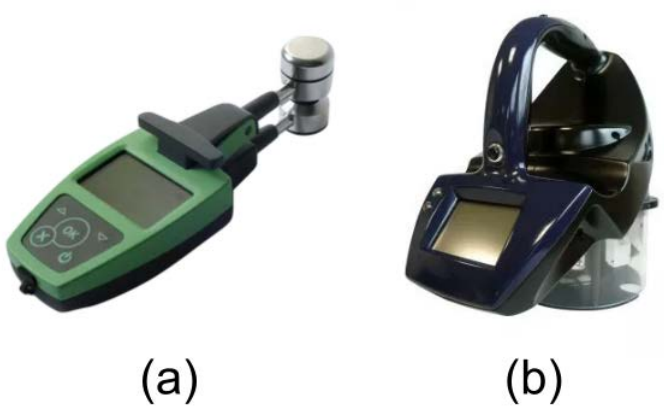

Figure 1.13: Two handheld fluorescence-based sensors used for the monitoring of plant status. Source: *Force A*.

In Rey-Caramés et al. (2016), the authors designed an experiment throughout the 2011 season for the quantification of the spatio-temporal variation of leaf chlorophyll and nitrogen in a commercial vineyard. They used a handheld fluorescence sensor (Figure 1.13b), demonstrating its suitability

for vineyard monitoring during a season. The same sensor was employed for the assessment of the spatial variability of grape composition during the 2010 campaign in a commercial vineyard. These kind of sensors have also been mounted on a ground vehicle for the on-the-go monitoring of the vineyard. In Diago et al. (2016b) the authors reported a study of how to calibrate fluorescence-based sensors from moving platforms for the assessment of grapevine vegetative status.

1.4 Sensing platforms

The different kind of sensors described in Section 1.3 can be installed on several platforms, and depending on them, the data collected from the same target can be very different. In this chapter, some of the most common monitoring platforms used in agriculture are described, divided depending on their utility for remote or proximal sensing.

Remote sensing is defined as a technique that allows the acquisition of images from earth surface from high altitude, while proximal sensing is performed by maintaining low distances between the sensor and the target that is measured (Fussell et al., 1986).

1.4.1 Remote sensing platforms

Until the 1960s, aerial images were the main development in remote sensing, but it was in 1960 when the first satellites were used for image acquisition of surfaces (Chuvieco Salinero, 2006). Nowadays, there have been many launches of sensing satellites for different purposes, like the Landsat program (United States Geological Survey, 2019) (Figure 1.14a) or the Sentinel family (European Space Agency, 2019). Imaging from manned airborne platforms at high altitude (Figure 1.14b) is also common for the monitoring of large areas in a few runs. Remote sensing is extensively used for geology and mineralogy, due to its ability of acquiring large areas in a short period of time, and this is also a trait that agriculture can benefit from. The latest developments on unmanned aerial vehicles (UAVs) and RPAS, commonly known as drones (Figure 1.14c), have positively influenced the application of local airborne sensing in agriculture in the last years.

In spite of the advantages of remote sensing, applied to crops that cover large areas, coarse image acquisition from satellites or very high airborne platforms lacks of a proper resolution for the detailed analysis of grapevines (Matese et al., 2015). Also, as launching ad-hoc satellites is virtually impossible for most actors in the indutry, the only way to obtain satellite data is by accessing to services provided by external organisations. Airborne platforms have the advantage that can be hired as a service, and they are able to record data at higher resolutions. Still, it is a very expensive alternative

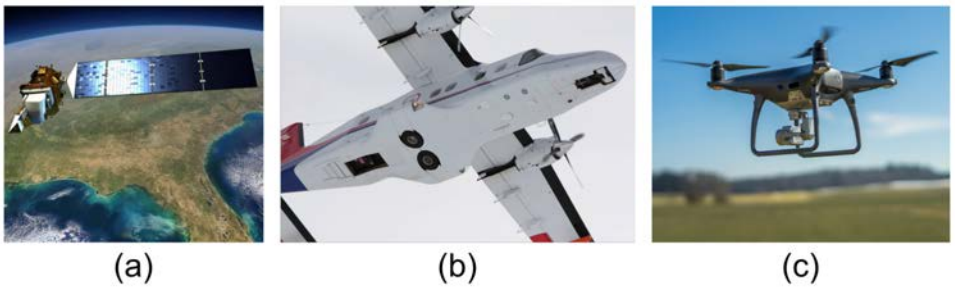

Figure 1.14: Examples of remote sensing platforms. (a) Satellite imagery, (b) airborne imagery, (c) remotely piloted aerial systems. Source: *NERC Airborne Research Facility* and *Landsat*.

and not within everyone's reach. RPAS have addressed the low-resolution and high-cost features. Because of their lower flight altitude, delivering high-resolution images, and their low-cost tendency in the last years, they have become a popular solution for remote sensing. Still, it should not be forgotten that the worldwide trend in industrial viticulture is to use a vertical trellising. This means that, from an aerial point of view, the width of the canopy is rarely larger than 40 cm, and many interest elements like mid-low leaves, branches or grapes are not visible. The fact that only the upper leaves in the canopy are scanned is also meaningful, as these have different behaviours for photosynthesis and transpiration (Escalona et al., 2015), and it is also not possible to sense the fruit (so no yield or fruit composition monitoring is possible). Even when top leaves are the ones of interest, there may exist some level of noise in the background in the image (Taylor et al., 2005), mainly caused by soil or grass (Tisseyre et al., 2008). Additionally, sensing from airborne platforms is affected by weather, and data acquisition can suffer from lower quality due to atmospheric disturbances.

Given all these reasons, the development of sensors for ground-based platforms (proximal sensing) has become a key factor for better DV solutions. The vast majority of the studies in viticulture make use of optical devices—RGB and spectral sensing—as some of them can be implemented in ground vehicles for on-the-go measurements (Matese and Di Gennaro, 2015).

1.4.2 Proximal sensing platforms

Proximal sensing, unlike remote sensing, is performed using sensors near the surface of the earth (Fussell et al., 1986). While many manual, portable sensors exist in the market (Section 1.3), current trends move toward sensing technologies mounted on moving ground vehicles. As previously discussed, grapevines are crops mostly planted in a vertical trellis system, hence monitoring from a lateral point of view allow for the high-resolution data

acquisition—*e.g.*, a vehicle moving between vineyard rows—would ideally offer high-resolution data collection.

One of the most basic set ups that can be deployed in the field is attaching the sensor directly on working agricultural vehicles. This has the advantage that monitoring can be performed at the same time that the vehicle is working on another task, or even this task can be determined by the information that the sensor is providing. The main drawback that this set up has is that, in some cases, the driver needs to be trained for the application of the technology, and plant monitoring is virtually limited to those moments in where the agricultural vehicle is working out in the field.

Another possibility is to install sensors in manned ground vehicles specifically designed for in-field monitoring. In this sense, vehicles like buggies or ATVs take a special role, as they can be adapted to very different environments and focused on the monitoring of a whole plot. A review article (Deery et al., 2014) has underlined the suitability of ground-based vehicles for crop phenotyping. During the development of this PhD Thesis, the majority of the work carried out in the field during four consecutive seasons has involved the use of an ATV (Figure 1.15). This vehicle has been conceived as a "mobile laboratory" in which many different kinds of sensing technologies have been installed for the on-the-go monitoring of several traits of grapevines.

The advantage of buggies or ATVs is that they can be specialised in plant data acquisition, without the need of adapting an already deployed agricultural vehicle for this end. This allows for the monitoring to be performed as many times as needed and in a faster way. The use of a specific vehicle for plant monitoring has the disadvantage that it not only adds the cost of the sensors, but the vehicle itself, and it also needs a person to, at least, drive the vehicle, if not for controlling the devices. Advances in the last years have driven to the development of different autonomous robotic platforms for the vineyard and other crops.

Robots are the future in agriculture, as they can act autonomously performing a wide range of applications in the field, and VineRobot and VineScout are good examples for this (Figures 1.16a and b, respectively). They are prototypes from different research projects that are fitted with different kinds of sensors for both automated manoeuvring and plant sensing: Light Detection and Ranging (LIDAR), for obstacle detection; fluorescence sensors, for grapevine status assessment; thermal cameras, for water status determination; etc. Robots have many advantages, such as their complete autonomy—allowing for a faster unsupervised plot monitoring, without the need of specialised personnel or training—or the ability of processing and delivering the information in real time. Nonetheless, we are in a stage in which robots are still expensive, in both purchasing and maintenance, and its availability is yet limited and far from full commercial deployment. With the continuous research and development, the hope is that robots become a

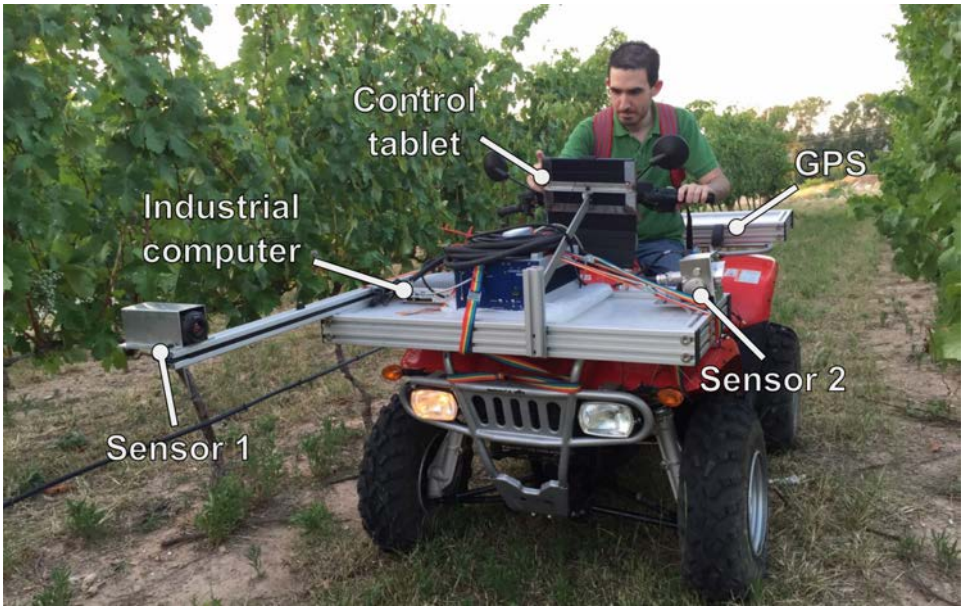

Figure 1.15: The "Televitis mobile lab", an ATV for vineyard monitoring designed by Televitis research group so that different sensors can be installed. Sensors are mounted on the frame structure of the vehicle, connected to an industrial computer (that acts as a hub) and controlled wireless by the driver using a tablet. Measurements can be georeferenced by attaching GPS signals. Source: *Televitis research group, University of La Rioja.*

settled down factor in modern agriculture.

1.5 Artificial intelligence

The ideal objective of AI has been to design machines capable of doing all that a human being can do. Nonetheless, there are huge and evident differences between a human's cognitive system and the machines we can build. Even so, AI is driving the world of today, and the trend is that year by year, AI will keep growing to improve our lives (Stajic et al., 2015). What is then driving this revolution in our society? The complex combination of mathematics, computing and massive data could be an accurate explanation of today's relentless advance of AI, as we have developed methods to let machines to learn. In mathematics we can find the unquestionable foundations of the vast majority of the concepts that machines are based on, and the latest developments on hardware and computing are the implementation of those concepts within the reach of everyone. Still, mathematics and computing are but tools that need to be fed with a third element, an already precious resource: data. We live in a data driven world, and data has become

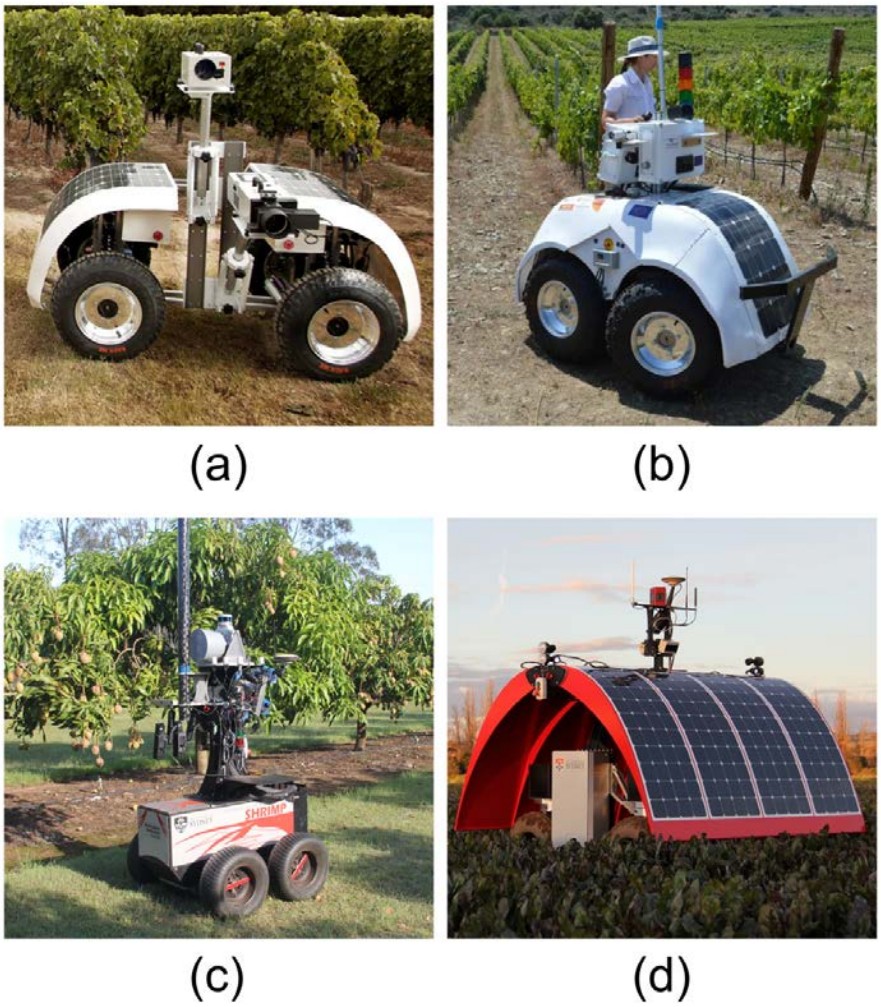

Figure 1.16: The (a) VineRobot, (b) VineScout, (c) Shrimp and (d) Ladybird robots. Prototypes from European and Australian projects. Source: *Televitis research group, University of La Rioja* and *Australian Centre for Field Robotics, The University of Sydney.*

a very powerful currency in many technological businesses. With the growth of worldwide communications and easiness of instant access to the Internet, it became possible to gather real-time tracking about one's online behaviour. Nearly every person in nowadays society has a device equipped with different sensors that gather data in form of voice, images or location, and can be instantly sent to social networks. Also, many kinds of transactions are also available through an smartphone connected to the Internet, like shopping, bank access, etc. We are definitely surrounded by data. Therefore, if mathematics and computing provide the AI tools to make a machine to learn, the

today's vast amount of data drives machines on what knowledge should they acquire (Sejnowski, 2018).

We are surrounded by the advances of AI at many levels. It is not inaccurate to name nowadays society as the Information Society, and AI has helped providing techniques and applications of natural language processing to manage huge amounts of information (Hirschberg and Manning, 2015). In economics, for example, AI is applied at many scales, as economics' decision models directly connect choices and values in a mathematically precise manner (Parkes and Wellman, 2015). Medicine has also benefited from learning machines (Buch et al., 2018), in applications like classifying suspicious skin lesions (Esteva et al., 2017) or identifying pulmonary tuberculosis on chest radiographs (Lakhani and Sundaram, 2017). Machines are able to drive cars autonomously on urban environments (Bojarski et al., 2016), and even science too has taken much advantage of AI (Appenzeller, 2017).

In agriculture, AI can be of much help with by transforming crop data into information useful to the farmer in the decision-making process. It is here where AI can be of much help (Jayaraman et al., 2015), to reduce environmental impact and increase sustainability. The combination of new digital technologies with AI create an opportunity to revitalise agriculture, increase the efficiency in farm operations and reduce environmental impact (Asseng and Asche, 2019). Digital technologies and AI have also help in agriculture with tools for data interoperability among storage systems (Hu et al., 2010), fertiliser management (Yuan et al., 2013) or for crop monitoring with the aid of computer vision (Patrício and Rieder, 2018). Still, further research is necessary for crop monitoring, as the increasing development trend in non-invasive sensing technologies (Section 1.3) open new opportunities to gather large and precise amounts of new data from crops and extract useful information.

The next section will go deeper into the tools AI have to give machines an useful knowledge to be of support in a digital agriculture application.

1.6 Machine learning

ML, in the core of AI, helps in the task of providing tools and methodologies to provide computers with learning capabilities so they can transform this huge amount of data into useful information (Jordan and Mitchell, 2015). ML frameworks are specific tools that AI has to develop mathematical models that acquire knowledge without explicit program, but by exposure of examples. In Section 1.3, many different kinds of sensors available to be used in agriculture have been presented, hence the current easiness of acquiring large quantities of data from crops. While digital agriculture is based on putting crop status in numbers, this data acquisition step should not be an end, but a mean to provide mechanisms and methodologies to transform the

numbers into information that is useful to take decisions. In the last decades, research and development in ML techniques has allowed to implement many data management and processing strategies (Government of Spain, 2019), and the present data-trending age is a perfect scenario to keep the research on new solutions in digital agriculture and transfer them to the industry.

ML can be defined as the field that studies techniques and methodologies to let computers solve specific tasks without the need of providing an explicit algorithm[1] (Samuel, 1959; Bishop, 2006). The term "learning" is extremely important in the concept, as learning has the implicit particularity that previous examples exist, and the process is carried out through exposition to and analysis of the examples (*i.e.*, acquiring experience). That is why ML needs to learn knowledge based on input samples. ML methods have the advantage that they are very flexible, hence their suitability to applications where knowledge is underlying and little is known about the domain (Domingos, 2002). When using ML methodologies, it should not be a goal to deeply identify the underlying rules that may exist in the data, but to construct a good and useful approximation that, although may not explain everything, would have enough discovered knowledge to apply it for other applications (Alpaydin, 2009).

According to García et al. (2015), the steps involving knowledge discovering using ML are:

1. **Problem Specification:** It involves gathering information about the application domain and the goals that need to be accomplished.

2. **Problem Understanding:** Including the comprehension of the selected data. It greatly relies on the previous knowledge about the domain that the experts have.

3. **Data processing:** Important step that may involve data cleaning, integration or reduction. Data processing is one of the most important steps, as much of the success or failure of a ML modelling may depend on how good the input data is processed.

4. **Machine Learning:** The core methodology to obtain models for the extraction of patterns from an input data. This step involves the selection of the most suitable ML task, the selection of a specific algorithm and the training and validation of the models.

5. **Evaluation:** Analysing the discovered patterns and interpreting their meaning.

[1] Attending to the Cambridge Dictionary's definition of the word: "a set of mathematical instructions or rules that, especially if given to a computer, will help to calculate an answer to a problem"

6. **Exploitation:** The implementation of the tuned and trained ML model for the incorporation of its knowledge in another system for further processing.

Combining digital technologies, ML and adequate methodologies will allow winegrowers to implement DV solutions to improve and optimise production systems (Tisseyre et al., 2007). But, the question arises, how can we make use of ML in a DV application? Figure 1.3 displays an scheme for ML modelling (Section 1.6) from non-invasive sensing technologies (Section 1.3) in an agricultural application.

Now that all elements in a DA application have been deeply discussed in previous sections, further detail on the use of ML is presented, making references again to Figure 1.3 in Section 1.2.

The first step is data acquisition (Figure 1.3a). The objective is to record data from a sensor (X) and, if necessary, link them with some kind of parameter of interest or reference data (y). Reference data is used to train prediction models that analyse underlying patters that could exists between X and y. Therefore, every sample in the data X should have a corresponding value in the data y to be used as input to for a ML algorithm. It is important to highlight that when acquiring reference data, it should cover a wide range of variability so that the ML algorithms will be able to learn from samples with different features.

Once the data are gathered, the next step is processing them (Figure 1.3b). Processing usually involves pre-processing of the raw data depending on the source sensor (*e.g.*, spectral treatments when using an spectrometer; temperature extraction when using a thermal camera; etc.) and then data processing common in all ML applications (*e.g.*, normalisation, discretisation, etc.) (García et al., 2015, 2016). At the end, the processed data should be converted into a set of examples (also known as samples) that represent the individuals from which data was gathered. Each sample is a collection of features, also defined as attribute or variables, that can be nominal or numeric.

The next step is the training of prediction models with ML algorithms (Figure 1.3c). After the samples have been defined, the question is, how can they be used for the training of the model that will better predict new unknown incoming samples (*e.g.*, examples whose y values are unknown). The training process of ML is arguably the most complex, and the one that mostly need of the experience of the user. First, a good knowledge of different ML algorithms and how they work is necessary. And second, consistent validation methods should be designed and applied as measurements of how good a trained model is.

The kind of prediction that ML algorithms can perform is called differently depending on the kind of variable that is predicted. When the target to predict is nominal (one category in a finite set), the prediction task is

called "classification". On the other hand, when the variable to predict is a number, it is called "regression". There are diverse kinds of algorithms for classification and regression, and each one of them can be more or less useful depending on the nature of the problem. Selecting an algorithm does not just imply using it, but effectively tuning its configuration parameters to maximise its performance.

The validation of a model is an indispensable process needed to a) monitor the behaviour of the training process and b) to obtain a statistical value of how precise the trained final model is (Wolpert, 1992). Having a dataset with N samples, when a model is trained with all of them, how can we be sure that it has a good generalisation capability for future predictions? One option would be to predict samples with known label, and see if the model was correct. Nevertheless, computing accuracy scores by predicting again the samples from the training dataset (samples with known labels) would be an error, as the model could be overfitted. Overfitting occurs when a model, after being trained, predicts the train data with very high accuracy, but fails in the prediction of new samples not present in the training process. One of the most used mechanisms to decrease and control overfitting is Cross Validation (CV). Cross Validation (CV) is a technique that is used to assess the performance of a ML algorithm when trained using a specific dataset. CV itself does not provide a trained model. On the contrary, it is used as a performance measurement, hence it should be used to prevent overfitting and select the optimum model configuration. As CV is an iterative process, it consists on the partitioning of the a dataset, the training of models and prediction of unknown samples, and the averaging of the performance statistics. This is called k-fold CV (Kohavi et al., 1995). In a k-fold CV, the dataset is equally and randomly split in k subsets, and k training-prediction iterations are performed. In each iteration, one of the k subsets is marked to be predicted, and a model is trained with the remaining subsets. Once trained, the marked subset is predicted and, as labels are known, an accuracy score is computed. This process is repeated over the remaining subsets, rotating the subset to be predicted, and finally the average computation is computed. CV is very useful when the dataset size is small. If there are enough samples in the dataset, it can be split in two subsets, for example in a 80%-20% ratio, and used them for training and testing, respectively. With the train subset, k-fold CV is performed to obtain a CV score, and then all the samples in it are used to train a model. That model is used for the prediction of the samples in the testing subset, and the test accuracy score is computed.

Once the best ML algorithm has been selected, and the best values for their parameters validated, a new model with the same configuration and all the samples in the dataset can be trained and used for its exploitation in another application (Figure 1.3d). In a DA application that make use

of non-invasive sensing technologies, this would mean the amalgamation of a sensor and a system with the trained model embedded. The latter may receive continuous data from the sensor, and give prediction outputs. In fact, this step is also a data gathering process. It is possible to take advantage of this and use the new gathered data to repeat the process in Figure 1.3 and retrain models to improve their performance.

Finally, as the goal of the process is to take decisions, the generated outputs are considered in the decision-making process, so the information obtained could drive plot management (Figure 1.3e).

The next sections describe in detail some ML algorithms.

1.6.1 Support vector machines

Support Vector Machines (SVMs) are kernel-based algorithms originally designed for binary classification, but currently are capable of performing multi-label classification (Herrera et al., 2016). They are defined as kernel-based algorithms because they make use of a kernel to transform the input into a higher dimensional space to lineally separate the samples. The base of SVMs were initially formulated by Vapnik and Chervonenkis (1964), but they were fully developed in the mid 1990s (Cortes and Vapnik, 1995). SVMs, that are considered among the most powerful learning algorithms for classification (Rosales-Pérez et al., 2017), have had great importance during the development and application of ML. These algorithms, unlike other approaches like Artificial Neural Networks (ANNs) (that require reinforcing training to get an optimal model, Section 1.6.2), are capable of train models on a deterministic way, *i.e.*, always delivering the best separation among the input labels. SVMs have demonstrated during the last decades their usefulness, extensively applied in many data-related solutions.

SVMs train models for the classification of a set of samples (Figure 1.17a) into two categories by finding the best decision boundary between them (Cristianini et al., 2000). A decision boundary is but a line (or a plane) in the attribute space of the samples that separate them. The classification of a new sample only requires to check in which side of the boundary the new sample lies. Nevertheless, the separation of the samples in two classes are not done directly on the attribute space, but on higher dimensional spaces after transformation using kernel functions (Figure 1.17b). Afterwards, the best decision boundary is calculated by maximising the distance between the boundary hyperplane and the closest samples from each class (the support vectors, Figure 1.17c).

The translation from the original attribute space to higher spaces is the key feature of SVMs. There are different kind of kernel methods to achieve this (for example: linear polynomial, or radial basis function kernels), and each one make very different transformations on the data. Choosing the best

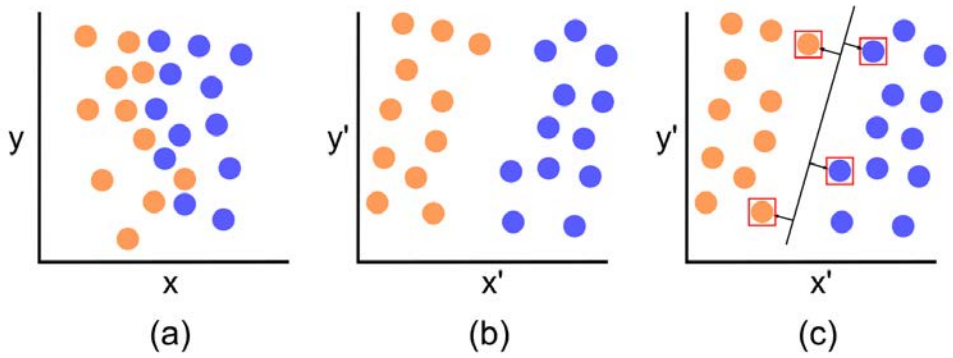

Figure 1.17: A Support Vector Machine transforms the original dataset (a) to a higher dimension space (b; for illustration purposes, the new space is represented also in two dimensions), and then generating a hyperplane—the black line—that maximises the distance to the support vectors—the samples with the red squares—in the new space (c).

one depends on the nature of the problem and the experience of the user. The selection of the hyperplane is also controlled by other several variables that need to be tuned.

Although SVMs were originally designed for binary classification, they can be used for regression (Drucker et al., 1997) and multi-label classification (Hsu and Lin, 2002). Still, in the majority of the cases, for multi-label classification, the SVM is not modified to admit more than two classes. On the contrary, binary classification is still performed. One-vs-one and one-vs-all approaches are followed. In the first case, having m classes, $\frac{m(m-1)}{2}$ binary classifiers are trained, each using only the samples of two classes; then, the prediction of an unknown sample is carried out by a voting scheme in which all the classifiers are used, and the most frequently predicted class is returned. On the other hand, in a one-vs-all, m classifiers are trained, one per class, using each all the samples from the class and the remaining samples as another unified class.

SVMs have been used for several applications in DV using spectral devices. In Al-Saddik et al. (2018), these classifiers were used for grapevine disease detection. Binary and multi-label classification models were trained per variety for the detection of healthy and infested leaves from spectral data. Results demonstrated that SVMs performed better than discriminant analysis classification, and that the ML approach was more able to successfully model the data after spectral pre-processing.

Yield estimation in vineyards has benefited from SVMs in several ways. Grape bunch detection has been performed on RGB images using computer vision and SVMs (Liu and Whitty, 2015). The authors demonstrated the good fitness of this technique over other ones like K-nearest neighbour (Reis

et al., 2012). There also are recent examples on data analysis supported by SVMs for berry number estimation (Aquino et al., 2017) or bud detection (Pérez et al., 2017; Díaz et al., 2018), demonstrating the usefulness of this ML approach in object detection.

1.6.2 Artificial neural networks

ANNs are a very popular ML approach used for both classification and regression. They are recognised as one of the most known benchmarks in ML, and these algorithms play a leading role in the field of AI (Muñoz-Ordóñez et al., 2018). The potential of ANNs have been proven for a very broad collection of applications: trajectory prediction (Zissis et al., 2015), cancer diagnosis (Ganesan et al., 2010; Bottaci et al., 1997), automatic game playing (Silver et al., 2016) or for solving problems in quantum mechanics (Carleo and Troyer, 2017).

The concept and design of ANNs are based on the behaviour of biological a neural network and, although a real simulation of brain neural networks is not sought, the main design of a layout and interconnection of neurons is implemented. The first mathematical concept about the functioning of ANNs was published by (McCulloch and Pitts, 1943), and taking that as a base, Rosenblatt (1958) proposed the idea of perceptron (Figure 1.18a).

The neuron or processing element, based on Rosenblatt's perceptrons, is the basic unit of an ANN. It receives n input signals, and these are modified (multiplied) by n different specific weights. Afterwards, the results are sum and used as input for an activation function, whose output is the output of the neuron. An ANN is therefore built when several neurons are connected in a layered pattern. The layout of an ANN is defined by the number of layers that it is composed of. One of the most common kind of ANNs used are Multilayer Perceptrons (MLPs). MLPs are a kind of neural networks that comprise at least three layers of neurons (Figure 1.18b) and use backpropagation in the training process (Hornik et al., 1989). In a fully connected ANN, the output of all the neurons in a layer are forwarded to (as the input of) all the neurons in the next layer. ANNs can be used for both classification or regression, depending on the structure in the last layer, the output one. If the output layer only contains one neuron, it can be used for the prediction of a real value (regression) or binary classification. If it is sought to train a classification model for more than two classes, the last layer should contain the same number of classes.

Backpropagation was a innovative concept introduced and developed in the 1970s and 80s (Werbos, 1974; Rumelhart et al., 1986). The training process of an ANN consists in the iterative exposure of the neurons to the samples in the training dataset, computing the prediction performance at each iteration, and adjusting the weights by backpropagation, from the last layer to the first one, to improve the output. This is repeated a certain

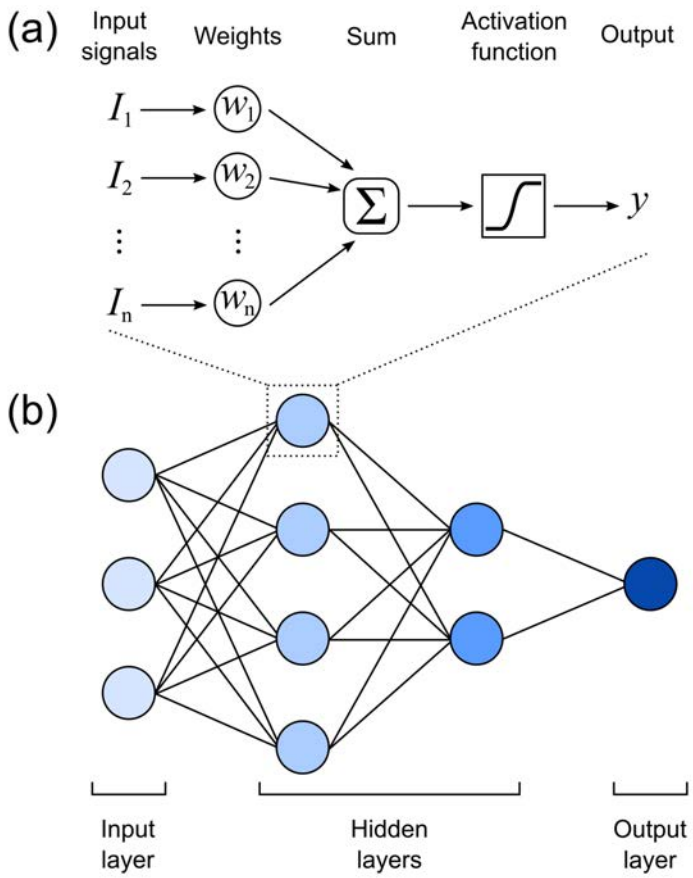

Figure 1.18: (a) Example of a processing element or neuron in an Artificial Neural Network. (b) A fully connected Multilayer Perceptron with two hidden layers.

number of times, and at each iteration, as the weights in the network are updated, the network improves its response for the prediction of the training data. The number of cycles the ANN is trained through is a very important aspect of the training process, as too much iterations could lead to high levels of overfitting in the model.

ANNs have been used, and currently still are, for different applications in viticulture. Mancuso et al. (1998) developed one of the first applications of neural networks for the classification of grapevine varieties from several ampelographic parameters. Recent research on varietal classification has also considered leaf features and NIR spectroscopy as input for ANNs in the classification of several grapevine cultivars (Fuentes et al., 2018), with high accuracy levels from the learning algorithms.

Grapevine water status estimation has been recently evaluated using

thermal readings and ANNs by King and Shellie (2016). Leaf temperature was predicted from several climatic parameters, with ANN models that were useful for the calculation of thermal indices for water status assessment (Section 1.3.4). Another combination of digital technologies and ML has been recently reported by Romero et al. (2018). In this work, the authors used MSI from RPAS for the monitoring of water stress spatial distribution in vineyards. ANNs modelling aided in the management of irrigation scheduling.

1.6.3 Convolutional neural networks

Deep Learning is a branch of ML that promotes the re-use of features and, progressively and using deeper layer architectures, obtains more abstract features at higher layers of representations (Bengio et al., 2013). Convolutional Neural Networks (CNNs) are the most common implementation of deep learning (LeCun et al., 2015), being extensively used in the last years in many scientific and industrial fields. Technically, any neural network with two or more hidden layers can be considered as a deep neural network, but CNNs have lately emerged as very effective tools in computer vision, like object detection or image classification. The concept on which CNNs are based on is not new (LeCun et al., 1990), but new developments in hardware, like parallel computing, have carry them to better levels.

A CNN is similar to a classical neural network, but with different kind of layers between the input (an image) and the output that are not fully connected. The hidden layers in CNNs are composed of several combinations of convolutional layers and pooling layers. After these group of layers, one or several fully connected layers are attached and connected to the output layer (Figure 1.19).

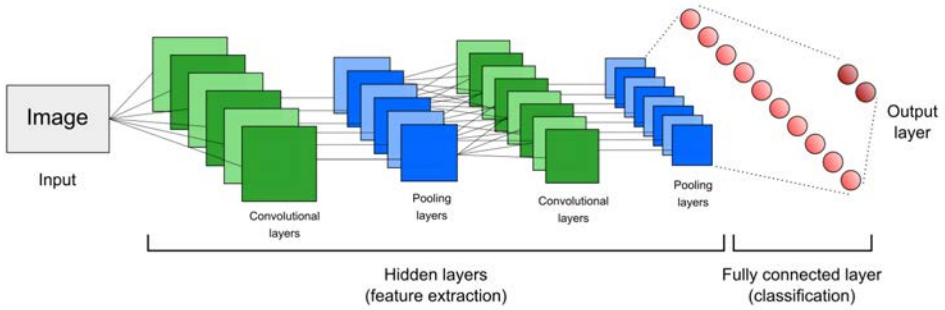

Figure 1.19: A CNN with two convolutional layers and two pooling layers used for features extraction from the input image. The last layer, a fully connected layer, perform the classification of the abstract features from the convolutional and pooling layers.

A convolutional layer contains a certain number of filters (kernel or con-

volutional matrix, used in digital image processing) that are connected to local zones in the image. The filters in the convolutional layers are responsible of automatically extracting features from the input image, whose size are reduced by the pooling layer. By adding more layers, the network is capable of extracting more information of the features, decomposing the image in smaller connected parts (features) that maximises the information for better classification rate. By iteration and backpropagation, the structure of the filters is modified to maximise the performance of the network.

In classical neural networks, the weights at each node are randomly initialised, and then adjusted by training. Nevertheless, this is not a common practice when using CNNs, where the filter values are not randomly generated at the beginning. It is usual to use a network that has been previously trained for image classification or object detection, being only necessary to make fine adjustments for the problem that needs to be solved (Yosinski et al., 2014). These pre-trained networks may have been built for the classification of common objects, like the ImageNet (Deng et al., 2009), AlexNet (Krizhevsky et al., 2012) or ZF Net (Zeiler and Fergus, 2014).

In agriculture, CNNs have recently been used for many applications. The huge potential of this kind of neural networks in computer vision has been employed for yield estimation in many crops. Sa et al. (2016) developed full fruit detection system based on RGB and NIR data and CNNs. The neural networks allowed for the retraining of the system to new fruits in an easy way by labelling new samples (images). Apple yield estimation was also possible from multi-geometry RGB images from an agricultural robot (Bargoti and Underwood, 2017). Results demonstrated that the improved segmentation performance with CNNs also translated to more accurate fruit detection when compared to other algorithms. Disease detection is an important application for which the use of CNNs is researched. Convolutional networks were used for visual pattern identification of different disease in leaf images (Mohanty et al., 2016), and were able to correctly classify 993 out of a thousand samples from 38 different classes. A similar approach was followed by Amara et al. (2017), that used thousands of RGB images for disease identification in banana leaves. Models were trained using CNNs, and they exhibit enough accuracy to consider them as a decision support tool to help farmers to identify the disease in their plants.

As exposed, CNNs have been massively used for image processing and computer vision, but the concept is not limited to this kind of input data. While the filters in the convolutional layers classically used are two-dimensional matrices, they can be adjusted to other dimensions in order to fit with different inputs. A recent PhD Thesis has studied how CNNs can be adapted to hyperspectral images (Windrim, 2018). The basic idea behind the proposed network is to, instead of convolving over the spatial dimension of the hyperspectral image, to perform the convolution over the spectral dimen-

sion (one image pixel, coded as a vector containing the reflectance values at each wavelength in the range). Therefore it is possible to take advantage of the potential of CNNs to extract all possible underlying relations from the spectra in an image.

1.6.4 Genetic algorithms

Genetic Algorithms (GAs) are metaheuristics methodologies that are based on natural selection of individuals depending on their adaptation (fitness) to the environment (Herrera et al., 1998). With the evolution in computing development, the first approximations of genetic algorithms were proposed by Fraser et al. (1970) and Crosby (1973), and several different strategies have been developed since. GAs are used in many applications in which parameter optimisation is required.

The basic concept of GAs is that a problem is coded so that each solution, a set of parameters (genes) that affects the result, is represented as an individual (a chromosome). A large set of individuals is defined and, through successive breeding and mutations in a iterative process, the best individuals are selected and passed to next generations. A GA requires for the problem to be defined as a function that, given a certain parameter set, returns a fitness value indicating how good that parameter set is for that problem. The fitness function should be deterministic, *i.e.,* it should always return the same value any time it is called with a specific set of input values. In general, a GA implements the following operators:

- **Initialisation:** A set of individuals (a generation) is generated and their parameters are randomly initialised.
- **Selection:** At each generation, several pair of individuals are selected for breeding. There are several kinds of selection methods, from random, to elitist selection (those individuals with the highest fitness values). There also are tournament methods in which the best individual from a reduced randomly subset is picked.
- **Mating or crossover:** Performed between two individuals from the selection step (the parents), it is used to generate one or more individuals that have genetic material (parameter values) randomly chosen from both parents. Selection and crossover is repeated a certain number of times at each generation to produce a sufficiently large offspring. There are also several types of crossing techniques (single-point, two-point, uniform crossover, etc.).
- **Mutation:** For each individual in the new offspring, one or many random parameters are selected for a mutation (a small change in the parameter) given a certain probability.

After a fixed number of generations (or any other stopping criterion), the best individual is selected from the last iteration, and it is considered as the best solution from the optimisation process.

GAs are very effective optimisation alternatives for those problems that cannot be coded into continuous, differentiable functions, for which other methodologies are more mathematically efficient, like gradient based approaches (Robbins and Monro, 1985). It should be noted that, because GAs are non-deterministic, stochastic methods, it is not assured that the best solution is found. They can get stuck in local maxima without improvements for many generations. For this reason, the tuning of the hyperparameters of the GA selected based on user's experience is a key aspect to achieve good results. A proper GA configuration should ideally reach high levels of both exploration—wide search in very different parameter spaces—and exploitation—deep search on a reduced parameter space to find the best solution in it.

In viticulture, GAs have been used for the optimisation of an neural network in grape bunch detection from RGB imaging (Behroozi-Khazaei and Maleki, 2017). Image segmentation was performed using colour features, selecting the best ANNs parameters with GAs. This work is a good example of the synergy that can exist between different AI techniques. Other agricultural applications make use of GAs. These were used by Arkeman et al. (2017) on satellite imagery for maximising economic factor and decrease environmental impact in agricultural practices. GAs also provided a key contribution for efficient irrigation management in Greece (Udias et al., 2018). The authors developed a decision support tool for soil and water assessment based on GA optimisation.

Chapter 2

Objectives

The main objective of this PhD Thesis is the development of innovative approaches through the combination of new artificial intelligence techniques and non-invasive sensing technologies for the assessment of relevant agronomical, physiological and qualitative traits in digital agriculture and viticulture].

The specific objectives achieved in this research work are:

- To make use of different machine learning algorithms on data from spectroscopy for in-field grapevine phenotyping and monitoring.
- The application of ensemble data analysis techniques for vineyard water status assessment with thermal imaging.
- To deploy hyperspectral imaging in the field, supported by intensive machine learning combinations, for the monitoring of different crop traits.

Chapter 3

Combining machine learning and spectroscopy for in-field grapevine monitoring

In this chapter, two published papers are presented on the use of spectroscopy for the in-field vineyard monitoring.

3.1 Machine learning for in-field grapevine varietal classification using a handheld spectrometer

Grapevine varietal classification demands slow, manual techniques like ampelography, that also relies on expert personnel. Although there are more recent methods for grapevine varietal classification, by using isoenzimes or genetic analysis,they are virtually impossible to be used under field conditions. With the advances and development in NIR spectroscopy and electronic miniaturisation, there are different industrial solutions for the spectral acquisition with portable devices. Along with sensor miniaturisation, the potential of ML algorithms, like ANNs and SVMs, opens new possibilities for the development of prediction models of a large number of grapevine varieties. The objective of the following paper was the use of a handheld NIR spectrometer for the in-field classification of 20 different grapevine varieties from three vineyards located at different regions and using data from two vintages. Additionally, the efficiency of ANNs and SVMs has been tested and compared for the classification task from leaf spectra. The results demonstrate that it is possible to develop accurate classification models for a high number of varieties with plants from a same zone and classification models for six varieties from three different vineyards. These outcomes open new paths in DV for the fast varietal identification under field conditions, an useful tool to several actors in viticulture and wine industry.

Overcome challenges

- To classify a high number of grapevine varieties using SVMs and ANNs.
- To use handheld spectroscopy under field conditions for phenotyping.
- To develop several classification models for a same zone (many varieties) or three different zones (at two vintages and phenological stages).

Paper information

- **Title of the publication**: Support Vector Machine and Artificial Neural Network Models for the Classification of Grapevine Varieties Using a Portable NIR Spectrophotometer
- **Authors:** Salvador Gutiérrez, Javier Tardáguila, Juan Fernández-Novales, María P. Diago
- **Published in:** PLOS ONE 10(11), e0143197
- **DOI:** 10.1371/journal.pone.0143197

Contributions of the PhD Thesis' author: The contribution of Salvador Gutiérrez was key at data analysis, machine learning modelling and statistical tests. Additionally, he wrote the full text at all stages in the review process.

PLOS | ONE

RESEARCH ARTICLE

Support Vector Machine and Artificial Neural Network Models for the Classification of Grapevine Varieties Using a Portable NIR Spectrophotometer

Salvador Gutiérrez, Javier Tardaguila, Juan Fernández-Novales, María P. Diago*

Instituto de las Ciencias de la Vid y del Vino, University of La Rioja, CSIC, Gobierno de La Rioja, Ctra. De Burgos Km. 6, 26007, Logroño, Spain

* mpaz.diago.santamaria@gmail.com

OPEN ACCESS

Citation: Gutiérrez S, Tardaguila J, Fernández-Novales J, Diago MP (2015) Support Vector Machine and Artificial Neural Network Models for the Classification of Grapevine Varieties Using a Portable NIR Spectrophotometer. PLoS ONE 10(11): e0143197. doi:10.1371/journal.pone.0143197

Editor: Monica Scali, Universita degli Studi di Siena, ITALY

Received: August 28, 2015

Accepted: November 2, 2015

Published: November 24, 2015

Data Availability Statement: Data are available at the following address: http://digital.csic.es/handle/10261/124880.

Funding: This work has received funding from the Spanish Ministry of Economy and Competitiveness (MINECO) under the INNGRAPE project (RTC-2014-3058-2).

Competing Interests: The authors have declared that no competing interests exist.

Abstract

The identification of different grapevine varieties, currently attended using visual ampelometry, DNA analysis and very recently, by hyperspectral analysis under laboratory conditions, is an issue of great importance in the wine industry. This work presents support vector machine and artificial neural network's modelling for grapevine varietal classification from in-field leaf spectroscopy. Modelling was attempted at two scales: site-specific and a global scale. Spectral measurements were obtained on the near-infrared (NIR) spectral range between 1600 to 2400 nm under field conditions in a non-destructive way using a portable spectrophotometer. For the site specific approach, spectra were collected from the adaxial side of 400 individual leaves of 20 grapevine (*Vitis vinifera* L.) varieties one week after veraison. For the global model, two additional sets of spectra were collected one week before harvest from two different vineyards in another vintage, each one consisting on 48 measurement from individual leaves of six varieties. Several combinations of spectra scatter correction and smoothing filtering were studied. For the training of the models, support vector machines and artificial neural networks were employed using the pre-processed spectra as input and the varieties as the classes of the models. The results from the pre-processing study showed that there was no influence whether using scatter correction or not. Also, a second-degree derivative with a window size of 5 Savitzky-Golay filtering yielded the highest outcomes. For the site-specific model, with 20 classes, the best results from the classifiers thrown an overall score of 87.25% of correctly classified samples. These results were compared under the same conditions with a model trained using partial least squares discriminant analysis, which showed a worse performance in every case. For the global model, a 6-class dataset involving samples from three different vineyards, two years and leaves monitored at post-veraison and harvest was also built up, reaching a 77.08% of correctly classified samples. The outcomes obtained demonstrate the capability of using a reliable method for fast, in-field, non-destructive grapevine varietal classification that could be very useful in viticulture and wine industry, either global or site-specific.

Introduction

The development of a fast and automatic procedure for grapevine varietal classification would bring a new valuable way in viticulture and wine industry due to the high economical and social impact of these businesses, offering new trends on vineyard monitoring and grape quality control.

Althought classic ampelometry [1] has been widely used for grapevine varietal identification by taking morphological differences between varieties into consideration, the necessity of human expert intervention makes virtually impossible its widespread utilization. Also, wet chemistry techniques based on isoenzymes [2] or DNA analysis [3–5] have been carried out. Still, these methods are labour and time-consuming, and not able to be performed under field conditions.

Near-infrared reflectance spectroscopy (NIRs) is a non-invasive technique, highly-suited analytical method for several agricultural applications due to its rapid data acquisition time, the capability of determining more than one parameter using the same measurement, and its easy fast usage and little sample preparation.

Spectroscopy has been previously applied for fruit composition assessment [6, 7]. Also, plant varietal discrimination has been accomplished using spectroscopy in crops such as wheat [8], bayberry [9], pear [10], tomato [11] and strawberry [12], using different organs. Recent studies have explored the use of leaf spectroscopy for grapevine varietal and clone identification using hyperspectral imaging under laboratory conditions throughout destructive methods [13, 14]. Also, these works used partial least squares discriminant analysis (PLS-DA) for the training of the models.

Machine learning techniques for the development of classification models are extensively applied in countless fields. Methods such as support vector machines (SVM) or artificial neural networks (ANN) have demonstrated their high reliability in the training of non-linear regression and classification models.

SVMs have arisen as very solid machine learning methods for supervised classification issues [15]. SVMs are kernel-based algorithms that transform data into a high-dimensional space and construct an hyperplane that maximizes the distance to the nearest data point of any of the input classes. Although SVM are originally designed to train binary classifiers, an extension for multiple classes is possible by reducing the multiclass problem into several binary classification ones, using *one-versus-all* or *one-versus-one* approaches. SVM models have been used for NIR varietal classification under laboratory conditions on sesame oil [16], waxy corn seed [17] or rice seed varieties [18].

ANN are machine learning models inspired on biological neural networks present in animal brains. The first approaches of the ANN concept was exposed by [19], and afterwards resurfaced with the introduction of the *error backpropagation* concept [20, 21]. ANN are formed by units named *processing elements* (PE) having similar behaviors than a biological neuron. Different functions—as data input, output, storage or forwarding—are distributed among all the PEs. The layout of a ANN is composed of a number of layers (one-layer or multi-layer designs) and a number of PE per layer. NIR varietal classification have been carried out using ANN models in tea plants [22] or herbal medicine [23].

Most studies have developed PLS-DA based models under laboratory conditions from NIR spectroscopy obtained through destructive methods. Also, these models were constructed using only a few number of varieties as classes. The importance of fast, in-field grapevine variety discrimination using a portable device could be crucial for viticulture and wine industry. Specially in viticulture—for nurseries, appellation boards or commercial vineyards—grapevine varietal classification is a matter of great interest, e.g., discrimination of unknown vines in

older vineyards, where it is usual the plantation of more than a single cultivar, or the recognition of not-allowed varieties in particular appellation regions.

The objective of this work was the classification of grapevine varieties using SVM and ANN models from in-field, portable and non-desctructive leaf NIR spectroscopy. Particularly, two approaches have been followed: the developing of a site-specific classification model for 20 grapevine varieties, comparing its performance vs a PLS-DA one; and the use of a dataset with samples from different vineyards, vintages and phenological stages for developing a global model that would cover samples from several sources.

Materials and Methods

Layout and experimental design

Site-specific model. The study was carried out on 12 August 2012 (one week after veraison) at a 1.43 ha commercial vineyard located in Vergalijo (Lat. 42° 27' 45.96", Long. 1° 48' 13.42", Alt. 325 m), Navarra, Spain, under permission of the owner of the vineyard plot. 20 grapevine (*Vitis vinifera* L.) varieties (Albariño, Cabernet Franc, Cabernet Sauvignon, Caladoc, Carmenere, Godello, Grenache, Malvasia, Marselan, Pedro Ximénez, Pinot Noir, Syrah, Tempranillo, Touriga Nacional, Treixadura, Verdejo, Viognier, Viura, White Grenache, White Tempranillo) were used in this study. Grapevines were trained to a vertically shoot-positioned trellis system, with North-South row orientation at 2 × 1 meters inter and intra row distances. Varieties were grafted on Richter 110 rootstock. Full irrigation was uniformly applied across the season for all varieties and these were well watered. The Relative Water Content (RWC) of leaves, measured following the method in [24], was maintained between 80% and 90% for all varieties.

Global model. Two additional sets of spectral measurements were acquired one week before harvest from two different vineyards, under permission of the manager and owner, located at the Rioja Regional Goverment's Experimental Vineyard (Logroño, Spain, Lat. 42° 26' 4.7", Long. 2° 30' 49.0", Alt. 480 m) on 23 September 2015 and Provedo Nurseries (Viana, Spain, Lat. 42° 27' 52.0", Long. 2° 23' 36.0", Alt. 371 m) on 1st October 2015 in order to test the behaviour and applicability of the model using samples from separated sites, vintages (samples for site-specific dataset were taken in 2012) and different stages of leaf development (August—after veraison—vs late September and October—harvest). For this model, six different varieties, grown in the three vineyard sites, were selected—Albariño, Grenache, Syrah, Tempranillo, Treixadura and Viura. At Rioja Government's Vineyard, grapevines were trained to a vertically shoot-positioned trellis system, with Northwest-Southeast row orientation at 3 × 1.2 meters inter and intra row distances. Varieties were grafted on Richter 110 rootstock. At Provedo Nurseries, grapevines were trained to a vertically shoot-positioned trellis system, with East-West row orientation at 3 × 1 meters inter and intra row distances. Varieties were grafted on Richter 110 rootstock. Full irrigation was uniformly applied across the season for all vineyard plots and grapevines were well watered.

Spectral measurement in the field

For the spectral acquisition, an integrated portable Near-infrared (NIR) spectral analyzer (microPHAZIR™, Thermo Fisher Scientific Inc., Waltham, MA, USA), working in reflectance mode (log1/*R*) in the range of 1600–2400 nm with an interval of 8.7 nm was used. Sensor integration time was 600 ms.

Spectral measurements were performed directly upon the adaxial surfaces of the leaves. For each leaf, five spectra were taken from different spots of the leaf blade. The mean of this five measurements was then considered as the average spectrum of the leaf. In every acquisition, the optical window of the NIR device was placed in direct contact with the surface of the leaf, making

sure that the sensor window was completely covered. To avoid the contamination of the adaxial surfaces with external pollutants, vinyl gloves were used at all times when handling the leaves.

For each one of the 20 varieties for the site-specific model, 10 vines and two adult leaves per vine of the mid-upper part of the shoot (nodes 6 to 12), a total of 20 leaves per variety, were selected and labeled with its variety name in order to be measured with a portable spectrometer device. Spectra were acquired under field conditions directly on the vine in a non-destructive way. A total of 400 leaves were measured.

For each one of the six varieties for the global model, four vines and two adult leaves per vine of the mid-upper part of the shoot (nodes 6 to 12), a total of eight leaves per variety, were selected and labeled with its variety name in each of the three vineyard plots sample. Spectra were acquired under field conditions directly on the vine in a non-destructive way. A total of 144 leaves (three places, six varieties per place, four vines per variety, two leaves per vine) were measured.

Spectral pre-processing and algorithms for modelling

The following pre-processing techniques and algorithms were used:

Scatter correction. Standard normal variate (SNV) followed by de-trending [25] [26] has been commonly used to remove the multiplicative interferences of scatter in the spectral signal. In SNV, average and standard deviation of all the data points are calculated individually for each spectrum. Then, the average value is substracted from the absorbance (zero-mean or centering) and the result is divided by the calculated standard deviation. De-trending subtracts from the data points a second degree least-squares fit polynomial calculated from the original data. Sometimes, no scatter correction is performed upon the raw spectra, hence two options for scatter correction were tested in this work: the application of SNV + De-trending (SNV+D) on the spectra before any other filtering, and the total omission of scatter correction (NoSNV+D).

Fig 1 plots, from the 400 samples, the average raw spectrum and the result of SNV + De-trending scatter correction.

Smoothing filtering. A lowpass smoothing filter that makes use of local least-squares polynomial approximation was developed in [27]. This method is able to preserve the shape,

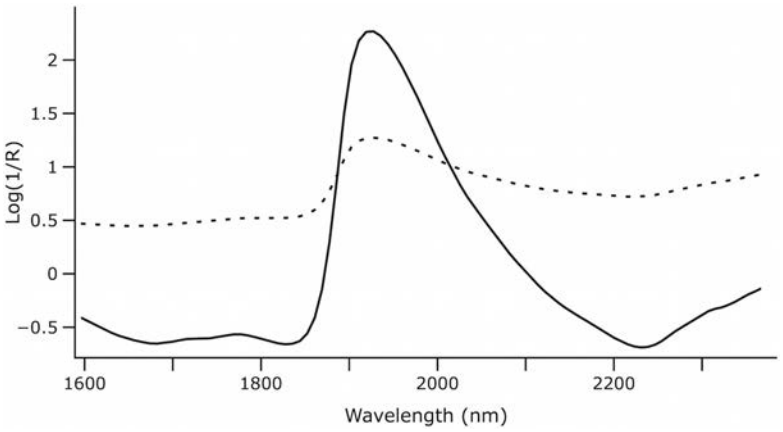

Fig 1. Average raw and pre-processed spectra with SNV+de-trending from the whole set of samples. Solid line: SNV+de-trending. Dashed line: Raw.

doi:10.1371/journal.pone.0143197.g001

height and width of waveform peaks. Savitzky-Golay filtering is usually followed by a first- or second-degree derivative. The smoothing is performed by using a moving window along the whole spectral signal. Typical values for this are in the range from 5 to 11, both included. In this work, the combination of two different derivative degrees (first-degree and second-degree) and two window sizes (5 and 11) were tested. So, four final parameter sets were defined for Savitzky-Golay filtering: first-degree derivative, window size 5 (D1W5); first-degree derivative, window size 11 (D1W11); second-degree derivative, window size 5 (D2W5); second-degree derivative, window size 11 (D2W11).

Classification algorithms. Two different machine learning classification algorithms (support vector machines and artificial neural networks) have been tested and compared with partial least squares discriminant analysis, widely used in spectroscopy. Sequential minimal optimization algorithm [28] working with a polynomial kernel was used in this study to train a SVM for varietal classification. Also, a multilayer perceptron was utilized as ANN classification method [29]. Partial least squares discriminant analysis (PLS-DA) has been extensively applied for classification problems, such as strawberry varieties [12], cooked ham quality [30], detection of expired vacuum-packed smoked salmon [31], Alpaca wool samples [32] or olive varietal identification [33]. PLS-DA expects to find a proper correlation of spectral variations and a set of defined classes. This is done by maximizing the covariance value between different class variables and rejecting variance within a class. In this study, PLS-DA models were trained with a maximum number of six latent variables and a uncertainty factor of 2.326.

For every one of the algorithms, the inputs were provided as the data points of the spectra (absorbance values of wavelengths 1600 nm to 2400 nm, with a step of 8.7 nm) and the classes were the identity labels of each variety.

One-way ANOVA was performed when comparing means for testing the influence of: (i) the application of a scatter correction method; (ii) the four Savitzky-Golay parameter values; (iii) the three classification algorithms and the interaction of the two previous factors. Tukey's range test was used as mean comparison method at a significance level $p = 0.05$.

Spectra pre-processing was done using the language and software environment *R*, version 3.1.3, and the additional packages *prospectr* [34] and *pracma* [35]. *Java Language Programming*, version 1.7, along with *Weka*, version 3.6, [36] were used for machine learning algorithms executions. PLS-DA models were developed using *WinISI* software package, version 1.5 (Infrasoft International, Port Matilda, PA, USA). Finally, statistical test were performed with *InfoStat* software (Córdoba, Argentina), version 2015.

Model training

A site-specific model for the classification of 20 varieties from the same vineyard plot was developed. In order to test the influence of the dataset population size in classifiers' behavior, two datasets were used for training and evaluating the machine learning models: 20 varieties (N = 20 varieties and n = 400 leaves) and a randomly selected subset of five varieties (N = 5 varieties and n = 100 leaves). An execution was performed for each one of the combination of datasets, with (SNV+D) and without (NoSNV+D) scatter correction, Savitzky-Golay filtering pretreatments (D1W5, D1W11, D2W5 and D2W11), algorithms (SVM and ANN) and their parameter sets (12 sets per algorithm), making a total of 384 executions. Due to the high number of samples (leaves), a *k*-fold with $k = 5$ was selected as Cross Validation method instead of the classic number of $k = 10$.

A global dataset with six varieties—24 leaves per variety—was built up using samples from the three vineyard plots all the measurements of this work were taken (Vergalijo 2012, Logroño and Viana 2015). The total number of samples was 144 (three places, six varieties per place,

eight leaves per variety). The same pre-processing algorithm and parameter set combinations were used as those employed for the site-specific model training, using again a 5-fold Cross Validation.

As previously mentioned, 12 parameter sets per machine learning algorithm have been used in order to test their influence in the classification results. These parameters are:

For SVM:

C: The trade-off between complexity of decision rule and frequency of error [15].

Exponent: The polynomial kernel exponent.

For ANN:

Hidden layer layout: The number of PEs present in the hidden layer of the network. *0*: no PEs (so, no hidden layer. Input PEs are directly connected to output PEs. No hidden layer layout can cast good results if the data is linearly separable). *a*: the number of PEs is the half of the sum of the number of attributes (inputs) and classes (outputs). *i*: the number of PEs is equal to the number of attributes. *o*: the number of PEs is equal to the number of classes.

Learning rate: It affects the speed that the minimum solution is reached by the ANN. Its value should be in the range [0, 1].

Momentum: It regulates the ANN capability of reaching a local minimum. The lower momentum value is set, the less likely the ANN converges to a local minimum (but more computational time will require). Its value must be in the range [0, 1].

The values used in this study for the above parameters are shown in Table 1.

A source code written in *Java* was developed for the automatic running of these combinations, taking a computation time of 5 hours and 45 minutes with the following hardware specifications: Intel Core i3, 2.93 GHz processor; 12.0 GB of RAM.

Table 1. Parameter sets for SVM and ANN algorithms.

	SVM		ANN		
	C	Exponent	Hidden Layer ‡	Learning Rate	Momentum
Parameter set 1	3.5	1	*0*	0.3	0.1
Parameter set 2	0.1	1	*0*	0.3	0.9
Parameter set 3	1	1	*0*	0.7	0.1
Parameter set 4	10	1	*a*	0.3	0.1
Parameter set 5	3.5	2	*a*	0.3	0.9
Parameter set 6	0.1	2	*a*	0.7	0.1
Parameter set 7	1	2	*i*	0.3	0.1
Parameter set 8	10	2	*i*	0.3	0.9
Parameter set 9	3.5	3	*i*	0.7	0.1
Parameter set 10	0.1	3	*o*	0.3	0.1
Parameter set 11	1	3	*o*	0.3	0.9
Parameter set 12	10	3	*o*	0.7	0.1

‡*0*: no processing elements (PEs) in hidden layer; *a*: PEs = (#attributes + #classes)/2; *i*: PEs = #attributes; *o*: PEs = #classes.
SVM: Support Vector Machine; ANN: Artificial Neural Network.

doi:10.1371/journal.pone.0143197.t001

Table 2. Comparison of means of percentage of correctly classified leaves for signal scatter correction attending to the algorithm used for N = 20 and N = 5 datasets.

Number of varieties	Scatter correction	PLS-DA	SVM	ANN
N = 20	**SNV+D**	44.8	75.8	78.4
	NoSNV+D	47.2	75.1	77.9
	significance	*n.s.*	*n.s.*	*n.s.*
N = 5	**SNV+D**	76.5	87.9 *a*	87.1
	NoSNV+D	75.8	85.1 *b*	86.7
	significance	*n.s.*	* *	*n.s.*

n.s.: not significant ($p \geq 0.05$); * *: $p < 0.01$; (Tukey's range test at a significance level $p = 0.05$). SNV+D: Standard Normal Variate followed by De-trending; PLS-DA: Partial Least Squares Discriminant Analysis; SVM: Support Vector Machine; ANN: Artificial Neural Network.

doi:10.1371/journal.pone.0143197.t002

Results

The influence of scatter correction, algorithms, and smoothing filtering was statistically tested with the dataset acquired for the site-specific mode.

Influence of scatter correction

Table 2 shows the mean comparison of the percentage of correctly classified grapevine leaves according to their variety for each algorithm when the scatter correction pre-processing was applied or omitted. For almost every case, the use of scatter correction had no statistical influence in the correctly classified percentage obtained, regardless of the algorithm. Only in the reduced dataset (N = 5), the application of SNV + De-trending performed significantly better when the SVM was used as classifier.

Influence of algorithms and Savitzky-Golay filters

Table 3 shows the comparison of means of correctly classified percentages attending to the algorithms and Savitzky-Golay pre-processing. Although there was a common and logical

Table 3. Correctly classified percentages of grapevine leaves for each Savitzky-Golay filter and algorithm combination for N = 20 and N = 5 number of varieties.

Number of varieties	Savitzky-Golay filter	PLS-DA	SVM	ANN	significance
N = 20	**D1W5**	45.3 B	77.5 A *a*	81.2 A *b*	* * *
	D1W11	44.4 B	69.7 A *b*	67.3 A *c*	* * *
	D2W5	51.0 B	78.0 A *a*	84.3 A *a*	* * *
	D2W11	43.2 B	76.7 A *a*	79.8 A *b*	* * *
	significance	*n.s.*	* *	* * *	
N = 5	**D1W5**	81.5 *a*	87.8 *b*	88.0 *b*	*n.s.*
	D1W11	72.5 B *b*	79.3 A *c*	81.0 A *c*	*
	D2W5	84.5 B *a*	91.2 A *a*	91.6 A *a*	* * *
	D2W11	66.0 B *c*	87.8 A *b*	86.9 A *b*	* * *
	significance	* *	* * *	* * *	

The values shown are the varieties correctly classified percentage. Each value is, in turn, the average of the results obtained using and not using scatter correction and, for SVM and ANN, the 12 parameter sets.

PLS-DA: Partial Least Squares Discriminant Analysis; SVM: Support Vector Machine; ANN: Artificial Neural Network.

Uppercase and italic lowercase letters attend respectively to row-wise (comparison among algorithms) and column-wise (comparison among Savitzky-Golay filters) values comparison. *n.s.*: not significant ($p \geq 0.05$); *: $p < 0.05$; * *: $p < 0.01$; * * *: $p < 0.001$.

doi:10.1371/journal.pone.0143197.t003

widespread worse response from the algorithms when the number of varieties to be classified is noticeably large, the SVM and ANN classifiers still achieved very good results for N = 20. When—for these two algorithms—the correctly classified percentages reached excellent numbers with N = 5 (values moving between 79.3% and 91.6%), this remarkable behaviour remained with a slight degradation when the number of classes was four times greater (correctly classified percentage values between 67.3% and 84.3%).

As it can be seen, both ANN and SVM algorithms performed widely better than PLS-DA. Though this classifier obtained notable results in the reduced dataset, the increase of the number of varieties heavily degraded the output of the algorithm, barely reaching the 50% correctly classified mark (Table 3).

The results in Table 3 show that the best behaviour was generally yielded by ANN, achieving up to an average of 84.3% correctly classified instances for N = 20 and 91.6% for N = 5. Statistical tests displayed that in every case, the use of ANN or SVM casts significantly better outputs than PLS-DA, demonstrating the high suitability and surpassing response from the two machine learning classifiers vs PLS-DA. The interaction of the algorithm and the Savitzky-Golay configuration was calculated for both N = 20 and N = 5 through statistical tests. For the first dataset, the test showed that the interaction of both factor was significant at $p < 0.05$. For N = 5 dataset the interaction was significant at $p < 0.01$. If the ANOVA was performed only for SVM and ANN (ignoring the PLS-DA results), a p-value of 0.024 for N = 20 and 0.649 for N = 5 (not shown in the table) was obtained. Thus, while in the first case the use of ANN was significantly better (*) with regard to SVM, for N = 5 there was no significantly difference (*n.s.*) in using any algorithm.

Regarding the four different Savitzky-Golay configurations, statistical tests showed that the parameter values selection for this pre-processing filter was significantly influential in the final output, except for PLS-DA algorithm having N = 20. Also, Table 3 displays that, in every one of the cases, the Savitzky-Golay configuration with higher correctly classified percentage was a second-degree derivative with a window size of 5 (D2W5). It is likewise consistent that the second best configuration fell upon a first-derivative and window size 5 Saviztky-Golay filtering (D1W5). Using a window size of 11 returned the worst outcomes for every algorithm, so it was an avoidable choice for this study (Table 3).

Site-specific grapevine variety classification

From the 192 executions for N = 20, the best result (the one with the highest correctly classified percentage) was obtained with the following configuration: ANN, SNV+D, D2W5, parameter set 10 (Fig 2 shows, for the 400 leaf samples, the average raw and processed spectra using the pre-processing from this combination). The overall correctly classified percentage was 87.25 (349 out of 400 samples properly classified) and the confusion matrix of this configuration is shown in Table 4.

Three varieties (Cabernet Franc, Cabernet Sauvignon and Touriga Nacional) achieved a perfect score, while six ones reached excellent results (percentage of correct classification greater than 90%): Albariño, Treixadura, Viognier, Grenache, Carmenere and Caladoc. Seven varieties obtained good results in their classification (greater or equal than 75% and less or equal than 90%): Viura, Godello, White Grenache, White Tempranillo, Pedro Ximénez, Syrah, Tempranillo and Pinot Noir. Finally, the three varieties with worst result (less than 75%) were Verdejo, Malvasia and Marselan. The classification of the Verdejo leaves resulted in a moderate output, with a 50% of correctly classified samples. From these 10 misclassified instances, three were predicted as Viura and two as Tempranillo. For Malvasia, the majority of the misclassified samples were also assigned to the Viura class.

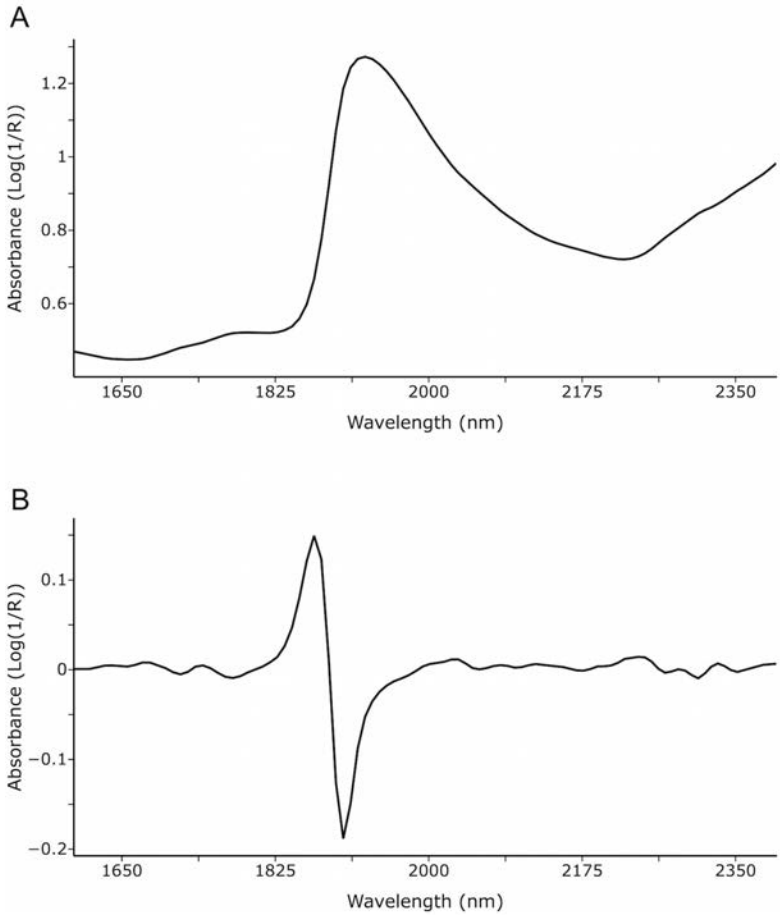

Fig 2. Average raw (A) and processed spectra (B) with SNV+de-trending+Savitzky-Golay filter (second-degree derivative, window size 5) from all samples.

doi:10.1371/journal.pone.0143197.g002

Global variety classification

From the 6-class global dataset model involving samples from different vineyards, vintages and phenological stages, the outcome with the highest correctly classified percentage was achieved with the following combination: ANN, NoSNV+D, D2W5, parameter set 6; reaching an overall result of 77.08% of correctly classified samples (111 out of 144). Table 5 shows the confusion matrix of this model.

Individually, the best classification results were obtained for Tempranillo and Grenache varieties, with a 91.7% and 87.5% correctly classified score respectively. Nonetheless, two varieties—Viura and Syrah—obtained a more modest score of correctly classified percentage, below the 70% mark in both cases.

Table 4. Confusion matrix from the execution with the best score (ANN, SNV+D, D2W5 and parameter set 10) with an overall correctly classified value of 87.25% (20 leaves per variety).

	Classified as																				
	Ve	M	V	A	T	G	WG	WT	PX	Vi	CF	Gr	CS	C	S	Te	PN	Ca	Ma	TN	%
Ve	**10**	1	3	0	0	1	1	1	0	0	1	0	0	0	0	2	0	0	0	0	50
M	0	**14**	5	0	0	0	0	0	0	0	0	0	0	0	1	0	0	0	0	0	70
V	1	3	**15**	0	1	0	0	0	0	0	0	0	0	0	0	0	0	0	0	0	75
A	0	0	0	**19**	0	0	0	0	0	1	0	0	0	0	0	0	0	0	0	0	95
T	0	0	0	0	**19**	0	0	0	0	0	0	0	0	0	0	0	1	0	0	0	95
G	0	0	0	0	0	**18**	1	0	0	0	0	0	0	0	0	0	1	0	0	0	90
WG	0	0	0	0	0	0	**16**	0	0	1	0	2	0	0	0	0	0	0	0	1	80
WT	0	0	0	0	0	1	0	**17**	0	0	0	0	0	1	0	0	0	0	0	1	85
PX	0	0	1	0	0	0	0	0	**18**	1	0	0	0	0	0	0	0	0	0	0	90
Vi	0	0	0	0	0	0	0	0	0	**19**	0	0	0	0	1	0	0	0	0	0	95
CF	0	0	0	0	0	0	0	0	0	0	**20**	0	0	0	0	0	0	0	0	0	100
Gr	0	0	0	0	0	0	0	0	0	0	1	**19**	0	0	0	0	0	0	0	0	95
CS	0	0	0	0	0	0	0	0	0	0	0	0	**20**	0	0	0	0	0	0	0	100
C	0	0	0	1	0	0	0	0	0	0	0	0	0	**19**	0	0	0	0	0	0	95
S	0	0	0	0	0	0	0	0	0	0	1	0	1	0	**18**	0	0	0	0	0	90
Te	0	0	0	0	0	0	1	1	0	0	0	0	0	0	0	**17**	1	0	0	0	85
PN	0	1	0	0	0	0	0	0	0	0	0	0	0	0	0	0	**18**	0	1	0	90
Ca	0	0	0	0	0	0	0	0	0	0	0	1	0	0	0	0	0	**19**	0	0	95
Ma	0	1	0	0	0	0	0	0	0	1	0	1	0	0	1	0	2	0	**14**	0	70
TN	0	0	0	0	0	0	0	0	0	0	0	0	0	0	0	0	0	0	0	**20**	100

Each row represents the actual variety and in which one was classified. Bolded values (diagonal of the matrix) are the number of samples properly classified. The last column shows the correctly classified percentage for each variety.

ANN: Artificial Neural Network; SNV+D: Standard Normal Variate followed by De-trending; D2W5: Second-degree derivative and window size 5 Savitzky-Golay filter.

Ve: Verdejo; M: Malvasia; V: Viura; A: Albariño; T: Treixadura; G: Godello; WG: White Grenache; WT: White Tempranillo; PX: Pedro Ximénez; Vi: Viognier; CF: Cabernet Franc; Gr: Grenache; CS: Cabernet Sauvignon; C: Carmenere; S: Syrah; Te: Tempranillo; PN: Pinot Noir; Ca: Caladoc; Ma: Marselan; TN: Touriga Nacional.

doi:10.1371/journal.pone.0143197.t004

Discussion

The present work has shown the possibility of grapevine varietal classification using a portable NIR spectrophotometer in the field along with SVM and ANN models. 20 different grapevine varieties were classified with an overall correct classification percentage of 87.25% in a site-specific approach. Similar recent studies such as [13] or [14] also reached high percentages in varietal (93.53%) and clone (98.8%) discrimination. Nevertheless, in [13], hyperspectral imaging was conducted with a camera operating between 380 nm and 1028 nm under laboratory conditions on leaf discs. The PLS-DA models obtained in [13] were trained for the discrimination of three grapevine varieties and resulted, for every one of then, in correctly classification percentages over 92%. Although a lower overall percentage was obtained in the present work (87.25%), it is important to highlight the fact that this result was achieved from training a model with 20 classes under field conditions. Only less than five points were lost when using a classifier that had more than six times the number of classes in [13]. Additionally, attention must be drawn to the fact that the present study achieved the grapevine classification goal using NIR measurements acquired under field conditions with a portable device, while in [13]

Table 5. Confusion matrix from the global dataset execution with the best score (ANN, NoSNV+D, D2W5 and parameter set 6) with an overall correctly classified value of 77.08% (24 leaves per variety).

	Classified as						
	V	Gr	T	Te	S	A	%
V	**15**	1	3	0	1	4	62.5
Gr	0	**21**	0	2	1	0	87.5
T	0	0	**22**	1	0	1	91.7
Te	1	3	1	**17**	2	0	70.8
S	1	0	0	6	**16**	1	66.7
A	0	0	1	0	3	**20**	83.3

Each row represents the actual variety and in which one was classified. Bolded values (diagonal of the matrix) are the number of samples properly classified. The last column shows the correctly classified percentage for each variety.

ANN: Artificial Neural Network; NoSNV+D: No application of Standard Normal Variate followed by De-trending; D2W5: Second-degree derivative and window size 5 Savitzky-Golay filter.

V: Viura; Gr: Grenache; T: Treixadura; Te: Tempranillo; S: Syrah; A: Albariño.

doi:10.1371/journal.pone.0143197.t005

hyperspectral imaging was performed using a camera under laboratory conditions and having full control of illumination status.

The discrimination and classification of grapevine varieties using in-field NIR spectroscopy can be feasible as ated in this work. The variation in spectral properties in relation to leaf biochemical composition and structure, which depends on many factors like the plant species, the developmental or microclimate position of the leaf on the plant [37], have been outlined as potent factors causing this spectra differentiation. Still, the leaf water content can be an influence due to the fact that the absorption band of water can be found at 1940 nm. However, in this work the differences in water content have not driven the discrimination of leaves according to their variety, as special care was paid to measure only leaves with RWC marks between 80% and 90%.

In regard to spectra pretreatments (scatter correction and smoothing filtering), [38] remarked that selection of suitable spectral pre-treatment is not easy, due to the strong likelihood of several different mathematical transformation being used. The selection of the best pre-treatment for spectra analysis must be based on the combination of statistical testing and the modeller's judgement [39]. Several factors can affect the results of applying different spectral pre-processing methods, ranging from sample nature to light conditions or spectra acquisition device's status, etc, so the fact that SNV followed by de-trending and a second-degree derivative, window size 5 Savitzky-Golay filter cast the best classification marks would not assure this behaviour will maintain in other plant varietal discrimination problems.

In every case, SVM and ANN outperformed PLS-DA, whether five or 20 classes were used in the training. PLS-DA extracts the principal components from the whole set of wavelengths, by linear combinations of them, and ranking them depending on the more explained variance. The fact that SVMs and ANNs develop non-linear models and the complete set of wavelength values are used may be the cause of this better performance (e.g., the training process of an artificial neural network already penalizes those input variables less useful in the discrimination goal); this was more clear when comparing the N = 20 models. Although ANN performed better than SVM in almost every case, the lack of statistical significance between their scores allows to affirm that both of them could be used for this type of varietal discrimination purposes.

The outcomes the global method have thrown support the applicability of ANN for a multi-vineyard, vintage and phenological stage grapevine varietal discrimination. Despite the lower score obtained from the global vineyard dataset, 77.08%, versus the one achieved by the site-specific dataset, 87.25%, these results accomplished the classification goal with a high level of satisfaction, specially when taking into account that the model contemplated samples from different vineyards, seasons and leaf age, according to different phenological stages. Divergences were found regarding the pre-processing and parameter set combination with the best scores for site-specific and global datasets. While the algorithm (ANN) and smoothing filtering (D2W5) remained the same for both, not applying SNV and de-trending worked better in the global dataset, unlike the original one, where this scatter correction method gave a better response. This behavior could be a consequence of the differences in phenological stages and vineyards' places at which the spectral measurements were acquired, given that leaf's maturity is influenced by the time of year, and phenotype is affected by the physiology and field environment of the grapevine [40–42]. A scatter correction step might hide the spectral representation of these phenomena. Still, as previously discussed, the use of SNV and de-trending showed no statistical influence in the results, so the divergence related to the employment of this scatter correction procedure brought no big issue. The same applies for the ANN parameter set, where the original dataset responded better with a different one (parameter set 10) than the global dataset (parameter set 6). The minor particularities of the Multilayer Perceptron ANN implementation (such as the concrete values of the configuration parameters) are always very influenced by the input data and experimenter criteria, and could not be generalized.

The high marks obtained in the present work by both studied datasets, attending specially to the large number of classes for the site-specific model and the significant heterogeneity for the global one, opens several ways of direct application for viticulture and wine industry, including precision viticulture, if spectral data are georeferenced. In addition to the novelty of the spectral range and the high number of classes discriminated, it is worth highlighting that the spectra used in this study were acquired in the field, where illumination conditions are far from being stable. ANNs have demonstrated a notable accuracy for both potential applications of: a vineyard-specialized varietal classification, e.g., given vineyard plots sharing environmental, climatic and seasonal features (as evidenced by the 20-class model); and the global and generalized classification of vineyards from heterogeneous sources (different sites, vintages and phenological stages), such as those found in a whole region or territory. But this reliability is not the only valuable feature of this method: the easy usage because of its fast, portable and non-destructive nature makes the present grapevine varietal discrimination approach prone for direct in-field applicability by commercial vineyards, nurseries, appellation boards, among others. The remarkable performance of the developed model under field conditions paves the way for the use of this type of portable NIR analyses as powerful phenotyping tools in viticulture and other crops.

Conclusions

The present study proposes a new classification method for the classification of grapevine varieties from in-field leaf NIR spectroscopy acquired through non-destructive methods. Modelling was approached in two ways: training the classifier with leaves from 20 varieties—building a site-specific model—and leaves from different vineyards, vintages and stages of development—building a global model. Support Vector Machines and Artificial Neural Networks showed a high reliability in the creation of grapevine leaf varietal classification models from in-field NIR spectroscopy using non-destructive data acquisition. The accuracy showed by both site-specific models, specially when the number of classes was high, along with the ability of properly train

the model from heterogeneous sources, allows to consider this NIR range suitable for in-field grapevine varietal discrimination.

The classification results cast by the trained models open a new window in viticulture and wine industry, specially due to its portable and non-destructive nature, allowing the fast and in-field discrimination of a high number of grapevine varieties.

Acknowledgments

This work has received funding from the Spanish Ministry of Economy and Competitiveness (MINECO) under the INNGRAPE project (RTC-2014-3058-2). The authors want to thank Vitis Navarra S.L. (Larraga, Navarra, Spain) and Viveros Provedo S.A. (Logroño, La Rioja, Spain) for providing the vineyards to carry out this study.

Special thanks to Victor Sicilia and Teresa Díaz for their help in the vineyard during data acquisition.

Author Contributions

Conceived and designed the experiments: MPD JT. Performed the experiments: MPD. Analyzed the data: SG JFN. Contributed reagents/materials/analysis tools: JT. Wrote the paper: SG JT JFN MPD.

References

1. Galet P. A practical ampelography. Cornell University Press.; 1979.
2. Altube H, Cabello F, Ortiz JM. Caracterización de variedades y portainjertos de vid mediante isoenzimas de los sarmientos. Vitis. 1991; 30(4):203–212.
3. Sefc KM, Lefort F, Grando MS, Scott KD, Steinkellner H, Thomas MR. Microsatellite markers for grapevine: a state of the art. In: Molecular Biology & Biotechnology of the Grapevine; 2001. p. 433–463. doi: 10.1007/978-94-017-2308-4_17
4. Borrego J, De Andrés MT, Gómez JL, Ibáñez J. Genetic study of Malvasia and Torrontes groups through molecular markers. American Journal of Enology and Viticulture. 2002; 53(2):125–130.
5. Pelsy F, Hocquigny S, Moncada X, Barbeau G, Forget D, Hinrichsen P, et al. An extensive study of the genetic diversity within seven French wine grape variety collections. Theoretical and Applied Genetics. 2010; 120(6):1219–1231. doi: 10.1007/s00122-009-1250-8 PMID: 20062965
6. Fernández-Novales J, López MI, Sánchez MT, García-Mesa JA, González-Caballero V. Assessment of quality parameters in grapes during ripening using a miniature fiber-optic near-infrared spectrometer. International Journal of Food Sciences and Nutrition. 2009; 60(sup7):265–277. doi: 10.1080/09637480903093116 PMID: 19626519
7. Pérez-Marín D, Paz P, Guerrero JE, Garrido-Varo A, Sánchez MT. Miniature handheld NIR sensor for the on-site non-destructive assessment of post-harvest quality and refrigerated storage behavior in plums. Journal of Food Engineering. 2010; 99(3):294–302. doi: 10.1016/j.jfoodeng.2010.03.002
8. Wang W, Paliwal J. Spectral data compression and analyses techniques to discriminate wheat classes. Transactions of the ASABE. 2006; 49(5):1607–1612. doi: 10.13031/2013.22035
9. Li X, He Y, Fang H. Non-destructive discrimination of Chinese bayberry varieties using Vis/NIR spectroscopy. Journal of Food Engineering. 2007; 81(2):357–363. doi: 10.1016/j.jfoodeng.2006.10.033
10. Fu X, Zhou Y, Ying Y, Lu H, Xu H. Discrimination of pear varieties using three classification methods based on near-infrared spectroscopy. Transactions of the ASABE. 2007; 50(4):1355–1361. doi: 10.13031/2013.23613
11. Xu HR, Yu P, Fu XP, Ying YB. On-site variety discrimination of tomato plant using visible-near infrared reflectance spectroscopy. Journal of Zhejiang University Science B. 2009; 10(2):126–132. doi: 10.1631/jzus.B0820200 PMID: 19235271
12. Sánchez MT, De la Haba MJ, Benítez-López M, Fernández-Novales J, Garrido-Varo A, Pérez-Marín D. Non-destructive characterization and quality control of intact strawberries based on NIR spectral data. Journal of Food Engineering. 2012; 110(1):102–108. doi: 10.1016/j.jfoodeng.2011.12.003
13. Diago MP, Fernandes AM, Millan B, Tardaguila J, Melo-Pinto P. Identification of grapevine varieties using leaf spectroscopy and partial least squares. Computers and Electronics in Agriculture. 2013; 99:7–13. doi: 10.1016/j.compag.2013.08.021

14. Fernandes AM, Melo-Pinto P, Millan B, Tardaguila J, Diago MP. Automatic discrimination of grapevine (Vitis vinifera L.) clones using leaf hyperspectral imaging and partial least squares. The Journal of Agricultural Science. 2015; 153(03):455–465. doi: 10.1017/S0021859614000252

15. Cortes C, Vapnik V. Support-vector networks. Machine Learning. 1995; 20(3):273–297. doi: 10.1023/A:1022627411411

16. Xie C, Wang Q, He Y. Identification of Different Varieties of Sesame Oil Using Near-Infrared Hyperspectral Imaging and Chemometrics Algorithms. PLOS ONE. 2014; 9(5):e98522. doi: 10.1371/journal.pone.0098522 PMID: 24879306

17. Yang X, Hong H, You Z, Cheng F. Spectral and Image Integrated Analysis of Hyperspectral Data for Waxy Corn Seed Variety Classification. Sensors. 2015; 15(7):15578–15594. doi: 10.3390/s150715578 PMID: 26140347

18. Kong W, Zhang C, Liu F, Nie P, He Y. Rice seed cultivar identification using near-infrared hyperspectral imaging and multivariate data analysis. Sensors. 2013; 13(7):8916–8927. doi: 10.3390/s130708916 PMID: 23857260

19. McCulloch WS, Pitts W. A logical calculus of the ideas immanent in nervous activity. The Bulletin of Mathematical Biophysics. 1943; 5(4):115–133. doi: 10.1007/BF02478259

20. Werbos P. Beyond regression: New tools for prediction and analysis in the behavioral sciences. PhD Thesis. 1974;.

21. Rumelhart DE, Hinton GE, Williams RJ. Learning representations by back-propagating errors. Nature. 1986; 323(6088):533–536. doi: 10.1038/323533a0

22. Li X, He Y. Discriminating varieties of tea plant based on Vis/NIR spectral characteristics and using artificial neural networks. Biosystems Engineering. 2008; 99(3):313–321. doi: 10.1016/j.biosystemseng.2007.11.007

23. Yang CW, Chen S, Ouyang F, Yang IC, Tsai CY. A robust identification model for herbal medicine using near infrared spectroscopy and artificial neural network. Journal of Food and Drug Analysis. 2011; 19(1).

24. Barrs HD, Weatherley PE. A re-examination of the relative turgidity technique for estimating water deficits in leaves. Australian Journal of Biological Sciences. 1962; 15(3):413–428.

25. Barnes RJ, Dhanoa MS, Lister SJ. Standard Normal Variate Transformation and De-trending of Near-Infrared Diffuse Reflectance Spectra. Applied Spectroscopy. 1989; 43(5):772–777. doi: 10.1366/0003702894202201

26. Dhanoa MS, Lister SJ, Barnes RJ. On the scales associated with near-infrared reflectance difference spectra. Applied Spectroscopy. 1995; 49(6):765–772. doi: 10.1366/0003702953964615

27. Savitzky A, Golay MJE. Smoothing and differentiation of data by simplified least squares procedures. Analytical Chemistry. 1964; 36(8):1627–1639. doi: 10.1021/ac60214a047

28. Platt J. Sequential minimal optimization: A fast algorithm for training support vector machines. Technical Report MSR-TR-98-14, Microsoft Research. 1998;.

29. Hornik K, Stinchcombe M, White H. Multilayer feedforward networks are universal approximators. Neural Networks. 1989; 2(5):359–366. doi: 10.1016/0893-6080(89)90020-8

30. Talens P, Mora L, Morsy N, Barbin DF, ElMasry G, Sun DW. Prediction of water and protein contents and quality classification of Spanish cooked ham using NIR hyperspectral imaging. Journal of Food Engineering. 2013; 117(3):272–280. doi: 10.1016/j.jfoodeng.2013.03.014

31. Ivorra E, Girón J, Sánchez AJ, Verdú S, Barat JM, Grau R. Detection of expired vacuum-packed smoked salmon based on PLS-DA method using hyperspectral images. Journal of Food Engineering. 2013; 117(3):342–349. doi: 10.1016/j.jfoodeng.2013.02.022

32. Canaza-Cayo AW, Cozzolino D, Alomar D, Quispe E. A feasibility study of the classification of Alpaca (Lama pacos) wool samples from different ages, sex and color by means of visible and near infrared reflectance spectroscopy. Computers and Electronics in Agriculture. 2012; 88:141–147. doi: 10.1016/j.compag.2012.07.013

33. Vanloot P, Bertrand D, Pinatel C, Artaud J, Dupuy N. Artificial vision and chemometrics analyses of olive stones for varietal identification of five French cultivars. Computers and Electronics in Agriculture. 2014; 102:98–105. doi: 10.1016/j.compag.2014.01.009

34. Stevens A, Ramirez-Lopez L. An introduction to the prospectr package; 2013. R package version 0.1.3.

35. Borchers HW. pracma: Practical Numerical Math Functions; 2015. R package version 1.8.3.

36. Hall M, Frank E, Holmes G, Pfahringer B, Reutemann P, Witten IH. The WEKA Data Mining Software: An Update. SIGKDD Explorations. 2009; 11(1):10–18. doi: 10.1145/1656274.1656278

37. Jacquemoud S, Ustin SL. Leaf optical properties: A state of the art. In: 8th International Symposium of Physical Measurements & Signatures in Remote Sensing; 2001. p. 223–332.

38. Fernández-Cabanás VM, Garrido-Varo A, Pérez-Marín D, Dardenne P. Evaluation of pretreatment strategies for near-infrared spectroscopy calibration development of unground and ground compound feedingstuffs. Applied Spectroscopy. 2006; 60(1):17–23. doi: 10.1366/000370206775382839 PMID: 16454905

39. Delwiche SR, Reeves JB. The effect of spectral pre-treatments on the partial least squares modelling of agricultural products. Journal of Near Infrared Spectroscopy. 2004; 12:177–182. doi: 10.1255/jnirs.424

40. Sultan SE. Phenotypic plasticity for plant development, function and life history. Trends in Plant Science. 2000; 5(12):537–542. doi: 10.1016/S1360-1385(00)01797-0 PMID: 11120476

41. Nicotra AB, Atkin OK, Bonser SP, Davidson AM, Finnegan EJ, Mathesius U, et al. Plant phenotypic plasticity in a changing climate. Trends in Plant Science. 2010; 15(12):684–692. doi: 10.1016/j.tplants.2010.09.008 PMID: 20970368

42. Pélabon, Osler NC, Diekmann M, Graae BJ. Decoupled phenotypic variation between floral and vegetative traits: distinguishing between developmental and environmental correlations. Annals of botany. 2013; 111(5):935–944. doi: 10.1093/aob/mct050 PMID: 23471008

3.2 Machine learning for grapevine phenotyping under field conditions from a handheld spectrometer

Demonstrated the effectiveness of handheld NIR spectroscopy, the next published work was focused on its use for the non-destructive, fast grapevine phenotyping by ML techniques, specifically, for varietal classification or vineyard water status assessment from a single spectral signal. Plant water status monitoring has been always carried out using time-consuming, destructive methods, that carry limitations. The combination of NIR spectroscopy with different ML techniques was the goal of the experiments published in the following article. Classification results showed precise validation values, while water status regression models also yielded accurate predictions. These results show the great strength of portable NIR spectroscopy for the phenotyping of two important vineyard features from the same spectral measurement, for a fast, in-field vineyard monitoring.

Overcome challenges

- The in-field use of portable spectroscopy for two different grapevine phenotyping tasks.
- To predict the plant water status in the vineyard using NIR spectroscopy.
- To develop complex ML models using ensemble algorithms.

Paper information

- **Title of the publication**: Data Mining and NIR Spectroscopy in Viticulture: Applications for Plant Phenotyping under Field Conditions
- **Authors:** Salvador Gutiérrez, Javier Tardáguila, Juan Fernández-Novales, María P. Diago
- **Published in:** Sensors 16(2), 236
- **DOI:** 10.3390/s16020236

Contributions of the PhD Thesis' author: Salvador Gutiérrez performed all the data pre-processing, analysis and machine learning modelling. He also wrote the full text of the paper during all review stages.

sensors

MDPI

Article

Data Mining and NIR Spectroscopy in Viticulture: Applications for Plant Phenotyping under Field Conditions †

Salvador Gutiérrez, Javier Tardaguila, Juan Fernández-Novales and Maria P. Diago *

Instituto de Ciencias de la Vid y del Vino (University of La Rioja, CSIC, Gobierno de La Rioja) Ctra. De Burgos Km, 6, 26007 Logroño, Spain; salvador.gutierrez@unirioja.es (S.G.); javier.tardaguila@unirioja.es (J.T.); juan.fernandezn@unirioja.es (J.F.-N.)

* Correspondence: mpaz.diago.santamaria@gmail.com; Tel.: +34-94-189-4980 (ext.410065); Fax: +34-94-189-9728

† This paper is an extended version of our paper published in Proceedings of the 2nd International Electronic Conference on Sensors and Applications, online, 15–30 November 2015.

Academic Editor: Dirk Lehmhus
Received: 2 December 2015; Accepted: 4 February 2016; Published: 16 February 2016

Abstract: Plant phenotyping is a very important topic in agriculture. In this context, data mining strategies may be applied to agricultural data retrieved with new non-invasive devices, with the aim of yielding useful, reliable and objective information. This work presents some applications of machine learning algorithms along with in-field acquired NIR spectral data for plant phenotyping in viticulture, specifically for grapevine variety discrimination and assessment of plant water status. Support vector machine (SVM), rotation forests and M5 trees models were built using NIR spectra acquired in the field directly on the adaxial side of grapevine leaves, with a non-invasive portable spectrophotometer working in the spectral range between 1600 and 2400 nm. The ν-SVM algorithm was used for the training of a model for varietal classification. The classifiers' performance for the 10 varieties reached, for cross- and external validations, the 88.7% and 92.5% marks, respectively. For water stress assessment, the models developed using the absorbance spectra of six varieties yielded the same determination coefficient for both cross- and external validations (R^2 = 0.84; RMSEs of 0.164 and 0.165 MPa, respectively). Furthermore, a variety-specific model trained only with samples of Tempranillo from two different vintages yielded R^2 = 0.76 and RMSE of 0.16 MPa for cross-validation and R^2 = 0.79, RMSE of 0.17 MPa for external validation. These results show the power of the combined use of data mining and non-invasive NIR sensing for in-field grapevine phenotyping and their usefulness for the wine industry and precision viticulture implementations.

Keywords: variety classification; plant water status; non-destructive; SVM; rotation forest; regression tree; stem water potential

1. Introduction

In the context of the current worldwide industrial demand of quality and efficiency in crop and food production, the importance of phenotyping arises every day. Plant phenotyping refers to a quantitative description of the plant's physiological, biochemical and morphological properties, among others [1]. It consists of the identification of effects on the phenotype as a result of genotype differences and the environmental conditions to which a plant has been exposed [2]. The development of new usable technologies and its direct availability have driven the latest plant phenotyping approaches that have emerged and have already been applied in several environments [3]. These technologies have enabled the performance of phenotyping tasks with reduced time and monetary costs (much sought after by the industrial actors) and remain under the focus of researchers from different currents

of investigation, trying especially to provide realistic, applicable and suitable solutions. Proximal sensing approaches, such as spectroscopy sensors or hyperspectral imaging, have arisen in the last few years as fast, non-destructive resources for the gathering of crop spectral information that could characterize concrete phenotyping traits, providing the in-field methods with a high relevance due to their desirable capability of providing *in situ* results.

Viticulture has benefited from these results of recent research that have developed methods and procedures for several vine- and wine-related problems using near-infrared (NIR) spectroscopy. NIR spectroscopy is a potent technology widely used in several agricultural areas due to its non-destructive nature and multi-parametric capabilities [4]. Spectroscopic sensors have been proven to be fast for the real-time assessment of several grapevine-related traits, such as the grape composition [5], the grapevine petiole nutrient concentration assessment [6] or the identification of grape berry sunburn symptoms [7]. Therefore, the possibility of the use of NIR technology for grapevine phenotyping arises as an attractive and promising tool for precision viticulture, especially when taking into account the fact that this technique is able to characterize more than one parameter using the same spectral measurement.

NIR devices are able to acquire large amounts of spectral data, making it necessary to manage them in efficient and automatic ways. Data mining has become one of the most valuable research fields in the latest few years due to its knowledge discovery power, direct applicability in several areas and, especially, its proven effectiveness in those problems where it is applied. Data mining through, among others, machine learning techniques have provided procedures for both descriptive (characterizations of the properties of the data) and predictive (learning and induction of the data for forecasting) tasks [8,9]. Some of the most widespread applications of predictive techniques are decision trees [10], decision forests [11] and, particularly, artificial neural networks (ANNs) [12] and support vector machines (SVMs) [13], employed in several research areas, such as medicine [14], business and industry [15] or biology [16]. Support vector machines [13,17] are supervised learning methods used for classification and regression through the nonlinear mapping of the input data. SVMs transform the original dataset into a higher dimension using a kernel function and find an optimal separating hyperplane, the best one that maximally separates the samples. Rotation forests [18] are machine learning ensemble methods that make use of several classification trees (hence the name) to build a meta-classifier. A rotation forest can be used both for classification or regression, depending on the kind of tree-based algorithm used. A robust regression tree is the M5 learner [19], which, although not as familiar as other estimation methods in spectroscopy, like partial least squares (PLS) [20], has demonstrated robustness and efficiency in other applications, such as pan evaporation prediction [21], low-flow forecasting modeling [22] or the water level-discharge relationship [23].

Two important grapevine phenotyping topics are varietal discrimination and water status assessment, tasks addressed in the literature and where spectroscopy especially has played a significant part in the last few years. Current varietal discrimination methods have some lack of aspects that are relevant for an industrial point of view, e.g., their need for a highly trained expert or their destructive nature [24]. Water status assessment especially suffers from this last issue, as well as its time and labor-consuming nature, along with the lower representative capacity (limited number of samples measured) derived from it [25]. Grapevine varietal discrimination using spectroscopic data has been recently attempted by hyperspectral imaging under laboratory conditions [24]. Both in-lab or in-field water status assessment via spectroscopy have also been aimed at, attending to several plant water condition indicators, such as stem water potential [26,27], leaf water potential [26,28,29] or leaf stomatal conductance [26]. It is worth highlighting that each and every one of the mentioned studies has one common factor: the use of partial PLS as the model training algorithm. PLS is a widespread statistical technique commonly used in spectroscopy for the regression of chemometric parameters. Qualitative prediction (e.g., discrimination among discrete classes) can also be achieved using PLS (as in [30], where a binary classification is translated into a regression of two natural numbers) or via a purest discrete classification method, like partial least squares discriminant analysis (PLS-DA) [31]. Still,

discrimination models built with PLS-based approaches have not yielded remarkable results when taking into account a considerably large amount of classes. Hence, the attractive attempt to apply less often used data mining techniques for the modeling of NIR spectra, thus making it possible to carry fast, in-field solutions for these two grapevine phenotyping approaches into commercial and industrial demands.

The goal of this study was to evaluate the combined use of different data mining techniques along with a non-destructive NIR portable sensor for the in-field grapevine phenotyping of two concrete traits: the variety classification and the estimation of the plant water status.

2. Experimental Section

2.1. Experimental Layout, Acquisition of NIR Spectra and Reference Measurements

Two experiments regarding grapevine varietal classification and plant water status were conducted.

Both experiments were carried out during late August and early September 2012 in a vineyard located in Vergalijo, Navarra, Spain (latitude 42°27'45.96" N, longitude 1°48'13.42" W, altitude 325 m). Vines of different varieties were planted in 2009 and trained to a vertical shoot-positioned trellis system at 2 × 1 m inter- and intra-row distances, with a north-south row orientation.

For both experiments, spectra acquisition was performed in the field with an integrated portable NIR spectral analyzer (microPHAZIR^{TM}, Thermo Fisher Scientific Inc., Waltham, MA, USA) operating in the range of 1600 to 2400 nm with a step of 8.7 nm (a total of 100 data points per spectrum). All spectra were returned by the device in absorbance mode and in this form were used for analysis.

For the grapevine varietal classification, 10 varieties were used: Cabernet Sauvignon, Caladoc, Carmenere, White Grenache, Pedro Ximenez, Pinot Noir, Tempranillo, Treixadura, Viognier and Viura. For each variety, 10 vines and two adult leaves per vine were selected from the mid-upper part of the shoot (Nodes 6 to 12) for the measurement of its spectrum on the adaxial side, making up a total of 20 leaves per variety. Five spectra per leaf (from different positions of the surface) were taken, and their average was considered the final spectrum of that leaf. Therefore, a total of 200 leaves (10 varieties, 20 leaves per variety) were used, and the name of the corresponding variety was linked to each measurement for the training of the varietal classification model.

For the assessment of the grapevine water status, measurements were carried out in six varieties during two days: Godello, Grenache, Pedro Ximenez (29 August 2012; vapor pressure deficit: 0.87 kPa; average temperature: 21.7 °C; average relative humidity: 68%), Carmenere, Marselan and Tempranillo (5 September 2012; vapor pressure deficit: 0.89 kPa; average temperature: 19.8 °C; average relative humidity: 62%). As in the varietal discrimination experiment, 10 vines and two adult leaves per vine were selected from the mid-upper part of the shoot (Nodes 6 to 12) for each variety. A total of 120 leaves (6 varieties, 20 leaves per variety) were measured, thus for the training of the water status assessment model. Spectra acquisition was done on the adaxial side of the leaves. Afterwards, the midday stem water potential ψ_{stem} (14:00, solar noon) of each leaf was measured as the reference method of water stress [32]. Stem water potential was determined using a Scholander pressure bomb (Model 600, PMS Instruments Co., New York, NY, USA). The selected leaves were driven into dark adaptation by covering them with aluminum foil bags one hour before the ψ_{stem} measurement.

In order to test the robustness of the algorithms, a second model for water status assessment was developed involving samples of a given variety (to analyze the ψ_{stem} prediction capability within one variety) acquired at different seasons and vineyards (to test the prediction capability with samples at different phenological stages). Thirty-six leaf spectral measurements of Tempranillo were acquired in 12 August 2015 in a vineyard located in Tudelilla, La Rioja (42°18'17.9208", −2°7'15.8376"; vapor pressure deficit: 1.74 kPa; average temperature: 26.7 °C; average relative humidity: 53%) using the same procedure as in 2012. A new variety-specific dataset for Tempranillo was built up merging these 36 samples and the 20 samples of Tempranillo taken in 2012, making up a total of 56 samples.

For both variety discrimination and water status assessment, the optical window of the NIR device was fully covered and vinyl gloves were used when taking the measurements in order to avoid contamination from external light and pollutants.

2.2. Spectra Pre-Processing and Data Mining Algorithms

2.2.1. Pre-Processing

An outlier detection analysis was performed before any other spectral treatment. It consisted of the following procedure: at measurement time, the acquired spectrum was compared by the sensor with a previously taken grapevine leaf's spectrum signature and labeled according to whether the signal was from a leaf or not. All spectra that did not belong to a grapevine leaf were treated as outliers and thus removed.

Scatter correction and spectral derivative were applied to the raw spectra, in order to diminish the physical variability between samples because of scatter and to remove both additive and multiplicative effects in the spectra, respectively [33]. Standard normal variate (SNV) followed by de-trending [34,35] was used as a scatter correction method. Afterwards, a Savitzky–Golay smoothing and derivative process [36] was applied with a window size of five and a second-degree derivative.

2.2.2. Data Mining Algorithms

Due to the different nature of the phenotyping features addressed in this work, distinct data mining algorithms for classification and regression were applied for grapevine varietal discrimination and water status assessment, respectively.

Varietal Discrimination

For grapevine varietal discrimination, SVMs were used. The ν-SVM algorithm [37] was used in this study, implemented in LIBSVM [38], the post-processed spectra data points, linked with its variety label (the class), being the input of the algorithm. A second-degree polynomial kernel and a ν value of 0.1 were set as the parameters of the algorithm.

The classifiers evaluation was performed attending not only to the confusion matrix, but also to a deeper analysis involving the true and false positive rates, precision values and receiver operating characteristic (ROC) curves' area (area under the curve, AUC). The true positive rate refers to the proportion of samples that were discriminated as a specific class among all samples, which truly corresponded to that class (it is similar to the correctly classified percentage divided by 100). The *false positive rate* is the proportion of samples that were classified as a specific class, but belonged to a different one, among all examples that were not of that class. The precision represents the proportion of the samples that were correctly classified in their class among all those that were classified as that given class. The AUC is the measure of the area that lies under the ROC curve. An ROC curve is a graphic representation of true positive *versus* false positive rates by varying a given threshold. ROC curves' AUC is a common metric for the evaluation of a classifier. A perfect classifier would achieve an AUC of 1, while a system that classifies instances in a random way would obtain a 0.5 value.

Water Status Assessment

To address the grapevine water status assessment, regression with rotation forest and M5 trees was applied. The spectral data points were used as the input of the algorithm and each sample's ψ_{stem} measurement as the value to predict. *Weka* software, Version 3.6, [39] was used for the development of the regression models.

Algorithm Validation

For the assessment of the algorithms' results, calibration, cross-validation and external testing were carried out. For each one of the experiments, its dataset was divided into two subsets, training

and test, comprising 80% and 20% of the original samples, respectively. The test set was never used for the training of any of the models. In the calibration assessment, the models were developed using the training set and validated with the same one. In the cross-validation, a *k*-fold method was performed upon the training dataset with a *k* value of 5 (in order to maintain the 80:20 ratio, obtaining five executions where, in each one of them, the model is trained with 80% of the samples and evaluated testing the remaining 20%). Finally, the prediction results were obtained via an external validation, training and testing the models with the training and test datasets, respectively. The test set was obtained in a stratified way (e.g., the same number of samples for each grapevine variety was selected). For the varietal classification, 160 and 40 samples were assigned to the training and test datasets, respectively. For the water status assessment, the multi-variety models' datasets contained 96 and 24 instances, respectively, while the Tempranillo-specific models' datasets involved 45 samples for the training subset and 11 samples for the test subset.

Figure 1 shows a diagram of the datasets and the different calibration and validation processes used in both experiments.

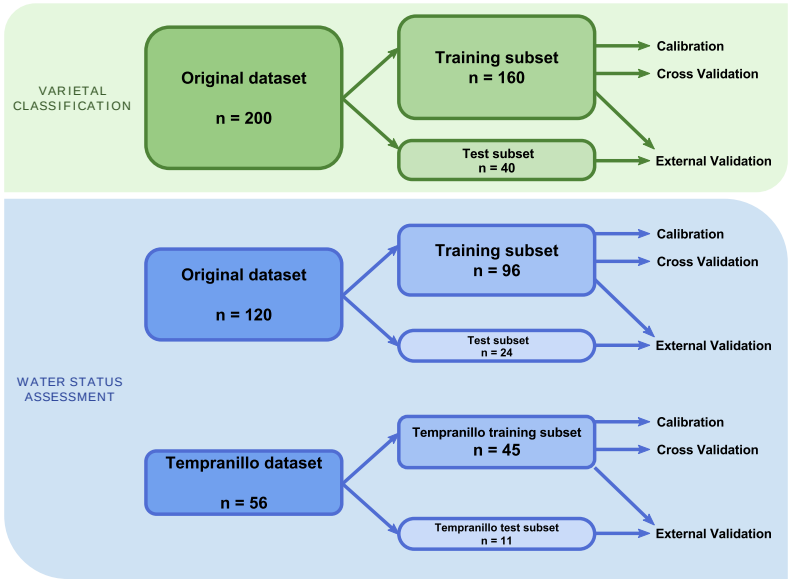

Figure 1. Diagram of the datasets used in both experiments and the different calibration and validation processes.

3. Results

3.1. Grapevine Varietal Discrimination

The spectral outlier analysis performed before the development of the models resulted in the removal of one sample of White Grenache due to spectral mismeasurement. One hundred percent of correctly classified samples were obtained in the calibration of the SVM classifier trained with the training dataset, reaching perfect scores in the confusion matrix (data not shown). Table 1 presents the confusion matrix from the 5-fold cross-validation of the SVM classifier trained with the training dataset. One hundred forty-one samples out of 159 were successfully discriminated (88.7%). The confusion matrix shows that the Cabernet Sauvignon variety obtained a perfect score in its discrimination, while all other varieties were above the 80% mark, excluding the Viognier variety, which obtained a score of 75% (12 out of 16 correctly discriminated samples).

Sensors **2016**, *16*, 236

Table 1. Confusion matrix of grapevine varietal classification using support vector machines and a 5-fold cross-validation. The diagonal of the matrix corresponds to the number of samples that were properly classified. The last column displays, for each variety, the correctly classified percentage (n = 159).

		Predicted Variety										
		CS	**CL**	**CR**	**WG**	**PX**	**PN**	**TE**	**TR**	**VO**	**VU**	**%**
Actual variety	**CS**	**16**	0	0	0	0	0	0	0	0	0	**100.0**
	CL	0	**15**	0	0	0	0	0	0	1	0	**93.8**
	CR	1	0	**15**	0	0	0	0	0	0	0	**93.8**
	WG	0	0	0	**12**	0	0	1	0	2	0	**80.0**
	PX	0	1	0	0	**13**	0	0	0	1	1	**81.3**
	PN	0	0	0	1	0	**14**	0	0	0	1	**87.5**
	TE	0	0	0	0	0	1	**15**	0	0	0	**93.8**
	TR	0	0	1	0	0	1	0	**14**	0	0	**87.5**
	VO	0	1	0	0	2	0	1	0	**12**	0	**75.0**
	VU	0	0	0	0	1	0	0	0	0	**15**	**93.8**

CS: Cabernet Sauvignon; CL: Caladoc; CR: Carmenere; WG: White Grenache; PX: Pedro Ximenez; PN: Pinot Noir; TE: Tempranillo; TR: Treixadura; VO: Viognier; VU: Viura.

Table 2. Detailed accuracy by class of the grapevine varietal classification using support vector machines and a 5-fold cross-validation (n = 159).

Class	True Positive Rate	False Positive Rate	Precision	AUC
Cabernet Sauvignon (CS)	1.000	0.007	0.941	0.997
Caladoc (CL)	0.938	0.014	0.882	0.997
Carmenere (CR)	0.938	0.007	0.938	0.998
White Grenache (WG)	0.800	0.007	0.923	0.985
Pedro Ximenez (PX)	0.813	0.021	0.813	0.980
Pinot Noir (PN)	0.875	0.014	0.875	0.976
Tempranillo (TE)	0.938	0.014	0.882	0.997
Treixadura (TR)	0.875	0.000	1.000	0.999
Viognier (VO)	0.750	0.028	0.750	0.992
Viura (VU)	0.938	0.014	0.882	0.992
Weighted average	0.887	0.013	0.888	0.991

AUC: area under the receiver operating characteristic (ROC) curve.

Table 2 shows a detailed accuracy analysis by class for the SVM classifier in the cross-validation process. Similar to the confusion matrix's correctly discriminated percentage (Table 1), one class obtained the highest value for the true positive rate (Cabernet Sauvignon). Nevertheless, due to a sample of the Carmenere class incorrectly assigned to the Cabernet Sauvignon class, the precision value of this variety did not reach the maximum. Additionally, although the Treixadura variety did not obtain a perfect true positive score, the fact that no other instance was classified as that variety (Table 1) led to a perfect precision mark for this variety class. The average AUC yielded by the cross-validation was 0.991, moving between 0.976 and 0.999 (achieved by the Treixadura variety) for class-specific values.

Table 3 shows the confusion matrix from the external validation of the SVM classifier, where the model was trained using 159 samples and validated with the prediction of 40 external ones. The average correctly discriminated percentage was slightly higher than that of the 5-fold cross-validation, reaching the 92.5% mark, where 37 out of 40 instances were properly classified. Seven varieties obtained 100% correctly classified samples, while Pinot Noir, Tempranillo and Viognier had one misclassified sample, dropping their percentage to 75%.

Table 3. Confusion matrix of grapevine varietal classification using support vector machines and an external validation of 40 samples. The diagonal of the matrix corresponds to the number of samples that were properly classified. The last column displays, for each variety, the correctly classified percentage (n = 40).

		Predicted Variety										
		CS	**CL**	**CR**	**WG**	**PX**	**PN**	**TE**	**TR**	**VO**	**VU**	**%**
Actual variety	**CS**	**4**	0	0	0	0	0	0	0	0	0	**100.0**
	CL	0	**4**	0	0	0	0	0	0	0	0	**100.0**
	CR	0	0	**4**	0	0	0	0	0	0	0	**100.0**
	WG	0	0	0	**4**	0	0	0	0	0	0	**100.0**
	PX	0	0	0	0	**4**	0	0	0	0	0	**100.0**
	PN	0	0	0	0	0	**3**	0	0	0	1	**75.0**
	TE	0	0	0	0	0	1	**3**	0	0	0	**75.0**
	TR	0	0	0	0	0	0	0	**4**	0	0	**100.0**
	VO	0	0	0	1	0	0	0	0	**3**	0	**75.0**
	VU	0	0	0	0	0	0	0	0	0	**4**	**100.0**

CS: Cabernet Sauvignon; CL: Caladoc; CR: Carmenere; WG: White Grenache; PX: Pedro Ximenez; PN: Pinot Noir; TE: Tempranillo; TR: Treixadura; VO: Viognier; VU: Viura.

The detailed accuracy per class for the external validation is displayed in Table 4. Confirming the results in the confusion matrix of Table 3, seven varieties obtained a value of one in the true positive rate, but two of them—White Grenache and Viura—did not achieve a perfect score, because some samples were misclassified as those varieties. It is remarkable that two classes that obtained a precision value of one (Tempranillo and Viognier) did not reach a full true positive rate, meaning that all samples that were classified as Tempranillo and Viognier were in effect leaves of those varieties. According to the AUC values, eight out of 10 classes yielded the perfect score, increasing the average AUC for all of the classes to the 0.997 mark.

Table 4. Detailed accuracy by class of the grapevine varietal classification using support vector machines and an external validation of 40 samples (n = 40).

Class	True Positive Rate	False Positive rate	Precision	AUC
Cabernet Sauvignon (CS)	1.000	0.000	1.000	1.000
Caladoc (CL)	1.000	0.000	1.000	1.000
Carmenere (CR)	1.000	0.000	1.000	1.000
White Grenache (WG)	1.000	0.028	0.800	0.993
Pedro Ximenez (PX)	1.000	0.000	1.000	1.000
Pinot Noir (PN)	0.750	0.028	0.750	0.972
Tempranillo (TE)	0.750	0.000	1.000	1.000
Treixadura (TR)	1.000	0.000	1.000	1.000
Viognier (VO)	0.750	0.000	1.000	1.000
Viura (VU)	1.000	0.028	0.800	1.000
Weighted average	0.925	0.008	0.935	0.997

AUC: area under the receiver operating characteristic (ROC) curve.

3.2. Assessment of Grapevine Water Status

3.2.1. Multi-Variety Model

The spectral outlier analysis tagged one sample of Godello and another of Grenache as mismeasured spectra, so both were removed before the development of the regression model. The ranges of ψ_{stem} per variety are shown in Table 5. It can be observed that Cermenere and Tempranillo were the most water stressed varieties, while Pedro Ximenez and Godello experienced no water scarcity. Grenache and Marselan exhibited a similar ψ_{stem} range, indicative of an incipient moderate water stem.

Sensors **2016**, *16*, 236

Table 5. Stem water potential (ψ_{stem}) ranges per variety.

ψ_{stem}	Variety					
	Godello	**Pedro Ximenez**	**Grenache**	**Carmenere**	**Tempranillo**	**Marselan**
Min	−0.90	−0.65	−1.15	−1.45	−1.85	−1.02
Max	−0.62	−0.42	−0.85	−1.10	−1.62	−0.85

Table 6 shows the statistical summary for the ψ_{stem} values of the sampled population and the result of the calibration, cross- and external validations of the stem water potential estimation using a rotation forest and M5 trees.

Table 6. Statistic overview and results of the ψ_{stem} (MPa) estimation using a rotation forest and M5 trees.

Statistics					**Rotation Forest and M5 Trees**					
					Calibration (n = 94)		**5-Fold Cross-Validation (n = 94)**		**External Validation (n = 24)**	
n	**Min**	**Max**	**Mean**	**SD**	**R^2**	**RMSE**	**R^2**	**RMSE**	**R^2**	**RMSE**
118	−1.85	−0.42	−1.03	0.396	0.97	0.083	0.84	0.164	0.84	0.165

n: number of samples; Min: minimum; Max: maximum; SD: standard deviation; RMSE: root-mean-square error in MPa.

The determination coefficient (R^2) and root-mean-square error (RMSE) of calibration were 0.97 and 0.083, respectively. For both validation processes, these values were R^2 = 0.84, RMSE: 0.164, for the cross-validation (having a training dataset with 94 samples) and R^2 = 0.84, RMSE: 0.165, for external validation (with a test dataset having 24 samples).

The regression plots for cross- and external validation models are displayed in Figure 2, along with the prediction bands at a 95% of confidence. To perform a deeper analysis of the predicted outcomes, a manual clustering into four groups was performed for the samples according to the absolute error value $|\varepsilon|$ = measured ψ_{stem} − predicted ψ_{stem}: minimal error ($|\varepsilon| < 0.1$). low error ($0.1 \leq |\varepsilon| < 0.2$), moderate error ($0.2 \leq |\varepsilon| < 0.4$) and high error ($|\varepsilon| \geq 0.4$). For the cross-validation (Figure 2a), 40 samples obtained a minimal error (42.6% of the samples), 34 a low error (36.2%), 18 a moderate error (19.1%) and 2 a high error (2.1%). In the external validation (Figure 2b), 16 samples obtained a minimal error (66.7%), 5 a low error (20.8%), 2 a moderate error (8.3%) and 1 a high error (4.2%). Two samples for the cross-validation (Figure 2a) and another one for the external validation (Figure 2a) were present in the regression models, samples that obtained an absolute error value greater than 0.4 MPa. In both plots, these high error samples were driven by the divergence of the regression line from the 1:1 line. Further, the samples with the minimal and low error values did considerably fit better to the diagonal line 1:1 than the high error samples. The prediction bands at a 95% confidence only excluded a few samples in both cases. For the cross-validation (Figure 2a), four samples lied out of the precision bands, meaning that 95.7% of the samples were inside both bands. For the external validation results (Figure 2b), 95.8% of the samples lied between the 95% confidence bands, while only one sample was kept out.

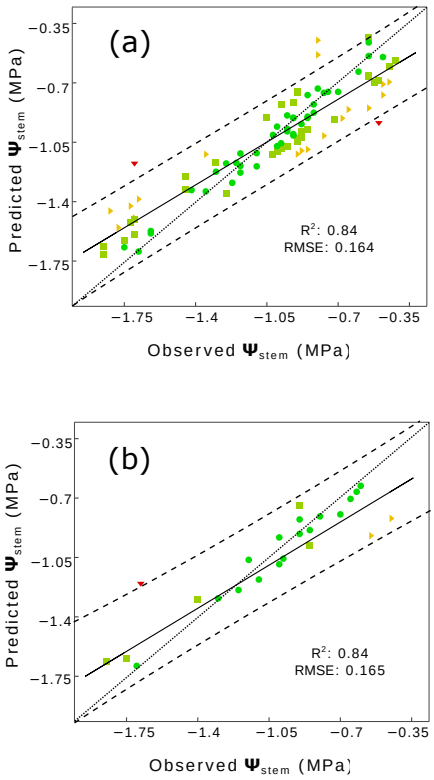

Figure 2. Regression plot for ψ_{stem} estimation using a Rotation Forest and M5 trees with a 5-fold cross (**a**) and external (**b**) validations. Prediction confidence bands are shown at a 95% level (dashed lines). Solid line represents the regression line and dotted line refers to the 1:1 line. Each points' color and shape refers to its absolute error value $|\varepsilon|$ (the absolute value of the difference between the actual value and the predicted one) in MPa: green ●: $|\varepsilon| < 0.1$, minimal error; olive ■: $0.1 \leq |\varepsilon| < 0.2$, low error; orange ►: $0.2 \leq |\varepsilon| < 0.4$, moderate error; red ▼: $|\varepsilon| \geq 0.4$, high error.

3.2.2. Variety-Specific Multi-Vineyard Model

Table 7 shows the statistical summary for the ψ_{stem} values of the sampled population from the variety-specific model (involving samples of Tempranillo taken both in 2012 and 2015 from two different vineyards) and the result of the calibration, cross- and external validations of the stem water potential estimation using a rotation forest and M5 trees.

Table 7. Statistic overview and results of the ψ_{stem} (MPa) estimation for the variety-specific model (Tempranillo) using a rotation forest and M5 trees.

Statistics					Rotation Forest and M5 Trees					
					Calibration (n = 45)		5-Fold Cross-Validation (n = 45)		External Validation (n = 11)	
n	**Min**	**Max**	**Mean**	**SD**	**R^2**	**RMSE**	**R^2**	**RMSE**	**R^2**	**RMSE**
56	−1.85	−0.8	−1.447	0.314	0.92	0.098	0.76	0.159	0.79	0.168

n: number of samples; Min: minimum; Max: maximum; SD: standard deviation; RMSE: root-mean-square error in MPa.

Sensors **2016**, *16*, 236

The range of ψ_{stem}, in Table 7, illustrates a population of grapevines involving plants of very different water status, from no stressed plants (ψ_{stem} = −0.8 MPa) to severely stressed plants (ψ_{stem} = −1.85 MPa), the mean being ψ_{stem} (−1.45 MPa), indicative of high water stress.

The determination coefficient R^2 and RMSE of calibration were 0.92 and 0.098, respectively, while for both validation processes, these values were R^2 = 0.76, RMSE: 0.159 (cross-validation), and R^2 = 0.79, RMSE: 0.168 (external validation).

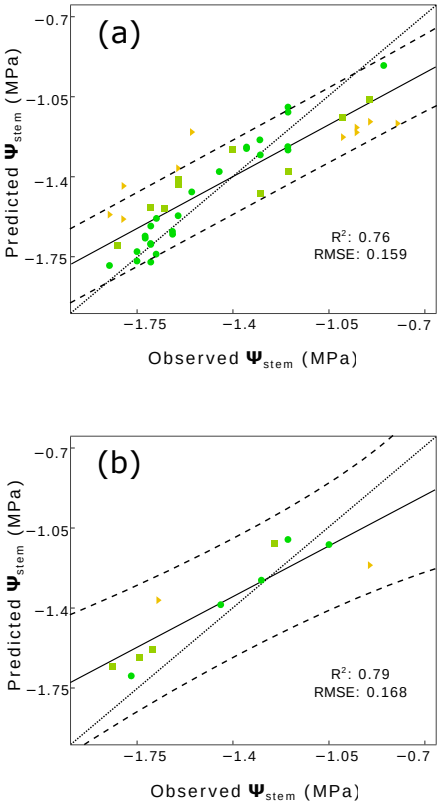

Figure 3. Regression plot for ψ_{stem} estimation of the variety-specific model (Tempranillo) using a Rotation Forest and M5 trees with a 5-fold cross (**a**) and external (**b**) validations. Prediction confidence bands are shown at a 95% level (dashed lines). Solid line represents the regression line and dotted line refers to the 1:1 line. Each points' color and shape refers to its absolute error value $|\varepsilon|$ (the absolute value of the difference between the actual value and the predicted one) in MPa: green ●: $|\varepsilon| < 0.1$, minimal error; olive ■: $0.1 \leq |\varepsilon| < 0.2$, low error; orange ►: $0.2 \leq |\varepsilon| < 0.4$, moderate error; red ▼: $|\varepsilon| \geq 0.4$, high error.

Figure 3 shows the regression plots for the two validation processes and their prediction bands at a 95% of confidence. In the 5-fold cross-validation (Figure 3a), 25 samples obtained a minimal error value, 10 a low error and 10 a moderate one. Five out of 45 samples lied out the prediction bands, keeping 88.9% of the samples inside them. In Figure 3b (external validation), all of the samples were inside the confidence bands, where 5 of them obtained a minimal error value, 4 a low one and 2 a moderate error value.

4. Discussion

In this work, the appraisal of two important phenotyping features in agriculture—grapevine varietal discrimination and water status assessment—has been aimed at from an innovative approach that successfully combines an in-field measurement, using a proximal and non-invasive sensor, with different data mining processing methods. The results obtained have displayed the potential of effectively applying data mining techniques upon the spectral information retrieved from a non-destructive and proximal NIR sensor for grapevine plant phenotyping of two key traits.

Regarding variety classification, most of the widely-used methods for grapevine varietal discrimination have traditionally been either destructive or time-consuming, like classic ampelometry [40] (which is subjected to expert visual description, but still prone to a considerable level of bias due to its human nature), DNA analysis [41] or wet chemistry techniques [42] (carried out by trained people and through destructive methods).

In our work, the 10-class variety classification models using SVMs from non-invasively acquired leaf spectra have yielded 88.7% and 92.5 values of correctly discriminated samples for cross- and external validations, respectively. These high percentages allow one to be reasonably optimistic about the suitability of SVMs for the grapevine varietal classification. These correctly-classified percentages are also supported by the high scores of additional classification statistics, such as the average precision (obtaining in several cases a perfect score and high mean values) and AUCs (an average of 0.991 and 0.997 for cross- and external validation, respectively).

Only very recently, grapevine varietal classification has been attempted by hyperspectral imaging [24] and an NIR portable spectrophotometer [43]. In [24], hyperspectral imaging in the range between 280 nm and 1028 nm was used along with PLS for the classification of 300 leaves from three different varieties (Tempranillo, Grenache and Cabernet Sauvignon), under laboratory conditions. The cross-validation method used (Monte Carlo) yielded more than 92% of correctly classified samples in all cases. The outcomes reached in the present work, even when a large number of varieties was selected for the training, highlights the accuracy shown by data mining techniques for the same goal, particularly when the spectra were collected in the field and in a non-destructive way, different from [24], where a hyperspectral camera was used indoors under controlled illumination conditions. In [43], the authors used a portable NIR spectrophotometer of the same range as the one in this work for the acquisition of leaves' spectra. Artificial neural networks (ANNs) and sequential minimal optimization for the training of SVMs were tested as classification algorithms for the development of two grapevine discrimination models for two different approaches: a site-specific model for 20 varieties (yielding 87.25% of correctly classified samples, using ANNs) and a global model using six varieties from different vineyards and seasons (obtaining 77.08%, again with ANNs). The higher percentages obtained in the present study could be explained by the selected SVM algorithm, ν-SVM algorithm, *versus* sequential minimal optimization, as well as the reduced number of classes.

Varietal discrimination using NIR spectroscopy has also been recently performed for waxy corn seed [44] using SVM and in strawberry [45] and plum [46] using PLS-D. From these works, it is remarkable that a purer data mining technique, SVMs [44], behaved better than the statistical method PLS, commonly used in spectroscopy and chemometrics, confirming the high suitability and adaptability of machine learning approaches for any kind of problem and specifically NIR spectroscopy. Five- and four-class varietal discrimination using PLS-DA was achieved in [45,46] obtaining 69% and up to 96.5% values of correctly classified samples, respectively, presenting lower than and similar accuracies as in the present grapevine varietal discrimination, but taking into account that the number of varieties was reduced by half.

The proven flexibility, generalization capability and accuracy in so many dissimilar fields for discrimination issues given by data mining techniques, and confirmed by the results of the grapevine varietal classification via SVMs, demonstrates how well the numerous data mining algorithms fit in classification problems, specifically when working with NIR spectroscopy from proximal sensors.

Sensors **2016**, *16*, 236

Current water status assessment methods are mostly destructive, labor intensive, thus expensive, and, in many cases, only capable of being implemented in a limited number of samples, jeopardizing their representativeness and not suitable for characterizing the spatial variability of a vineyard's water status. Therefore, new non-invasive and fast approaches are needed.

For the regression of ψ_{stem} conducted through rotation forests and M5 trees, the calibration R^2 and RMSE reached the 0.97 and 0.083 values, respectively, while both validation results were virtually identical (R^2 = 0.84; RMSE = 0.165). A relatively large divergence between calibration and validation results was found, where the latter's RMSE nearly doubled that of the calibration. Still, this difference of 0.082 MPa, although, as said, being relatively wide, remains small in absolute terms, particularly when compared to the standard deviation of the population ψ_{stem} values (0.396), that is almost five-times larger. The high score of the determination coefficient of calibration is an aspect that could be generally expected when using data mining and machine learning techniques. Moreover, the training of decision trees is very sensitive to the examples used as input, having a high importance for the algorithm (that tries to extract underlying rules and correlations between the independent and dependent variables), so high results are likely to be obtained when testing with the same set that the algorithm was trained. The use of the calibration results should be carefully treated when applying data mining algorithms, and they should be contrasted with values that came from validation processes. However, the high results obtained for both cross- and external validations concede a considerable level of confidence in the suppression of any overfitting problem.

Additionally, the good outcomes obtained from the variety-specific model (although slightly lower than the multi-varietal one) show the robustness of the application of data mining algorithms for the accurate prediction of ψ_{stem} of samples from different seasons and locations when properly training the models with both kinds of examples. This could enable affirming that support vector machines are able to assess the grapevine water status within one variety and to discard the variety as a driving factor in good water status prediction. Still, should the variety-specific model have a higher number of samples and/or a wider range in the water status reference parameter (ψ_{stem}), the model's performance would have probably yielded higher R^2 and RMSE values. It should not be omitted that the Tempranillo dataset, compared to the multi-varietal one, contained a lower number of samples (56 *vs.* 120) and a narrower ψ_{stem} range ([−1.85, −0.8] *vs.* [−1.85, −0.42], MPa).

Stem water potential, as an indicator of plant water stress, has been previously predicted by NIR-based models developed using PLS regression [26–29], returning determination coefficients between 0.71 and 0.85 (and error values around 0.1 and 0.2 MPa). The in-field multi-varietal study performed in the current work, using rotation forests and M5 trees, returned a similar determination coefficient for cross- and external validations, highlighting that a considerably higher number of varieties was used. The fact that both studies ([26] and this one) clearly resulted in high ψ_{stem} correlations from two different and scarcely overlapped NIR regions may drive one to conclude the adequate suitability of NIR spectral measurements from non-destructive sensors in water status prediction.

Models for the grapevine ψ_{leaf} [28] and ψ_{stem} in olive trees [27] were developed by VIS/NIR spectroscopy. These works have in common the use of PLS as a model training method, returning moderated values of cross-validation correlation (R^2 from 0.45 to 0.74) that are noticeably surpassed by the results from the rotation forest and M5 trees models described in this work, allowing one to confirm the effective application of data mining techniques to NIR spectral data for the estimation of ψ_{stem}, hence the assessment of plant water status. Additionally, it must be highlighted that the spectral range used in this study (1600 to 2400 nm) completely covered the absorption band (O–H) corresponding to the water vibrational band (1940 nm) [47], which could be one of the reasons for the high sensitivity in ψ_{stem} changes; thus, a good predictive model could be obtained from this spectral range.

To the best of our knowledge, scarce studies have made use of data mining algorithms for water status assessment. In [48], the authors built an artificial neural network for the in-lab relative water

content (RWC) estimation from grapevine leaf's hyperspectral imaging working in the range from 900 nm to 1700 nm. The authors asserted that the generated models (with average absolute error below the 3% mark) were shown to be leaf side, varietal and even clone dependent. Although no direct comparison can be made with the present work, because RWC was used as a water status indicator instead of ψ_{stem}, both results have displayed the accuracy of the combination of NIR spectroscopy along with data mining and machine learning techniques for the reliable assessment of plant, grapevine specifically, water status.

The selection of a proper estimation method for a concrete algorithm and dataset is crucial for the evaluation of the results. In multivariate chemometrics, a classic approach of performance evaluation has been the dataset split into calibration (or training) and test partitions [49]. Although the use of the same dataset for the training and testing is not generally recommended, because the obtained results are overly optimistic [9], its value could be considered as an upper limit to what may be expected in other settings (e.g., cross- and external validation). k-fold and leave-one-out cross-validation methods [50] have been broadly extended in data mining and chemometrics. The selection of $k = 5$ for the cross-validation in the present work, maintaining the 80:20 ratio as in the external validation, can lead to a higher consistency and reliability on the obtained results in both experiments.

It is also remarkable the duality brought by the spectral measurements obtained with the same NIR sensor. The capability of effectively addressing these two grapevine phenotyping traits from a single leaf spectral measurement along with its rapid, non-destructive and in-field nature makes the almost direct implementation of a grapevine phenotyping system on an NIR device a reasonable goal supported by the precision obtained in the developed models and the characterization of concrete and sufficient sets of samples for the training.

5. Conclusions

Combining non-invasive sensors and data mining algorithms may be a powerful tool that could allow one to perform grapevine phenotyping tasks and forward the results to the user directly in the field. The proven good behavior of different data mining techniques along with the non-invasive, fast and responsive nature of a portable NIR sensor for the in-field grapevine varietal classification and water status assessment opens a way for the direct application of the models in embedded portable systems.

The two phenotyping traits addressed in this study—grapevine discrimination and water status assessment—deserve major attention in modern viticulture, as they are key factors in breeding, grape quality production and sustainability. Their robust prediction from non-invasively acquired data is expected to have a positive impact in precision viticulture and, extensively, several other agricultural areas. These are very likely to benefit from the application of the results obtained by the prediction models due to their almost direct application of the training process via data mining to a portable NIR device.

Acknowledgments: This work has received funding from the Spanish Ministry of Economy and Competitiveness (MINECO) under the INNGRAPEproject (RTC-2014-3058-2). The authors want to thank Vitis Navarra S.L. (Larraga, Navarra, Spain) for providing the vineyards to carry out this study. Special thanks to Victor Sicilia, Teresa Díaz and Borja Millan for their help in the vineyard during data acquisition.

Author Contributions: Maria P. Diago and Javier Tardaguila conceived of and designed the experiments. Maria P. Diago performed the experiments. Salvador Gutiérrez and Juan Fernández-Novales analyzed the data. Javier Tardaguila contributed reagents/materials/analysis tools. Salvador Gutiérrez, Javier Tardaguila, Juan Fernández-Novales and Maria P. Diago wrote the paper.

Conflicts of Interest: The authors declare no conflict of interest.

References

1. Walter, A.; Liebisch, F.; Hund, A. Plant phenotyping: From bean weighing to image analysis. *Plant Methods* **2015**, *11*, doi:10.1186/s13007-015-0056-8.

2. Minervini, M.; Scharr, H.; Tsaftaris, S. Image Analysis: The New Bottleneck in Plant Phenotyping [Applications Corner]. *IEEE Signal Process. Mag.* **2015**, *32*, 126–131.
3. Fiorani, F.; Schurr, U. Future scenarios for plant phenotyping. *Annu. Rev. Plant Biol.* **2013**, *64*, 267–291.
4. Roberts, C.A.; Workman, J., Jr.; Reeves, J.B., III. *Near-Infrared Spectroscopy in Agriculture*; American Society of Agronomy: Madison, WI, USA, 2004.
5. Cozzolino, D.; Esler, M.; Dambergs, R.; Cynkar, W.; Boehm, D.; Francis, I.; Gishen, M. Prediction of colour and pH in grapes using a diode array spectrophotometer (400–1100 nm). *J. Near Infrared Spectrosc.* **2004**, *12*, 105–112.
6. Smith, J.; Schmidtke, L.; Müller, M.; Holzapfel, B. Measurement of the concentration of nutrients in grapevine petioles by attenuated total reflectance Fourier transform infrared spectroscopy and chemometrics. *Aust. J. Grape Wine Res.* **2014**, *20*, 299–309.
7. Rustioni, L.; Rocchi, L.; Guffanti, E.; Cola, G.; Failla, O. Characterization of grape (Vitis vinifera L.) berry sunburn symptoms by reflectance. *J. Agric. Food Chem.* **2014**, *62*, 3043–3046.
8. Han, J.; Kamber, M.; Pei, J. *Data Mining: Concepts and Techniques: Concepts and Techniques*; Elsevier: Harrisburg, PA, USA, 2011.
9. Witten, I.H.; Frank, E. *Data Mining: Practical Machine Learning Tools and Techniques*; Morgan Kaufmann: Burlington, VT, USA, 2005.
10. Quinlan, J.R. Induction of decision trees. *Mach. Learn.* **1986**, *1*, 81–106.
11. Rokach, L. Decision forest: Twenty years of research. *Inf. Fusion* **2016**, *27*, 111–125.
12. Rumelhart, D.E.; Hinton, G.E.; Williams, R.J. Learning representations by back-propagating errors. *Nature* **1986**, doi:10.1038/323533a0.
13. Cortes, C.; Vapnik, V. Support-vector networks. *Mach. Learn.* **1995**, *20*, 273–297.
14. Lavrač, N. Selected techniques for data mining in medicine. *Artif. Intell. Med.* **1999**, *16*, 3–23.
15. Giudici, P. *Applied Data Mining: Statistical Methods for Business and Industry*; John Wiley & Sons: New York, NY, USA, 2005.
16. Hirschman, L.; Park, J.C.; Tsujii, J.; Wong, L.; Wu, C.H. Accomplishments and challenges in literature data mining for biology. *Bioinformatics* **2002**, *18*, 1553–1561.
17. Boser, B.E.; Guyon, I.M.; Vapnik, V.N. A training algorithm for optimal margin classifiers. In Proceedings of the Fifth Annual Workshop on Computational Learning Theory. Pittsburgh, PA, USA, 27–29 July 1992; pp. 144–152.
18. Rodriguez, J.J.; Kuncheva, L.I.; Alonso, C.J. Rotation forest: A new classifier ensemble method. *IEEE Trans. Pattern Anal. Mach. Intell.* **2006**, *28*, 1619–1630.
19. Quinlan, J.R. Learning with continuous classes. In Proceedings of the 5th Australian Joint Conference on Artificial Intelligence, Hobart, Australia, 16–18 November 1992; pp. 343–348.
20. Wold, S.; Sjöström, M.; Eriksson, L. PLS-regression: A basic tool of chemometrics. *Chemom. Intell. Lab. Syst.* **2001**, *58*, 109–130.
21. Kisi, O. Pan evaporation modeling using least square support vector machine, multivariate adaptive regression splines and M5 model tree. *J. Hydrol.* **2015**, *528*, 312–320.
22. Štravs, L.; Brilly, M. Development of a low-flow forecasting model using the M5 machine learning method. *Hydrol. Sci. J.* **2007**, *52*, 466–477.
23. Bhattacharya, B.; Solomatine, D.P. Neural networks and M5 model trees in modeling water level–discharge relationship. *Neurocomputing* **2005**, *63*, 381–396.
24. Diago, M.; Fernandes, A.; Millan, B.; Tardaguila, J.; Melo-Pinto, P. Identification of grapevine varieties using leaf spectroscopy and partial least squares. *Comput. Electron. Agric.* **2013**, *99*, 7–13.
25. Jones, H.G. Irrigation scheduling: Advantages and pitfalls of plant-based methods. *J. Exp. Bot.* **2004**, *55*, 2427–2436.
26. De Bei, R.; Cozzolino, D.; Sullivan, W.; Cynkar, W.; Fuentes, S.; Dambergs, R.; Pech, J.; Tyerman, S. Non-destructive measurement of grapevine water potential using near infrared spectroscopy. *Aust. J. Grape Wine Res.* **2011**, *17*, 62–71.
27. Poblete-Echeverría, C.; Ortega-Farías, S.; Lobos, G.; Romero, S.; Ahumada, L.; Escobar, A.; Fuentes, S. Non-invasive method to monitor plant water potential of an olive orchard using visible and near infrared spectroscopy analysis. *Acta Hortic.* **2014**, *1057*, 363–368.
28. Vila, H.; Hugalde, I.; di Filippo, M. Estimation of leaf water potential by thermographic and spectral measurements in grapevine. *RIA Rev. de Investig. Agropecu.* **2011**, *37*, 46–53.

29. Santos, A.O.; Kaye, O. Grapevine leaf water potential based upon near infrared spectroscopy. *Sci. Agric.* **2009**, *66*, 287–292.
30. Perez, D.; Sanchez, M.; Cano, G.; Garrido, A. Authentication of Green Asparagus Varieties by Near-Infrared Reflectance Spectroscopy. *J. Food Sci.* **2001**, *66*, 323–327.
31. Naes, T.; Isaksson, T.; Fearn, T.; Davies, T. *A User Friendly Guide to Multivariate Calibration and Classification*; NIR publications: Chichester, UK, 2002.
32. Scholander, P.F.; Bradstreet, E.D.; Hemmingsen, E.; Hammel, H. Sap pressure in vascular plants negative hydrostatic pressure can be measured in plants. *Science* **1965**, *148*, 339–346.
33. Rinnan, Å.; van den Berg, F.; Engelsen, S.B. Review of the most common pre-processing techniques for near-infrared spectra. *TrAC Trends Anal. Chem.* **2009**, *28*, 1201–1222.
34. Barnes, R.; Dhanoa, M.; Lister, S. Standard Normal Variate Transformation and De-trending of Near-Infrared Diffuse Reflectance Spectra. *Appl. Spectrosc.* **1989**, *43*, 772–777.
35. Dhanoa, M.; Lister, S.; Barnes, R. On the scales associated with near-infrared reflectance difference spectra. *Appl. Spectrosc.* **1995**, *49*, 765–772.
36. Savitzky, A.; Golay, M. Smoothing and differentiation of data by simplified least squares procedures. *Anal. Chem.* **1964**, *36*, 1627–1639.
37. Williamson, R.; Bartlett, P. New support vector algorithms. *Neural Comput.* **2000**, *12*, 1207–1245.
38. Chang, C.C.; Lin, C.J. LIBSVM: A library for support vector machines. *ACM Trans. Intell. Syst. Technol.* **2011**, *2*, doi:10.1145/1961189.1961199.
39. Hall, M.; Frank, E.; Holmes, G.; Pfahringer, B.; Reutemann, P.; Witten, I.H. The WEKA data mining software: An update. *ACM SIGKDD Explor. Newsl.* **2009**, *11*, 10–18.
40. Galet, P. *A practical Ampelography*; Cornell University Press: New York, NY, USA, 1979.
41. Pelsy, F.; Hocquigny, S.; Moncada, X.; Barbeau, G.; Forget, D.; Hinrichsen, P.; Merdinoglu, D. An extensive study of the genetic diversity within seven French wine grape variety collections. *Theor. Appl. Genet.* **2010**, *120*, 1219–1231.
42. Altube, H.; Cabello, F.; Ortiz, J. Caracterización de variedades y portainjertos de vid mediante isoenzimas de los sarmientos. *Vitis* **1991**, *30*, 203–212.
43. Gutiérrez, S.; Tardaguila, J.; Fernández-Novales, J.; Diago, M.P. Support vector machine and artificial neural network models for the classification of grapevine varieties using a portable NIR spectrophotometer. *PLOS ONE* **2015**, *10*, doi: 10.1371/journal.pone.0143197.
44. Yang, X.; Hong, H.; You, Z.; Cheng, F. Spectral and Image Integrated Analysis of Hyperspectral Data for Waxy Corn Seed Variety Classification. *Sensors* **2015**, *15*, 15578–15594.
45. Sánchez, M.T.; de la Haba, M.J.; Benítez-López, M.; Fernández-Novales, J.; Garrido-Varo, A.; Pérez-Marín, D. Non-destructive characterization and quality control of intact strawberries based on NIR spectral data. *J. Food Eng.* **2012**, *110*, 102–108.
46. Pérez-Marín, D.; Paz, P.; Guerrero, J.E.; Garrido-Varo, A.; Sánchez, M.T. Miniature handheld NIR sensor for the on-site non-destructive assessment of post-harvest quality and refrigerated storage behavior in plums. *J. Food Eng.* **2010**, *99*, 294–302.
47. Shenk, J.S.; Workman, J.J.; Westerhaus, M.O. Application of NIR spectroscopy to agricultural products. *Pract. Spectrosc. Ser.* **2001**, *27*, 419–474.
48. Diago, M.; Pou, A.; Millan, B.; Tardaguila, J.; Fernandes, A.; Melo-Pinto, P. Assessment of grapevine water status from hyperspectral imaging of leaves. *Acta Hortic.* **2014**, *1038*, 89–96.
49. Brereton, R.G. *Applied Chemometrics for Scientists*; John Wiley & Sons: New York, NY, USA, 2007.
50. Wong, T.T. Performance evaluation of classification algorithms by *k*-fold and leave-one-out cross validation. *Pattern Recognit.* **2015**, *48*, 2839–2846.

Chapter 4

Machine learning and thermal imaging for vineyard water status monitoring

As exposed in Section 3.2, vineyard water status assessment is an extremely important aspect, especially in the current context of climate change. Many works have been published demonstrating the utility of thermal imaging for plant water status assessment, due to the physiological relation between grapevine water stress and canopy temperature. Nevertheless, almost all works published only report correlations between thermal indices and water status values that, although high, are hardly applicable for the prediction of new samples. ML algorithms are ideal for the training of prediction models from a specific set of variables, like data gathered from a thermal camera. In the following paper, the objective was the use of ML and data captured with a thermal camera mounted on an ATV for vineyard water status monitoring, developing a new ML prediction model using measurements from several phenological stages within the same campaign. Good prediction models were obtained from the experiments, while the best statistical values were yielded by models that did not need the measurement of reference temperatures. Therefore, thermal indices were not needed to obtain acceptable prediction models. The outcomes obtained with the combination of thermal images and ML expose this methodology as a promising alternative for the on-the-go water status monitoring of great areas under field conditions, demonstrating its utility for many industrial applications.

Overcome challenges

- To exploit the combination of ML techniques for the development of several water status prediction models, instead of simple correlations between thermal indices and water stress indicators.

- To use a thermal camera in a moving ground vehicle under field conditions for plant water assessment.
- To use ML modelling with data from seven weeks to perform prediction tasks at any time within a campaign.

Paper information

- **Title of the publication**: Vineyard water status assessment using on-the-go thermal imaging and machine learning
- **Authors:** Salvador Gutiérrez, María P. Diago, Juan Fernández-Novales, Javier Tardáguila
- **Published in:** PLOS ONE 13(2), e0192037
- **DOI:** 10.1371/journal.pone.0192037

Contributions of the PhD Thesis' author: Salvador Gutiérrez contributed to the experimental design and data acquisition in the field. He also performed data pre-processing, analysis and machine learning modelling. Salvador Gutiérrez wrote the full text of the paper during all review stages.

PLOS ONE

RESEARCH ARTICLE

Vineyard water status assessment using on-the-go thermal imaging and machine learning

Salvador Gutiérrez, María P. Diago, Juan Fernández-Novales, Javier Tardaguila*

Instituto de Ciencias de la Vid y del Vino (University of La Rioja, CSIC, Gobierno de La Rioja), Finca La Grajera, Ctra. Burgos Km. 6, 26007 Logroño, Spain

* javier.tardaguila@unirioja.es

OPEN ACCESS

Citation: Gutiérrez S, Diago MP, Fernández-Novales J, Tardaguila J (2018) Vineyard water status assessment using on-the-go thermal imaging and machine learning. PLoS ONE 13(2): e0192037. https://doi.org/10.1371/journal.pone.0192037

Editor: Hernâni Gerós, Universidade do Minho, PORTUGAL

Received: March 6, 2017

Accepted: December 27, 2017

Published: February 1, 2018

Data Availability Statement: Data are available at DOI: 10.6084/m9.figshare.5808720.

Funding: This work is part of the RESOLVE project, for which the authors acknowledge the financial support provided by transnational funding bodies, being partners of the FP7 ERA-net project, CORE Organic Plus, and the cofund from the European Commission. Salvador Gutiérrez would like to acknowledge the research founding Formación para el Personal Investigador grant 299/2016 by Universidad de La Rioja, Gobierno de La Rioja. Dr.

Abstract

The high impact of irrigation in crop quality and yield in grapevine makes the development of plant water status monitoring systems an essential issue in the context of sustainable viticulture. This study presents an on-the-go approach for the estimation of vineyard water status using thermal imaging and machine learning. The experiments were conducted during seven different weeks from July to September in season 2016. A thermal camera was embedded on an all-terrain vehicle moving at 5 km/h to take on-the-go thermal images of the vineyard canopy at 1.2 m of distance and 1.0 m from the ground. The two sides of the canopy were measured for the development of side-specific and global models. Stem water potential was acquired and used as reference method. Additionally, reference temperatures T_{dry} and T_{wet} were determined for the calculation of two thermal indices: the crop water stress index (CWSI) and the Jones index (I_g). Prediction models were built with and without considering the reference temperatures as input of the training algorithms. When using the reference temperatures, the best models casted determination coefficients R^2 of 0.61 and 0.58 for cross validation and prediction (RMSE values of 0.190 MPa and 0.204 MPa), respectively. Nevertheless, when the reference temperatures were not considered in the training of the models, their performance statistics responded in the same way, returning R^2 values up to 0.62 and 0.65 for cross validation and prediction (RMSE values of 0.190 MPa and 0.184 MPa), respectively. The outcomes provided by the machine learning algorithms support the use of thermal imaging for fast, reliable estimation of a vineyard water status, even suppressing the necessity of supervised acquisition of reference temperatures. The new developed on-the-go method can be very useful in the grape and wine industry for assessing and mapping vineyard water status.

Introduction

Water utilization has become a critical issue in sustainable agriculture, and because of reasons such as water scarcity and climate change, its management is increasingly required to be more accurate. In viticulture, irrigation has a direct impact on vine yield and grape quality, so the implementation of precision watering systems could be considered as useful tools for the

Maria P. Diago is funded by the Spanish Ministry of Economy, Industry and Competitiveness (MINECO) with a Ramon y Cajal grant RYC-2015-18429.

Competing interests: The authors have declared that no competing interests exist.

precise application of water regimes based on water status reports of the vineyard plot [1]. Several authors have studied different physiological parameters for the monitoring of the plant water status [2±4], and the direct measurement of the plant has been widely put into action for the measurement of the water status, instead of moisture measurements of the soil [5]. A key factor in the precise water management in vineyards may lie on the development of reliable tools for assessing the vine water status and its spatial variation directly in the field. This goal is virtually unreachable by the classical measurement devices due to their labor demanding, time-consuming nature and necessity of expert and trained personnel.

Infrared thermography is a technique based on the relationship between leaf stomatal closure or aperture and its surface temperature [6]. When leaf transpires, water is lost through stomata and leaf temperature decreases. However, if transpiration stops, leaf temperature increases as no heat dissipation is ocurring. Likewise, the temperature of the canopy has been correlated with specific plant physiological parameters, such as the stomatal conductance (g_s) [5, 7±9]. Technological advances in thermal imaging have delivered new opportunities in the acquisition of plant thermal responses to water status variations [8, 10±12]. In this fashion, thermal cameras are very prone to be used as portable devices for the estimation of plant water status and to help in the set up of irrigation schedules [10, 13, 14]. Still, further advancement based on canopy temperature has led to the development of thermal indices, such as the crop water stress index (CWSI) [15] and the conductance index (I_g) [6], thatÐby previously taking reference temperaturesÐseek for the diminishing of environmental variations that could affect the canopy temperature. As a result, several studies exploring semi-supervised irrigation scheduling system based on thermal information have been recently published [16±18]. Nevertheless, in the majority of the cases, the computation of thermal indices relies on mandatory acquisitions of edge temperatures, typically T_{wet} and T_{dry} for minimal and maximal temperatures, respectively, with the need of inducing extreme temperatures using adapted leaves or special devices [9]. This hinders the development of fully automated thermal methods for the estimation of plant water status. Hence, the overcome of the measurement of reference temperatures would stand for a substantial improvement in this matter in order to automate this technology in industrial applications.

In-field, non-invasive assessment of grapevine water status and its variability within the vineyard would be a valuable tool in precision viticulture. Correlation analyses between thermal indices and physiological parameters such as g_s and stem water potential Ψ_{stem} have been carried out in the field using non-destructive portable sensors in commercial vineyards bringing compelling correlation levels [19, 20]. The main advantages these methods brought were the easy implementation and processing and immediate response. Nonetheless, it is needed for the device to be constantly managed by active human resources and it is only possible to make measurements on individual specific spots, factors that would make it difficult to expand the measurements for the fast monitoring of a whole vineyard. This main pitfall has been partially resolved by aerial thermal imaging [21±24], that successfully covered large extensions of vineyard. However, in the majority of cases the aerial point of view comes with a reduced spatial resolution in the measurements that shrink several meters of the canopy into a few number of pixels, losing a definite amount of information. This brings the opportunity of developing thermal systems for the grapevine water status estimation capable of gathering detailed canopy informationÐfrom a close lateral point of viewÐand to cover large areas for the monitoring of a vineyard variabilityÐusing stop-and-go and on-the-go approaches, as already attempted by other works [25, 26]. Moreover, the removal of constant human supervision would allow the possibility of mounting automatic acquisition systems in on-work agricultural vehicles.

The demonstrated high level of performance machine learning has provided in a vast number of problems from very different nature presents it as one of the most important algorithm-

provider research field. Regardless the area, if the problem can be properly modeled into an adequate input, machine learning algorithms could be very suitable for the discovering of underlying rules and latent connections between the provided information, for the categorization into specific identities (classification) or the estimation of real numbers (regression) [27, 28]. In recent years, several viticulture-related problems have been addressed using data mining and machine learning approaches [29±33]. Rotation forests [34] are prediction algorithms based on ensemble learning methods that can perform classification or regression tasks depending on the tree-based algorithm provided. Rotation forests build several trees after making use of principal component analysis to the randomly split input attributes.

The goal of this study was to develop a new on-the-go system involving thermal imaging and machine learning to assess the vineyard water status. Specifically, the objective was not only to analyze and find high levels of correlations between thermal information and physiological water status parameters, but to provide full trained, robust prediction models. These are fed with a huge amount of data from a wide period of time that covered an entire campaign, and are capable to return reliable estimations for the characterization of a whole vineyard plot and to be used in the irrigation decision making process.

Materials and methods

Experimental layout

The experiment was performed throughout seven weeks from early-July to early-September, 2016, in a 5 ha commercial vineyard of Tempranillo variety (*Vitis vinifera* L.) under permission of its owner. The vineyard plot was situated in Tudelilla, La Rioja, Spain (Lat. 42Ê18' 18.26º, Long. -2Ê7' 14.15º, Alt. 515 m). Grapevines, planted in 2002, were grafted on rootstock R-110 and trained to a vertically shoot-positioned (VSP) trellis system, having a North-South row orientation at 2.60 × 1.20 meters inter and intra row distances. To induce an extensive level of variability in the sample units and to obtain better trained prediction models, three different water regimes were deployed in a randomized complete block design [35] with four blocks (Fig 1). The three water treatments were:

- T0, full irrigation: two parallel water pipelines providing 6 L/h.
- T1, moderate irrigation: one water pipeline providing 3 L/h.
- T2, no irrigation: the plants were not irrigated during the whole experiment.

Irrigation was scheduled to be applied two hours per day, five days a week.

Each treatment involved four replications, therefore 12 different combinations of treatment and replication were present in the vineyard and located in three different parallel, equally-distanced vine rows. For each replication, comprising 25 plants (around 25 m of length), only the 15 middle ones were the ones in which the measurements were taken. The first and last groups of five plants were discarded to avoid edge effect (Fig 2A).

Acquisition of thermal images

On-the-go thermal measurements were acquired using a thermal camera (FLIR A35, FLIR® Systems, Inc., Bilerica, MA, USA) that was mounted in the front part of an all-terrain vehicle at a height from the floor of 1 m (Fig 2B) and connected to an industrial computer. The individual in this manuscript has given written informed consent (as outlined in PLOS consent form) to publish these case details. The camera was focused to the left at a distance from the canopy of approximately 1.2 m and with 48Ê× 39Êhorizontal and vertical field of views (FOV,

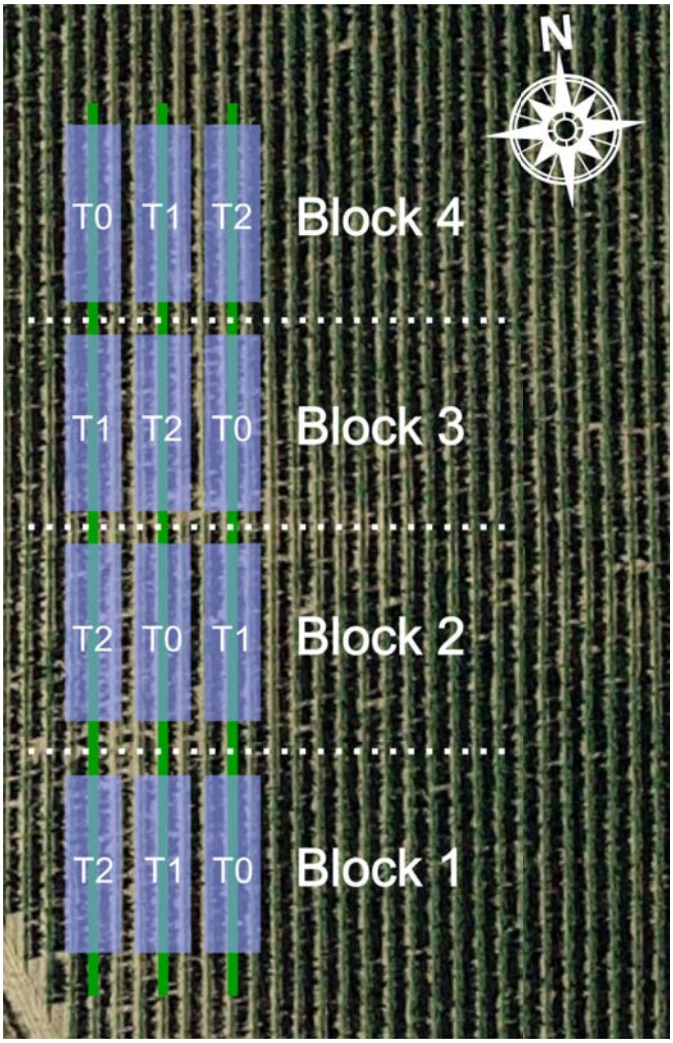

Fig 1. Experimental layout and water treatment replications. Each one of the four horizontal blocks comprised the three different water regimes applied. T0: full irrigation treatment. T1: moderate irrigation treatment. T2: no irrigation treatment.

https://doi.org/10.1371/journal.pone.0192037.g001

Fig 2A), respectively. This distance and FOVs provided images covering canopy scenes of 1.07 m horizontally and 0.85 m vertically, approximately. Acquisition of the thermal images, at 60 frames per seconds (FPS), was performed in both east and west sides of the canopy at an average speed of 5 km/h at solar noon (between 14:00 and 15:00 hours, local time).

Thermal images processing

At a recording framerate of 60 FPS, a treatment replication's length of 25 m and an average speed of 5 km/h, the number of thermal frames captured per each replication was approximately

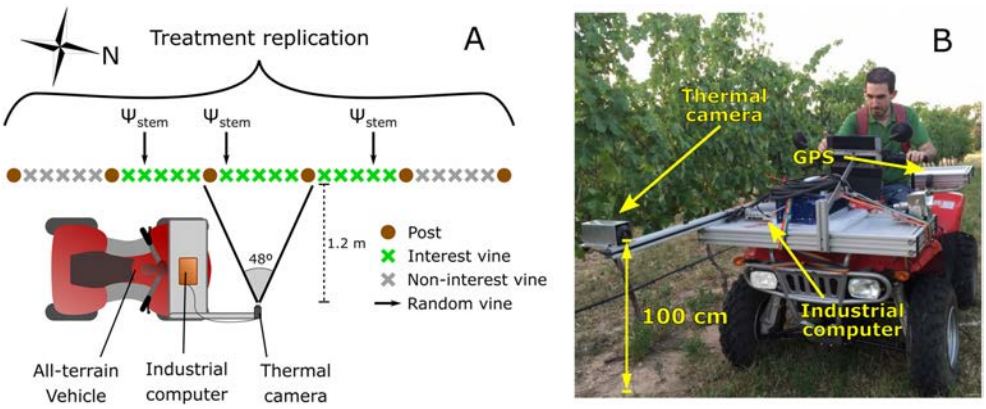

Fig 2. Detail from a treatment replication and thermal system (A) and picture of the actual on-the-go system (B). The thermal camera was connected to an industrial computer and controlled by the driver.

https://doi.org/10.1371/journal.pone.0192037.g002

1080. In order to reduce the amount of redundant information, not every frame from the recordings was used in the processing of the imagesÐonly those frames having no overlapping were thus used for the calculation of different thermal statistics. If a treatment block of 25 m length is covered by 1080 frames, and each frame displayed approximately a horizontal length of 1.07 m, one out of 46 consecutive frames would have no overlapping. Thus, each treatment replication consisted of roughly 23 frames, and only the 14 middle ones were used since they comprised the 15 middle plants of the replication (the plants in which the water status measurements were taken).

To support the thermal images segmentation and develop different canopy temperature indices, T_{wet} and T_{dry} reference temperatures were acquired using an evaposensor (Skye Instruments, Llandrindod Wells, UK) having two artificial leaves: a dry one (dry reference) and another one covered with a black cotton wick and receiving continuous water absorption for the wet reference [36]. Reference temperatures were acquired once per each measurement day.

To remove the influence of the sky, soil and fruiting zone in the top and bottom part of the thermal images respectively, the middle section of the thermal images was selected, named as area of interest, and used for the calculation of the different statistics and thermal indices (Fig 3). The area of interest had a size of 320 × 135 pixels, from a total image resolution of 320 × 256 pixels.

The average temperature (T_{canopy}), the median and the standard deviation were the statistics extracted from the thermal frames. Additionally, two thermal indices, the crop water stress index (CWSI) and the conductance index (I_g) were calculated, using the reference temperatures, as follows, according to [37] and [6], respectively:

$$CWSI = \frac{T_{canopy} - T_{wet}}{T_{dry} - T_{wet}} \quad (1)$$

$$I_g = \frac{T_{dry} - T_{canopy}}{T_{canopy} - T_{wet}} \quad (2)$$

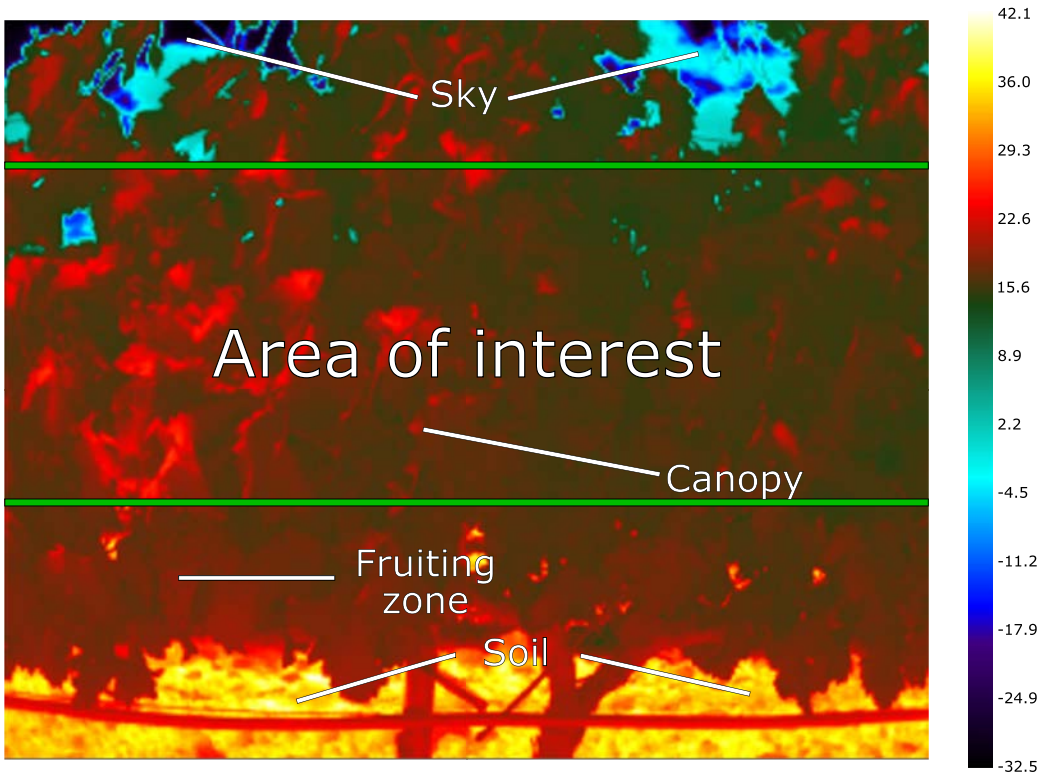

Fig 3. Canopy thermal image taken on-the-go at 5 km/h. The middle section between the green bars was defined as the area of interest. Total image resolution was 320 × 256 pixels, while the area of interest had a size of 320 × 135 pixels. The temperature values are expressed in degrees Celsius.

https://doi.org/10.1371/journal.pone.0192037.g003

FLIR ResearchIR 4.40 (FLIR® Systems, Inc., Billerica, MA, USA) and MATLAB 8.5.0 (The MathWorks Inc., Natick, MA, USA) were used for the processing of the thermal images.

Measurement of grapevine water status

Plant water status measurements were also performed at solar noon (between 14:00 and 15:00 hours, local time) simultaneously to thermal image acquisition. During the whole campaign, the air temperature, relative humidity (for vapor pressure deficit (VPD) calculation [38]) and incoming solar irradiance were additionally recorded in the same hours from a weather station located in the vineyard. The reference method used for the measurement of the plant water status was the midday stem water potential Ψ_{stem}. As shown in Fig 2A, a random vine was selected from each group of five plants (of the 15 middle ones in each replication) and its Ψ_{stem} was measured upon a leaf taken from the central part of the canopy. A Scholander pressure bomb (Model 600, PMS, Instruments Co., Albany, NY, USA) was used for the stem water potential determination [39]. The selected leaves were covered with aluminum foil bags to drive them into dark adaptation one hour before the measurements.

With 12 different replications and three selected plants per block, a total of 36 measurements of the plant water status were performed per day. Therefore, since the study was

conducted across seven different weeks, and one day per week, a total of 252 water status measurements were used for the training of the prediction models.

Machine learning algorithms and model development

Two different approaches were attempted for the extraction of the statistics that trained the prediction models: the use of T_{dry} and T_{wet} reference values for segmentation of the area of interest (the removal of all temperatures outside the T_{wet} and T_{dry} range) and calculation of thermal indices; and the extraction of the same statistics without segmentation and avoiding the calculation of the thermal indices.

A combination of rotation forests and decision trees (reduced error pruning tree, Weka's REPTree implementation [40]) was used for the development of the regression models. Two kind of models were built:

- **Using T_{dry} and T_{wet} reference temperatures and thermal indices**, with the following input attributes: air temperature, average canopy temperature, median of the canopy temperature, standard deviation of the canopy temperature, CWSI and I_g.
- **Avoiding the use of reference temperatures and thermal indices**, with the following input attributes: air temperature, average canopy temperature, median of the canopy temperature and standard deviation of the canopy temperature.

In both cases, the Ψ_{stem} was used as the plant water status reference value to predict.

Side-specific models for east and west sides of the canopy were individually built, each one including 252 samples. Additionally, a global dataset comprising samples from both east and west sides of the canopy was also generated. This global set was intended to be as similarly represented as those datasets from east and west side, therefore 126 samples from the east dataset and the same amount from the west dataset were picked to build a global set with 252 samples. This selection was pseudorandomly performed, taking the same amount of samples per canopy side, water regime and measurement day, in order to build a model from a well-represented input data.

In order to provide a complete set of performance statistics, calibration, 10-fold cross-validation and external prediction were carried out. The datasets were not completely used for the training of the regression models, but they were split in a 80-20 ratio, labeling the two originated subsets as train (80% of the original dataset) and test (the remaining 20%) sets. This division was not totally random. Samples representing the whole range of the stem water potential values obtained were extracted to the test set, also taking the same number of samples per measurement day. The calibration and cross validation were performed using the train set, while the prediction was achieved by training the model with the train set and predicting the test set.

Results

Vineyard status overview

A wide range of stem water potential values was covered throughout the whole experiment, obtaining Ψ_{stem} values at midday of the 252 samples from -2.05 MPaÐmeaning high level of water stressÐto -0.40 MPaÐno stress. The mean and standard deviation Ψ_{stem} values of -1.23 MPa and 0.298 MPa confirmed a high level of variability desirable for the development of representative plant water status prediction models.

Table 1 shows an overview by days in terms of VPD, incoming solar irradiance, canopy temperatures recorded by thermal imaging and Ψ_{stem} values.

Table 1. Mean values according to measurement days for vapor pressure deficit (VPD), incoming solar irradiance, canopy temperatures (by canopy side and irrigation treatment) and stem water potential (Ψ_{stem}) determined at solar noon, between 14:00 and 15:00. *N* = 12 per irrigation treatment for the statistical tests of canopy temperatures and Ψ_{stem} (MPa).

		Jul, 6	Jul, 13	Jul, 20	Jul, 28	Aug, 11	Aug, 23	Sep, 8
VPD (kPa)		2.71	1.11	2.49	3.22	1.77	3.43	1.28
Irradiance (W/m^2)		890.95	631.82	348.61	895.11	841.89	827.01	291.30
East temp. (ÊC)	**T0**	20.7	15.6	24.6	23.5 A	17.2	25.4 A	19.4 A
	T1	22.2	16.3	25.1	24.9 B	16.8	27.1 B	19.6 A
	T2	22.1	16.4	24.8	23.2 A	16.7	27.9 B	20.5 B
		n.s.	*n.s.*	*n.s.*	**	*n.s.*	***	***
West temp. (ÊC)	**T0**	22.5	16.0	24.7	25.2	16.8 A	26.8 A	20.4 A
	T1	23.8	16.9	25.2	27.0	17.4 B	28.5 B	20.5 A
	T2	22.6	16.1	25.4	25.5	18.0 C	29.1 B	21.1 B
		n.s.	*n.s.*	*n.s.*	*n.s.*	***	***	**
Ψ_{stem} (MPa)	**T0**	-0.97 A	-1.04 A	-1.00 A	-1.18 A	-1.19 A	-1.13 A	-0.56 A
	T1	-1.15 B	-1.28 B	-1.25 B	-1.26 AB	-1.47 B	-1.41 B	-0.96 B
	T2	-1.14 B	-1.22 B	-1.31 B	-1.31 B	-1.52 B	-1.65 C	-1.76 C
		***	***	***	**	***	***	***

Jul: July. Aug: August. Sep: September.

Dissimilar capital case letters within columns represent statistically different means among east and west temperatures and Ψ_{stem}, using Tukey's range test at a significance level p = 0.05.

n.s.: not significant ($p \geq 0.05$);

**: $p < 0.01$;

***: $p < 0.001$.

https://doi.org/10.1371/journal.pone.0192037.t001

VPD values ranged from 1.11 kPa (July 13th) to 3.43 kPa (August 23rd) while irradiance values were found to be above 800 W/m^2 for most of the measuring dates, with the exception of the 13th and 20th of July, and the 8th of September. The values observed in the last date can be explained by the generalized meteorological behavior in the end of the season, as a decrease of irradiance and temperatures is prone to be found. Canopy temperatures were generally distinguishable between treatments, presenting slightly higher values in the west side. Additionally, the water status values presented an increasing trend throughout the summer as a consequence of season progress and water treatments' effectiveness.

Statistically significant differences between the temperatures of the irrigation treatments were not found for either east or west sides in the first three days, while they were present in the last two ones. In July 28th, the east side of the canopy casted significant differences, while the west side did not, but the opposite occurred in August 11th. In the case of Ψ_{stem}, all the dates presented statistically significant differences between the most extreme irrigation treatments (T0 and T2) while for the last two dates all three treatments were significantly different.

Vineyard water status prediction models using T_{dry} and T_{wet} reference temperatures

The performance statistics of the prediction models trained with thermal indices are summarized in Table 2 for east and west models, and additionally for the global model trained with samples from both sides of the canopy.

For the models built with the thermal information from the east side of the canopy, determination coefficients R^2 of 0.83 and 0.61 were obtained for calibration and cross validation, casting RMSE values of 0.139 MPa and 0.190 MPa, respectively (Table 2). The performance of

Table 2. Performance statistics for the stem water potential (Ψ_{stem}) prediction models using T_{dry} and T_{wet} reference temperatures.

	N = 200				N = 50	
	Calibration		Cross validation		Prediction	
Canopy side	R^2	RMSE	R^2	RMSE	R^2	RMSE
East	0.83	0.139	0.61	0.190	0.57	0.206
West	0.81	0.148	0.57	0.202	0.58	0.204
Global	0.73	0.182	0.39	0.237	0.52	0.233

A 10-fold cross validation was used.

N: number of samples. RMSE: root mean square error (MPa). East: dataset having all the samples from the east side of the canopy. West: dataset having all the samples from the west side of the canopy. Global: dataset having non-repeated samples from both east and west sides of the canopy.

https://doi.org/10.1371/journal.pone.0192037.t002

the prediction stage did not lied far from that of the cross validation, producing a R^2 value of 0.57 and a RMSE of 0.206 MPa.

The results given by the west side models remained fairly similar, with a calibration R^2 of 0.81 (RMSE of 0.148 MPa) and a cross validation R^2 of 0.57 (RMSE of 0.202 MPa), being the latter slightly lower than that from the east side models. The prediction result was 0.58 for the determination coefficient with a root mean square error of 0.204 MPa (Table 2).

The performance achieved by the global models was lower in all the stages: calibration, cross validation and prediction, although in this last case the determination coefficient was closer to the ones from east and west models, as opposed to calibration and cross validation. Nevertheless, the RMSE values of cross validation and prediction remained very similar: 0.237 and 0.233 MPa respectively.

The regression plots for the cross validation and prediction results for east and west models are displayed in Fig 4. In Fig 4A, a high distribution along the measured Ψ_{stem} values was achieved, and few samples fell outside the 95% prediction bands. The regression plot of the cross validation from the west side (Fig 4C) followed the same trend as well, having a good distribution throughout the whole water potential range. Additionally, the higher spreading level of the samples from the 1:1 line in Fig 4C drove the increased RMSE value of the west side model presented in Table 2.

The prediction plots for both east and west sides (Fig 4) displayed a virtually identical behavior, in terms of determination coefficient and root mean square errors. In Fig 4B, all the samples but one were located within the 95% prediction bands, and a wide coverage throughout the Ψ_{stem} range was scored (values from -2.1 to -0.4 MPa). Regarding the prediction plot considering the west side of the canopy, two samples lied outside the prediction bands, but a very similar fit around the regression line was achieved by the samples, casting a coincident R^2 value (Table 2).

A statistical t-test analysis of the slopes showed no significant differences between the equations of each side for both cross validation ($p = 0.47$) and prediction ($p = 0.86$).

Vineyard water status prediction models without T_{dry} and T_{wet} reference temperatures

Table 3 shows the statistics obtained by the stem water potential models that were trained without the reference temperatures.

The determination coefficients R^2 obtained for the calibration process were above the 0.80 mark (0.83 for east and 0.81 for west), with RMSEs of 0.136 and 0.142 MPa, respectively. R^2 values around 0.60 were achieved in the cross validation, with very similar RMSE values around 0.190 MPa for both canopy sides. The prediction results were slightly better than those

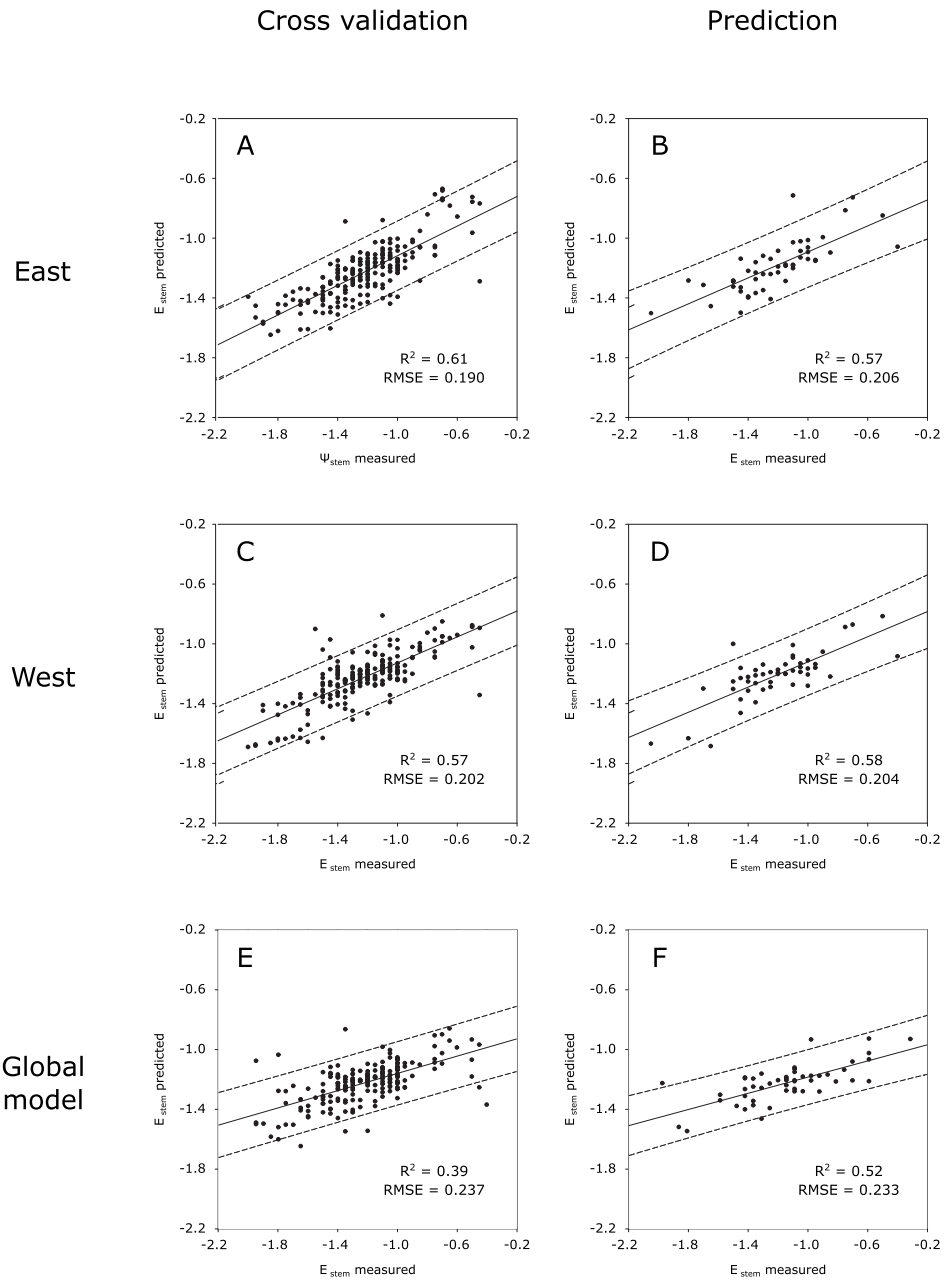

Fig 4. Regression plots for the water status prediction models with T_{dry} and T_{wet} reference temperatures. Plots from east (A, B) and west (C, D) sides of the canopy and from the global model trained with data from both sides (E, F); and for cross validation (A, C, E) and prediction (B, D, F). The dashed lines are the prediction confidence bands at 95%. The dotted lines represent the 1:1 line with slope 1.

https://doi.org/10.1371/journal.pone.0192037.g004

Table 3. Performance statistics for the stem water potential (Ψ_{stem}) prediction models without the use of T_{dry} and T_{wet} reference temperatures.

	N = 200				N = 50	
	Calibration		Cross validation		Prediction	
Canopy side	R^2	RMSE	R^2	RMSE	R^2	RMSE
East	0.83	0.136	0.59	0.195	0.60	0.191
West	0.81	0.142	0.62	0.190	0.65	0.184
Global	0.75	0.170	0.45	0.224	0.56	0.216

A 10-fold cross validation was used.

N: number of samples. RMSE: root mean square error (MPa). East: dataset having all the samples from the east side of the canopy. West: dataset having all the samples from the west side of the canopy. Global: dataset having non-repeated samples from both east and west sides of the canopy.

https://doi.org/10.1371/journal.pone.0192037.t003

of cross validation, in terms of R^2 and RMSE: 0.60, 0.191 MPa (east side) and 0.65, 0.184 MPa (west side, Table 3). The performance statistics obtained from the global models were lower than those from the site-specific datasets.

Comparing these outcomes with those from the models trained with the reference temperatures, the statistics were very similar in the calibration and cross validation, but the models without T_{dry} and T_{wet} brought better R^2 and RMSE values in the prediction. In the calibration, both kind of models achieved the same R^2 values (and almost identical RMSEs), while in the cross validation the best statistics came from the west side models, being the opposite in the models with reference temperatures (Table 2). Still, these values followed the same overall trend.

The regression plots for the cross validation and prediction models trained without T_{dry} and T_{wet} reference temperatures (for east, west and both sides) are grouped in Fig 5.

The cross validation outcomes covered a high Ψ_{stem} range, with samples along the whole range (Fig 5A and 5C) and similar distribution around the 1:1 line. This resulted in similar RMSE values (Table 3). Additionally, the R^2 values were nor far from each other, driven by the almost identical trend from the regression lines (as no significant differences were found between the slopes of both sides' equations, for both cross validationÐ $p = 0.93$Ðand predictionÐ $p = 0.89$).

In Fig 5B and 5D, displaying the regression plots for the prediction results, higher determination coefficients can be found comparing to those from the prediction outcomes of the models trained with the reference temperatures (Fig 4B and 4D). Nevertheless, contrary to the latter, in this case the best results came from the west side of the canopy instead of the east side, with a higher fit to the regression line (meaning a higher R^2 value) and a lower RMSE value (meaning a lower average distance of the samples from the 1:1 line).

Discussion

The results presented in this study highlight the actual prospect of obtaining on-the-go, fast assessment of a vineyard's water status directly on the field using proximal thermal imaging and machine learning algorithms. On-the-go assessment has a big advantages *vs*. other developed techniques for plant water status assessment or direct measurement of plant-based reference parameters [4], that are slower, manually controlled and with a lower capability of automatically characterizing a whole vineyard plot. It has also been proven that machine learning models, trained with data from seven days along a whole campaign, were capable of yielding plant water status prediction without the need of taking previous reference temperatures. This would allow a fastest, direct usage of this solution for in-field scenarios. The outcomes obtained using the models trained with reference temperatures demonstrated that canopy

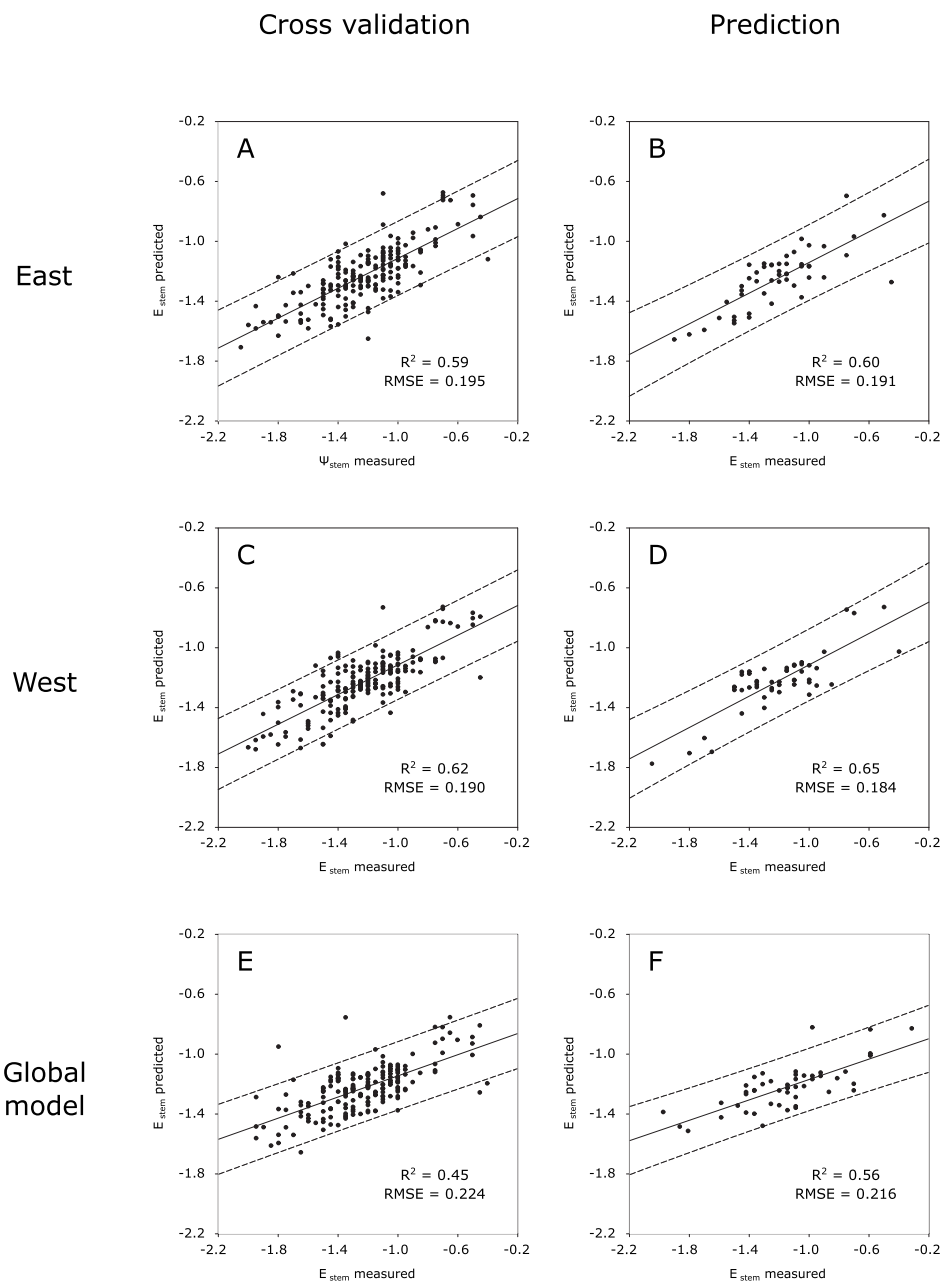

Fig 5. Regression plots for the water status prediction models without thermal indices. Plots from east (A, B) and west (C, D) sides of the canopy and from the global model trained with data from both sides (E, F); and for cross validation (A, C, E) and prediction (B, D, F). The dashed lines are the prediction confidence bands at 95%. The dotted lines represent the 1:1 line with slope 1.

https://doi.org/10.1371/journal.pone.0192037.g005

temperatures, along with T_{dry} and T_{wet} and weather parameters (such as the air temperature), would be very suitable for the useful prediction of the vineyard water status. Furthermore, the fact that similar results in cross validation (and even better outcomes in prediction) were achieved by the models trained without reference temperatures, brought high robustness into the models. This could allow to affirm that their implementation in industry and commercial environments is greatly feasible, also removing the necessity of the reference temperature measurement phaseÐand the calculation of thermal indices.

The relation between environmental status and canopy thermal response was clearly displayed throughout the whole experiment. Incoming solar irradiance casted high values most of the days, positively correlating with the high temperatures of the canopy in both sides. Nevertheless, two specific dates did not follow this trend, as in July 20th the canopy temperatures were particularly high for the relatively low irradiance received, and in August 11th the temperatures stayed very low regardless of the high amount of solar irradiance captured. This behavior seemed to be in contradiction with the expected response, but it is clearly explained by the VPD factor. As previously observed by other authors [11, 22, 41±43], VPD has a strong relationship with stomatal conductance and canopy temperature. In the case of July 20th, in spite of the low irradiance value, the increase of leaf temperature was mainly driven by the increase of VPD. Likewise, when the VPD, hence the evaporative demand increases, so does the actual rate of water vapor exchange through the leaf stomata. In this situation, the plant regulates this water loss by closing their stomata, leading to leaf temperature increase. On the other hand, in August 11th the low VPD value may not have led to stomata closure, hence leaf evapotranspiration was not impaired, and let the plants to cool down their leaf surface. Reported in other works [11, 41, 44], it exists a general correlation between VPD and water status, as higher VPD values limit the plants' capability of a proper transpiration, although in the case of the present study the plant water status is mainly steered by the applied water regimes rather than the VPD. All these physiological behaviors confirm the usefulness of measuring the canopy temperature to assess the water status of a vineyard.

A good effectiveness was accomplished in canopy side-specific models. The vineyard plot in which the experiment was conducted had a North-South row orientation, soÐat measurement time (between 14:00 and 15:00, local time)Ðthe east side was shaded but with a whole morning of direct sunlight accumulated, while the west side started an afternoon of illumination from the sun. The row orientation does have a direct impact upon the canopy temperature and, thus, upon the plant response and acclimation [45]. Therefore, the development of two distinct models for each side of the canopy was a necessary step to allow the machine learning algorithms to adapt their rule extraction ability to the specific canopy thermal information that was present in each face. The fact that the global model provided poorer results could be explained by an assumed confused information given to the algorithms, as the plant thermal response would be very different for each side of the canopy. Still, the side-specific models were able to successfully develop adequate prediction rules for the two datasets and to cast similar performance statistics, demonstrating the possibility of a fairly acceptable water status estimation of a vineyard if the thermal measurements are taken from the same side of the canopy. In a real scenario, the development and implementation of two canopy side-specific models could be totally feasible and their application would only depend on the side of the input data.

The use of machine learning approaches for the grapevine water status estimation proved to be effective. It is visible the high suitability of machine learning algorithms for the solution of specific problemsÐgrapevine water status predictionÐbut from very different kinds of inputÐspectral information and thermal imaging. In the case of the latter, the variables used (thermal and weather data) were selected in order to provide a decent amount of information from a thermal image. Although small differences would be present between two of the

attributes used, mean and median of the canopy temperature, they could be sufficient for the algorithms to extract informative rules from them. Moreover, the use of principal component analysis by rotation forests would deal with potential cases of collinearity. Additionally, a desirable behavior was obtained from the machine learning models. The fact that considerably similar results were casted by cross validation and prediction increases the reliability of the techniques in their appraisal ability.

The relationship between leaf temperatureÐtaken directly in the fieldÐand water status of different kind of crops has been widely studied in diverse research works. For example, airborne thermal imaging has been used for the mapping of cotton water status (represented by the leaf water potential Ψ_{leaf}) [17], and the same authors attempted the estimation of water status of the same kind of crop using ground-based thermal images [16], obtaining good results. Although the models presented in the present study returned lower performance statistics than those from [16, 17], the prediction capability of the machine learning algorithms was greatly supported by the high amount of data and its wide variability. The input samples employed in the training of the models (from very different phenological stages) were able to develop a whole prediction model capable of making Ψ_{stem} predictions in different moments within a wide time period. In grapevine, as in the present work, CWSI along with air temperature were used for the mapping of the water status (Ψ_{leaf}) of a Pinot noir vineyard [21]. The same authors also studied the effect of different phenological stages in the evolution of the CWSI in grapevines [22]. In [46], the vineyard water status variability was monitored using aerial thermal and multispectral imagery. These studies, providing R^2 values from 0.50 to 0.73, along with the results presented in the current research work, confirm the strong correlation of the canopy temperature with the grapevine water status, being possible to find underlying rules for the appraisal of an important reference value, such as water potential. The results reported by other authors from aerial thermal imaging of grapevines, as in [23, 24] or [46] also opened the possibility of estimate water status using thermal information from a lateral view, that would allow to gather a richer amount of information than that from zenith point of view. Some comparable works based on lateral thermal imaging but in static and manual approaches can be found in the literature. In [19] and [20], the authors used thermal imaging laterally acquired in a commercial vineyard to correlate the thermal indices CWSI and I_g with different plant water status reference parameters, with R^2 values up to 0.78 and 0.70. The results from the on-the-go estimation of the grapevine water status represent an improvement not only regarding the possibility of quickly assessing and mapping a whole vineyard plot (instead of taking isolated thermal measurements), but also presenting a robust model trained with a collection of a high number of samples from different dates, and additionally removing the necessity of acquiring reference temperatures, using only the data provided by the canopy and air temperature.

The main pitfalls of other developed techniques plant water status assessment, such as the necessity of supervised measurement or the hard adaptation for the characterization of a whole vineyard plot makes on-the-go approaches a very suitable candidate for grapevine monitoring. The on-the-go proposal detailed in this work opens a large number of new opportunities in the implementation of this technological solution for the estimation of grapevine water status. Contrary to the developments that can be found in other related works, as in [19, 47, 48] or [49], involving manual and static measurements, the acquisition of thermal images from a moving vehicle expandsÐin the context of precision viticultureÐthe possibility of monitoring a whole vineyard plot in a faster and automated way. The delineation, for example, of different zones with homogeneous irrigation regimes could be feasible, and it could save higher amounts of water and money. Other plant water status estimation studies carried out with thermal imaging made use of information from aerial sources ([16, 17, 20±24]). Still, the

acquisition of canopy side-aimed data that covers a larger area may assure a higher robustness in the given prediction. Additionally, the temporal flexibility of the approach from the present work arises as an advantage *vs*. airborne solutions, due to the fact that aerial acquisitions are very subjected to meteorological conditions and legal requirements. An on-the-go implementation of the proposal in the present work would be easily deployed directly in the field. A thermal system could be installed in an agricultural vehicle (e.g. a tractor conducting different viticulture operations), making constant measurements and giving real-time information to the driver or the manager. This possibility of covering large areas of a vineyard also makes available, jointly to an attached global positioning system, the creation of thermal-based maps of the plot that could provide detailed information about the water status of the monitored zones, making it an useful tool for irrigation scheduling in the decision-making process.

Conclusion

The present work introduced a new methodology for the on-the-go assessment of vineyard water status using thermography and machine learning algorithms. The results obtained open a way for the implementation of a vineyard water status appraisal system available to be set up in a moving vehicle, given the fact that the use of data from a whole campaign for the training of the models brought stronger reliability. Also, good prediction results has been achieved without the need of reference temperatures, thus removing the requirement of the supervised acquisition of these values. This advantage could clear new paths in sustainable viticulture, making possible the deployment of solutions that could characterize in an automatic and continuous way a whole vineyard for a more accurate application of irrigation in viticulture, that is a very needed requirement in the current context of climate change and water scarcity.

Acknowledgments

The authors acknowledge Carlos Poblete for his support in the design of the experimental layout and Daniel Sepúlveda and Marjolaine Chatin for their help with the measurement of the stem water potential. Special thanks to Luis Angel García for his support and to Bodegas Vivanco, for providing the vineyard to conduct the study. This work is part of the RESOLVE project, for which the authors acknowledge the financial support provided by transnational funding bodies, being partners of the FP7 ERA-net project, CORE Organic Plus, and the cofund from the European Commission. Salvador Gutiérrez would like to acknowledge the research founding FPI grant 299/2016 by Universidad de La Rioja, Gobierno de La Rioja. Dr. Maria P. Diago is funded by the Spanish Ministry of Economy, Industry and Competitiveness (MINECO) with a Ramon y Cajal grant RYC-2015-18429.

Author Contributions

Conceptualization: Salvador Gutiérrez, Javier Tardaguila.

Data curation: Salvador Gutiérrez.

Funding acquisition: María P. Diago, Javier Tardaguila.

Investigation: Salvador Gutiérrez, María P. Diago, Juan Fernández-Novales, Javier Tardaguila.

Methodology: María P. Diago, Juan Fernández-Novales, Javier Tardaguila.

Project administration: María P. Diago, Javier Tardaguila.

Software: Salvador Gutiérrez.

Supervision: Javier Tardaguila.

Validation: Salvador GutiÊrrez.

Writing ± original draft: Salvador GutiÊrrez.

Writing ± review & editing: Salvador GutiÊrrez, MarÂa P. Diago, Juan FernÂndez-Novales, Javier Tardaguila.

References

1. Keller M. The science of grapevines: anatomy and physiology. Academic Press; 2015.
2. Acevedo-Opazo C, Tisseyre B, Guillaume S, Ojeda H. The potential of high spatial resolution information to define within-vineyard zones related to vine water status. Precision Agriculture. 2008; 9(5):285±302. https://doi.org/10.1007/s11119-008-9073-1
3. Acevedo-Opazo C, Tisseyre B, Taylor J, Ojeda H, Guillaume S. A model for the spatial prediction of water status in vines (Vitis vinifera L.) using high resolution ancillary information. Precision Agriculture. 2010; 11(4):358±378. https://doi.org/10.1007/s11119-010-9164-7
4. FernÂndez J. Plant-based sensing to monitor water stress: Applicability to commercial orchards. Agricultural water management. 2014; 142:99±109. https://doi.org/10.1016/j.agwat.2014.04.017
5. Jones HG. Irrigation scheduling: advantages and pitfalls of plant-based methods. Journal of experimental botany. 2004; 55(407):2427±2436. https://doi.org/10.1093/jxb/erh213 PMID: 15286143
6. Jones HG, Stoll M, Santos T, De Sousa C, Chaves MM, Grant OM. Use of infrared thermography for monitoring stomatal closure in the field: application to grapevine. Journal of Experimental Botany. 2002; 53(378):2249±2260. https://doi.org/10.1093/jxb/erf083 PMID: 12379792
7. Costa JM, Grant O, Chaves M. Use of thermal imaging in viticulture: current application and future prospects. Springer; 2010.
8. Costa JM, Grant OM, Chaves MM. Thermography to explore plantÐ environment interactions. Journal of Experimental Botany. 2013; 64(13):3937±3949. https://doi.org/10.1093/jxb/ert029 PMID: 23599272
9. Jones HG. Use of infrared thermometry for estimation of stomatal conductance as a possible aid to irrigation scheduling. Agricultural and forest meteorology. 1999; 95(3):139±149. https://doi.org/10.1016/S0168-1923(99)00030-1
10. Grant OM, Tronina è, Jones HG, Chaves MM. Exploring thermal imaging variables for the detection of stress responses in grapevine under different irrigation regimes. Journal of Experimental Botany. 2007; 58(4):815±825. https://doi.org/10.1093/jxb/erl153 PMID: 17032729
11. Costa JM, Ortuño MF, Lopes CM, Chaves MM. Grapevine varieties exhibiting differences in stomatal response to water deficit. Functional Plant Biology. 2012; 39(3):179±189. https://doi.org/10.1071/FP11156
12. Fuentes S, De Bei R, Pech J, Tyerman S. Computational water stress indices obtained from thermal image analysis of grapevine canopies. Irrigation Science. 2012; 30(6):523±536. https://doi.org/10.1007/s00271-012-0375-8
13. Jones HG, Leinonen I. Thermal imaging for the study of plant water relations. Journal of Agricultural Meteorology. 2003; 59(3):205±217. https://doi.org/10.2480/agrmet.59.205
14. Grant OM, Chaves MM, Jones HG. Optimizing thermal imaging as a technique for detecting stomatal closure induced by drought stress under greenhouse conditions. Physiologia Plantarum. 2006; 127(3):507±518. https://doi.org/10.1111/j.1399-3054.2006.00686.x
15. Idso S, Jackson R, Pinter P, Reginato R, Hatfield J. Normalizing the stress-degree-day parameter for environmental variability. Agricultural Meteorology. 1981; 24:45±55. https://doi.org/10.1016/0002-1571(81)90032-7
16. Cohen Y, Alchanatis V, Sela E, Saranga Y, Cohen S, Meron M, et al. Crop water status estimation using thermography: Multi-year model development using ground-based thermal images. Precision Agriculture. 2015; 16(3):311±329. https://doi.org/10.1007/s11119-014-9378-1
17. Cohen Y, Alchanatis V, Saranga Y, Rosenberg O, Sela E, Bosak A. Mapping water status based on aerial thermal imagery: comparison of methodologies for upscaling from a single leaf to commercial fields. Precision Agriculture. 2016; p. 1±22.
18. Meron M, Tsipris J, Orlov V, Alchanatis V, Cohen Y. Crop water stress mapping for site-specific irrigation by thermal imagery and artificial reference surfaces. Precision agriculture. 2010; 11(2):148±162. https://doi.org/10.1007/s11119-009-9153-x

19. Pou A, Diago MP, Medrano H, Baluja J, Tardaguila J. Validation of thermal indices for water status identification in grapevine. Agricultural water management. 2014; 134:60±72. https://doi.org/10.1016/j.agwat.2013.11.010

20. Grant O, Ochagavía H, Baluja J, Diago M, Tardáguila J. Thermal imaging to detect spatial and temporal variation in the water status of grapevine (Vitis vinifera L.). The Journal of Horticultural Science and Biotechnology. 2016; 91(1):43±54. https://doi.org/10.1080/14620316.2015.1110991

21. Bellvert J, Zarco-Tejada PJ, Girona J, Fereres E. Mapping crop water stress index in a `Pinot-noir' vineyard: comparing ground measurements with thermal remote sensing imagery from an unmanned aerial vehicle. Precision agriculture. 2014; 15(4):361±376. https://doi.org/10.1007/s11119-013-9334-5

22. Bellvert J, Marsal J, Girona J, Zarco-Tejada PJ. Seasonal evolution of crop water stress index in grapevine varieties determined with high-resolution remote sensing thermal imagery. Irrigation Science. 2015; 33(2):81±93. https://doi.org/10.1007/s00271-014-0456-y

23. Bellvert J, Zarco-Tejada PJ, Marsal J, Girona J, González-Dugo V, Fereres E. Vineyard irrigation scheduling based on airborne thermal imagery and water potential thresholds. Australian Journal of Grape and Wine Research. 2016; 22(2):307±315. https://doi.org/10.1111/ajgw.12173

24. Sepúlveda-Reyes D, Ingram B, Bardeen M, Zúñiga M, Ortega-Farías S, Poblete-Echeverría C. Selecting Canopy Zones and Thresholding Approaches to Assess Grapevine Water Status by Using Aerial and Ground-Based Thermal Imaging. Remote Sensing. 2016; 8(10):822. https://doi.org/10.3390/rs8100822

25. Diago M, Bellincontro A, Scheidweiler M, Tardaguila J, Tittmann S, Stoll M. Future opportunities of proximal near infrared spectroscopy approaches to determine the variability of vineyard water status. Australian Journal of Grape and Wine Research. 2017; 23(3):409±414. https://doi.org/10.1111/ajgw.12283

26. Fernández-Novales J, Tardaguila J, Gutiérrez S, Marañón M, Diago MP. In field quantification and discrimination of different vineyard water regimes by on-the-go NIR spectroscopy. Biosystems Engineering. 2017;.

27. Han J, Pei J, Kamber M. Data mining: concepts and techniques. Elsevier; 2011.

28. Witten IH, Frank E, Hall MA, Pal CJ. Data Mining: Practical machine learning tools and techniques. Morgan Kaufmann; 2016.

29. Gutiérrez S, Tardaguila J, Fernández-Novales J, Diago MP. Support vector machine and artificial neural network models for the classification of grapevine varieties using a portable NIR spectrophotometer. PloS one. 2015; 10(11):e0143197. https://doi.org/10.1371/journal.pone.0143197 PMID: 26600316

30. Brillante L, Gaiotti F, Lovat L, Vincenzi S, Giacosa S, Torchio F, et al. Investigating the use of gradient boosting machine, random forest and their ensemble to predict skin flavonoid content from berry physicalÐmechan ical characteristics in wine grapes. Computers and Electronics in Agriculture. 2015; 117:186±193. https://doi.org/10.1016/j.compag.2015.07.017

31. Brillante L, Bois B, Mathieu O, Lévêque J. Electrical imaging of soil water availability to grapevine: a benchmark experiment of several machine-learning techniques. Precision Agriculture. 2016; 17(6):637±658. https://doi.org/10.1007/s11119-016-9441-1

32. Brillante L, Mathieu O, Lévêque J, Bois B. Ecophysiological Modeling of Grapevine Water Stress in Burgundy Terroirs by a Machine-Learning Approach. Frontiers in Plant Science. 2016; 7. https://doi.org/10.3389/fpls.2016.00796 PMID: 27375651

33. Gutiérrez S, Tardaguila J, Fernández-Novales J, Diago MP. Data mining and NIR spectroscopy in Viticulture: Applications for plant phenotyping under field conditions. Sensors. 2016; 16(2):236. https://doi.org/10.3390/s16020236 PMID: 26891304

34. Rodriguez JJ, Kuncheva LI, Alonso CJ. Rotation forest: A new classifier ensemble method. IEEE transactions on pattern analysis and machine intelligence. 2006; 28(10):1619±1630. https://doi.org/10.1109/TPAMI.2006.211 PMID: 16986543

35. Hinkelmann K, Kempthorne O. Randomized Block Designs, in Design and Analysis of Experiments: Introduction to Experimental Design. John Wiley & Sons, Inc.; 2007.

36. Harrison-Murray R. An electrical sensor for potential transpiration: principle and prototype. Journal of Horticultural Science. 1991; 66(2):141±149. https://doi.org/10.1080/00221589.1991.11516136

37. Jones H. Plants and Microclimate. Cambridge University Press, Cambridge. 1992;.

38. Murray FW. On the Computation of Saturation Vapor Pressure. Journal of Applied Meteorology. 1967; 6:203±204. https://doi.org/10.1175/1520-0450(1967)006%3C0203:OTCOSV%3E2.0.CO;2

39. Scholander PF, Bradstreet ED, Hemmingsen E, Hammel H. Sap pressure in vascular plants negative hydrostatic pressure can be measured in plants. Science. 1965; 148(3668):339±346. https://doi.org/10.1126/science.148.3668.339 PMID: 17832103

40. Hall M, Frank E, Holmes G, Pfahringer B, Reutemann P, Witten IH. The WEKA Data Mining Software: An Update. SIGKDD Explorations. 2009; 11(1):10±18. https://doi.org/10.1145/1656274.1656278

41. Möller M, Alchanatis V, Cohen Y, Meron M, Tsipris J, Naor A, et al. Use of thermal and visible imagery for estimating crop water status of irrigated grapevine. Journal of experimental botany. 2006; 58 (4):827±838. https://doi.org/10.1093/jxb/erl115 PMID: 16968884

42. Soar CJ, Speirs J, Maffei S, Penrose A, McCarthy MG, Loveys B. Grape vine varieties Shiraz and Grenache differ in their stomatal response to VPD: apparent links with ABA physiology and gene expression in leaf tissue. Australian journal of grape and wine research. 2006; 12(1):2±12. https://doi.org/10.1111/j.1755-0238.2006.tb00038.x

43. Schultz H, Stoll M. Some critical issues in environmental physiology of grapevines: future challenges and current limitations. Australian Journal of Grape and Wine Research. 2010; 16(s1):4±24. https://doi.org/10.1111/j.1755-0238.2009.00074.x

44. Prieto JA, Lebon É, Ojeda H. Stomatal behavior of different grapevine cultivars in response to soil water status and air water vapor pressure deficit. OENO One. 2010; 44(1):9±20. https://doi.org/10.20870/oeno-one.2010.44.1.1459

45. Intrigliolo D, Lakso A. Effects of light interception and canopy orientation on grapevine water status and canopy gas exchange. In: VI International Symposium on Irrigation of Horticultural Crops 889; 2009. p. 99±104.

46. Baluja J, Diago MP, Balda P, Zorer R, Meggio F, Morales F, et al. Assessment of vineyard water status variability by thermal and multispectral imagery using an unmanned aerial vehicle (UAV). Irrigation Science. 2012; 30(6):511±522. https://doi.org/10.1007/s00271-012-0382-9

47. Tardaguila J, Fernández-Novales J, Gutiérrez S, Diago MP. Non-destructive assessment of grapevine water status in the field using a portable NIR spectrophotometer. Journal of the Science of Food and Agriculture. 2017;. https://doi.org/10.1002/jsfa.8241

48. De Bei R, Cozzolino D, Sullivan W, Cynkar W, Fuentes S, Dambergs R, et al. Non-destructive measurement of grapevine water potential using near infrared spectroscopy. Australian Journal of Grape and Wine Research. 2011; 17(1):62±71. https://doi.org/10.1111/j.1755-0238.2010.00117.x

49. Santos AO, Kaye O. Grapevine leaf water potential based upon near infrared spectroscopy. Scientia Agricola. 2009; 66(3):287±292. https://doi.org/10.1590/S0103-90162009000300001

Chapter 5

On-the-go hyperspectral imaging and artificial intelligence in digital agriculture

As detailed in Section 1.3.3, HSI combines the potential of spectroscopy and the large data aggregation capability inherent to digital image. There are several published studies that make use of HSI for many applications in agriculture. Still, practically all of them have been developed under laboratory conditions, thus limiting the strength of this technology to indoor conditions.

A considerable part of the efforts during the research and development period from this PhD Thesis has been dedicated to overcome the challenge of carrying a hyperspectral camera to the field for the on-the-go vineyard monitoring, facing the new handicaps that this scenario carries, and designing useful applications for DA. Additionally, advanced ML techniques have been employed that, due to the large amount of data that hyperspectral image generates, were very useful tools for the modelling of different kinds of classifiers and regressors.

The works presented in this chapter are innovative due to the features present in the developed experiments (design of on-the-go HSI systems), also derived from collaboration with experts in robotics and HSI during my internship at the Australian Centre for Field Robotics, The University of Sydney, Australia.

5.1 In-field classification of a large number of grapevine varieties

As demonstrated in the published papers presented in Chapter 3, spectroscopy is an accurate technology for the task of grapevine varietal classification. The experiments developed in this paper went a step further than the ones presented in Chapter 3. They were designed to develop, using ANNs and SVMs, prediction models for 30 different international grapevine varieties with HSI from a mobile ground vehicle. Additionally, several statistical tests were conducted to compare the behaviour of each algorithm and the influence of their parameters. The obtained results showed that both algorithms were able to train models with a extremely high classification ratio. In general, ANNs were significantly better than SVMs. The experiments demonstrate that the powerful combination of on-the-go hyperspectral imaging and ML allow the precise, in-field classification of a large number of grapevine varieties, taking also into account that task monitoring can be carried out at different phenological stages.

Overcome challenges

- To use a hyperspectral camera in a moving ground vehicle under field conditions.
- To develop, using different ML algorithms, several classification models from a great number of grapevine varieties.
- To design an automated system for the identification of pixels (spectra) that belong to grapevine leaves.
- To use different parameter combinations in two ML techniques to model the spectra information obtained from two different phenological stages.

Paper information

- **Title of the publication**: On-the-go hyperspectral imaging under field conditions and machine learning for the classification of grapevine varieties
- **Authors:** Salvador Gutiérrez, Juan Fernández-Novales, María P. Diago, Javier Tardáguila
- **Published in:** Frontiers in Plant Science 9, 1102.
- **DOI:** 10.3389/fpls.2018.01102

Contributions of the PhD Thesis' author: Salvador Gutiérrez contributed to the experimental design and data acquisition in the field. He also performed data pre-processing, analysis and machine learning modelling. Salvador Gutiérrez wrote the full text of the paper during all review stages.

frontiers in Plant Science
ORIGINAL RESEARCH
published: 25 July 2018
doi: 10.3389/fpls.2018.01102

On-The-Go Hyperspectral Imaging Under Field Conditions and Machine Learning for the Classification of Grapevine Varieties

*Salvador Gutiérrez, Juan Fernández-Novales, Maria P. Diago and Javier Tardaguila**

Instituto de Ciencias de la Vid y del Vino - University of La Rioja, CSIC and Gobierno de La Rioja, Logroño, Spain

Grapevine varietal classification is an important plant phenotyping issue for grape growing and wine industry. This task has been achieved from destructive techniques like classic ampelography and DNA analysis under laboratory conditions. This work displays a new approach for the classification of a high number of grapevine (*Vitis vinifera* L.) varieties under field conditions using on-the-go hyperspectral imaging and different machine learning algorithms. On-the-go imaging was performed under natural illumination using a hyperspectral camera mounted on an all-terrain vehicle at 5 km/h. Spectra were acquired over two different leaf phenological stages on the canopy of 30 different varieties on a commercial vineyard located in La Rioja, Spain. A total of 1,200 spectral samples were generated. Support vector machines (SVM) and artificial neural networks (multilayer perceptrons, MLP) were used for the development of a large number of models, testing different algorithm parameters and spectral pre-processing techniques. Both classifiers yielded notable performance values and were able to train models with recall F1 scores and area under the receiver operating characteristic curve marks up to 0.99 for 5-fold cross validation. Statistical analyses supported that the best SVM kernel was linear and the best activation function for MLP was the hyperbolic tangent function. The prediction performance for individual varieties of MLP ranged from 0.94 to 0.99, displaying low levels of variability. In the case of SVM, slightly higher differences were obtained, ranging from 0.83 to 0.97 for individual varieties. These results support the possibility of deploying an on-the-go hyperspectral imaging system in the field capable of successfully classifying leaves from different grapevine varieties. This technology could thus be considered as a new useful non-destructive tool for plant phenotyping under field conditions.

Keywords: MLP, plant phenotyping, discrimination, sensors, proximal sensing, remote sensing, non-invasive sensors

OPEN ACCESS

Edited by:
Chuang Ma,
Northwest A&F University, China

Reviewed by:
Luigi Manfrini,
University of Bologna, Italy
Misao Itouga,
RIKEN Center for Sustainable Resource Science (CSRS), Japan

****Correspondence:***
Javier Tardaguila
javier.tardaguila@unirioja.es

Specialty section:
This article was submitted to Plant Systems and Synthetic Biology, a section of the journal Frontiers in Plant Science

Received: *22 February 2018*
Accepted: *09 July 2018*
Published: *25 July 2018*

Citation:
Gutiérrez S, Fernández-Novales J, Diago MP and Tardaguila J (2018) On-The-Go Hyperspectral Imaging Under Field Conditions and Machine Learning for the Classification of Grapevine Varieties. Front. Plant Sci. 9:1102. doi: 10.3389/fpls.2018.01102

1. INTRODUCTION

Plant phenotyping address the description of the plant's anatomical, physiological and biochemical properties (Walter et al., 2015). As grapevine growing and wine industry have a high economical and social impact, the interest of plant phenotyping is increasing in this context. In practice, however, phenotypes from controlled conditions rarely agree with those in f eld environments (Nelissen et al., 2014; Poorter et al., 2016). For this reason, in f eld plant phenotyping has become

a necessity, but it still remains as a diÿ cult task. The development of new technologies and methodologies for the precise phenotyping and monitoring of grapevines under f eld conditions would def nitely improve grape quality (and, thus, wine quality), a key factor for the industry.

Grapevine variety is a key feature of f nal product in terms of price, cultivation, etc. (Clarke and Rand, 2015). In the world, there exist several thousands of grapevine varieties, and ampelography has been the classic approach for their identif cation (Galet, 1979). Ampelography aims at extracting morphological differences between the leaves and grape berries, but it has always required specialized human resources. This methodology has gradually made way to modern and more precise identif cation approaches, such as wet chemistry (Altube et al., 1991) or DNA analysis (Sefc et al., 2001; Borrego et al., 2002; Pelsy et al., 2010). Nevertheless, the diÿ culty to fast and easily apply these techniques and their destructive nature makes them unable to be translated to a real time in-f eld application.

The advances in the research and development of applied spectroscopy—which involves the interaction between radiation and matter at specif c wavelengths—reveals this technology as a serious candidate to address the varietal classif cation goal. Likewise, many spectroscopic approaches have been developed toward this objective in several crops, such as barley malt (Porker et al., 2017), lotus seed (Guo et al., 2017b), pummelo (Li et al., 2016), or strawberry (Sánchez et al., 2012). Even works on in-f eld grapevine varietal classif cation using a near-infrared (NIR) device can be found in the literature (Gutiérrez et al., 2015, 2016). Hyperspectral imaging combines the potential of spectroscopy and the additional information that a two-dimensional space provides, and thus opens a new way to the development of spectroscopic methodologies. Particularly, hyperspectral images of grapevine leaves enable the development of varietal and clone classif cation models, as demonstrated by previous works (Diago et al., 2013; Fernandes et al., 2015). However, these studies worked with a very limited number of classes (no more than four), under laboratory conditions and required sample preparation. These pitfalls raise the necessity of taking a further step and deploying hyperspectral imaging directly in the f eld, opening a new frontier for the on-the-go classif cation of a large number of grapevine varieties, hence removing the requirements of laboratory conditions and even sample picking. This new application could be useful for commercial vineyards, nurseries, appellation boards, etc. Some authors have previously demonstrated the possibility of performing outdoor hyperspectral imaging in several crops (Underwood et al., 2017; Wendel and Underwood, 2017; Williams et al., 2017), and this bolsters the development of new on-the-go hyperspectral solutions for grapevine-related problems.

As exposed, hyperspectral imaging brings much richer data in relation to quantity and quality, but this feature also carries a big burden that needs to be handled: the huge amount of data that hyperspectral acquisitions implies. For this reason, eÿ cient and intelligent data analysis is an almost compelled necessity. Machine learning provides numerous techniques for predictive applications by learning and forecasting data (Han et al., 2011; Witten et al., 2016), and it has been extensively used in innumerable f elds. Two of the most reliable and adaptable algorithms for the development of supervised classif cation models are support vector machines (SVM) and artif cial neural networks (ANN).

SVM are algorithms that are based on a *kernel* that translates the input data into higher dimensional spaces (Capparuccia et al., 1995). In these, SVM try to f nd hyperplanes that maximize the distance to the nearest point (projected in the new dimensional space) of any of the input classes. The adequate selection of a kernel is crucial when applying SVM to a problem, as specif c kernels can f t better than other depending on the data modeled. SVM were originally conceived as binary classif ers, but multi-label classif cation SVM can be developed by splitting the original multi-class problem into several smaller binary classif cation ones using approaches as one-versus-all (training one model per class versus all the rest) or one-vs.-one (training one model per class for each one of the remaining classes). Applications based on SVM models can be widely found in plant science, like nitrogen evaluation (Gao et al., 2017), characterization of invasive grass distribution (Dronova et al., 2017) or seed development genetics (Ni et al., 2016). ANN are a popular machine learning approach extensively used for classif cation and regression purposes. Originally suggested by McCulloch and Pitts (1943), the modern concept of ANN was developed by Werbos (1974). ANNs try to emulate the behavior of a biological neural network, by deploying a net of basic interconnected units (neurons) and arranging them into a set of discrete layers (one-layer or multi-layer). In Rumelhart et al. (1986), *error backpropagation* feature was introduced, a process that f nds the gradients of the neurons' weights to adjust them, from the last layer to the f rst one. ANNs can also be found in multiple applications for plant science, e.g., leaf area index calculation (Yuan et al., 2017), rootstock genetics (Arab et al., 2017) or disease detection (Pérez-Bueno et al., 2016). For this reason, a deep analysis of how these algorithms and their multiple parameter settings behave with hyperspectral data is desirable, as they arise as powerful tools for the varietal classif cation objective.

The objective of this study was to develop a new application for the classif cation of a large number of grapevine (*Vitis vinifera* L.) varieties using on-the-go hyperspectral imaging under f eld conditions and machine learning algorithms.

2. MATERIALS AND METHODS

On-the-go hyperspectral imaging was performed in a commercial vineyard on a moving vehicle under f eld conditions and natural light, at two different phenological stages in a given season. A large amount of parameter combinations for spectral pre-processing and machine learning classif cation models were tested and statistically analyzed to evaluate the inf uence of the different parameters and obtain the best conf guration for the machine learning classif ers.

2.1. Experimental Layout

The study was conducted in a 1.8 ha commercial vineyard located in Logroño, La Rioja, Spain (Lat. 42° 2′ 4.5′′′′, Long.

-2° 30′ 49.6″″ Alt. 484 m), during two different days with clear weather corresponding to two different phenological stages of season 2017: 10 August—1 week post-veraison, at stage 36 of the modif ed Eichhorn and Lorenz system (Coombe, 1995)—and 11 October—1 week post-harvest, at stage 41. Grapevines (*Vitis vinifera* L.) were grafted on rootstock R-110 and trained to a vertically shoot-positioned trellis system. Plants were planted in 2001 with a Northwest-Southeast orientation at 3.00 × 1.20 m inter and intra row distances. Mechanical tillage was applied for vineyard soil management. Thirty different international grapevine varieties, uniformly irrigated across the season, were used in this study. From these, 16 white varieties were present: Baladí, Blanca Cayetana, Calagraño, Catalán Blanco, Chardonnay, Chenin Blanc, Cigüente, Palomino, Pardina, Parellada, Pedro Ximénez, Perruno Fino, Picapoll Blanco, Pinot Blanc, Sauvignon, Semillón. The other 14 were red varieties: Brancellao, Cabernet Franc, Cabernet Sauvignon, Calop Negro, Carnelian, Centurion, Concord, Crujidera, Pinot Noir, Rubired, Rufete, Sousón, Syrah, and Tempranillo. For each variety, 10 plants (along 12 m) were imaged. The 30 different varieties were randomly planted across the whole vineyard plot.

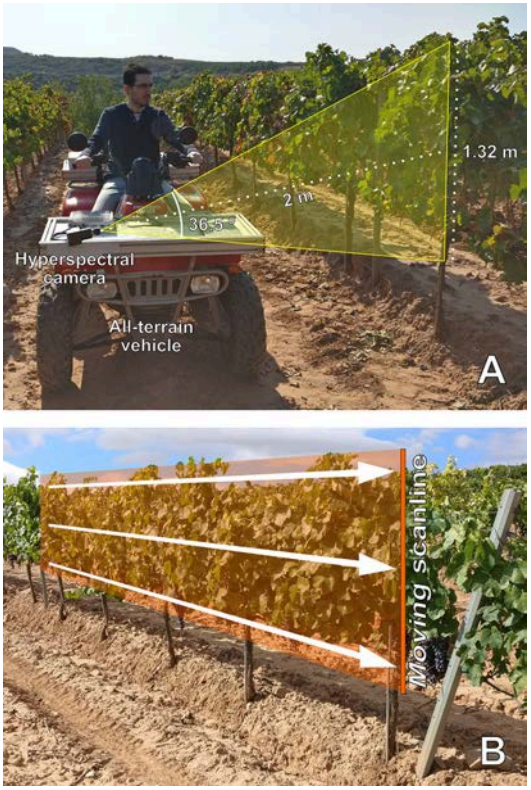

FIGURE 1 | (A) On-the-go hyperspectral imaging on an all-terrain vehicle in a vertically shoot positioned vineyard located in Logroño, La Rioja (Spain). Spectral acquisition was performed on the sun-exposed canopy side at 5 km/h. (The authors declare that written and informed consent has been obtained from the depicted individual in this image, for the publication of this identifiable image). **(B)** Construction of a two-dimensional hyperspectral image by push broom. The camera's scanline, that was acquiring spectral information from a vertical line over the vineyard canopy, was moved by the motion of the all-terrain-vehicle. Thus, the composition of the image was performed by this scanline dragging at constant speed.

2.2. On-The-Go Hyperspectral Imaging

The on-the-go acquisition of hyperspectral images was performed using a Resonon Pika L VNIR hyperspectral imaging camera (Resonon, Inc., Bozeman, MA, USA) mounted on the front part of an all-terrain vehicle (ATV) (Trail Boss 330, Polaris Industries, MN, USA), on a lateral point of view at 2.0 m of distance (**Figure 1A**). The camera covered the spectral range from 400 to 1,000 nm, with a spectral resolution of 2.1 nm (300 bands) and a spatial resolution of 900 pixels. Using an objective lens with a focal length of 8 mm, the f eld of view (FOV) was 36.5°, and casted a vertical recording line covering 1.32 m of the northeast canopy side, only with the natural illumination from the sun (between 10:00 and 12:00).

The camera conf guration was set up at 108 frames per second (FPS) with integration time of 6.53 ms, to maximize the trade-off between an acceptable image composition of the plants and spectral quality (avoiding signal saturation). In order to take into account the natural, variable illumination, at the beginning of the hyperspectral recording, for each variety, a Spectralon® white reference was manually presented to the camera and statically imaged. The dark current (that corresponds to inherent electronic noise) was measured with the camera lens covered. Afterwards, the 10 plants of that specif c variety were measured at a constant speed of 5 km/h. The horizontal movement from the ATV composed the whole hyperspectral image by push broom scanning (**Figure 1B**). The plants from each varietal recording comprised an average of 1,800 scanlines (columns in the hyperspectral image), 900 pixels each column. Therefore, each varietal hyperspectral image was composed of, on average, 1,620,000 pixels (i.e., spectra).

All the raw information from the camera (acquired as light intensity) was translated into ref ectance, using the following equation:

$$R(\bar{\mathbf{d}}_r, \lambda) = \frac{G(\bar{\mathbf{d}}_r, \lambda) - D(\bar{\mathbf{d}}_r, \lambda)}{W(\bar{\mathbf{d}}_r, \lambda) - D(\bar{\mathbf{d}}_r, \lambda)} \quad (1)$$

where $\bar{\mathbf{d}}_r$ is a position, λ is a wavelength, G is the intensity of the light ref ected by the target, W is the intensity of the light coming from the white reference, and D is the dark current. Afterwards, the absorbance $(\log 1/R)$ was calculated as the f nal unit to be used in computation. From this absorbance spectra, the f rst and last group of 25 bands were discarded to avoid the noise commonly present in both spectral signal's tails. Therefore, each spectrum comprised a total of 250 bands.

2.3. Building the Datasets

From the raw hyperspectral images, a semi-automatic dataset building process programmed in Python 3.6.1 was performed in two steps: the segmentation and filtering of the leaf spectra, and the generation of the samples for each grapevine variety.

2.3.1. Segmentation and Filtering of Leaf Spectra

The following procedure was applied to each variety hyperspectral image. From the $n \times m$ image (where m is the number of columns and n the number of pixels in each column), one manually selected average leaf spectrum was extracted and used as signature spectrum (the pure reference spectrum of a leaf of that image). Afterwards, for each column, all the spectra corresponding to leaves were automatically selected and averaged as described:

A Saviztky-Golay smoothing and derivative (Savitzky and Golay, 1964) was applied to the leaf signature spectrum. Afterwards, for each column, each one of its pixels were picked and its spectrum in absorbance was extracted, applying the same Savitzky-Golay smoothing and derivative. Then, the correlation coeÿcient between the pixel spectrum and the signature spectrum was computed, and if the Pearson's r was greater than 0.90, the spectrum was therefore positively identified as a leaf's spectrum and added into a selected leaves set. After all the pixels in the column were tested, the average spectrum from the selected leaves set was computed and considered as the average spectrum from all the leaves in that column. **Figure 2** represents a visual summary of this procedure.

After all the columns were processed, m mean spectra (one per column) were extracted for each variety altogether. On average, for all the varieties, the mean spectra was computed from 481 pixels (a 53.4% of the column pixels).

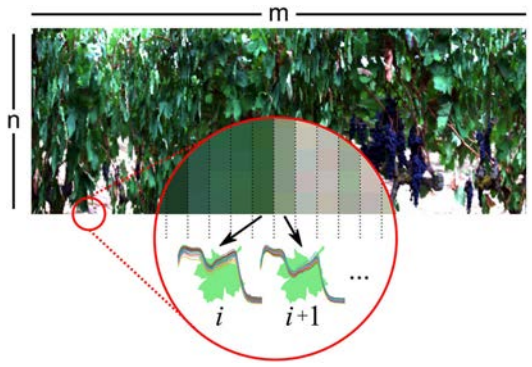

FIGURE 2 | Each $m \times n$ hyperspectral image was processed column by column. For each column i, each pixel (spectrum) was compared with a signature leaf spectrum. If a certain threshold of belonging was surpassed, the pixel was marked as leaf pixel. Afterwards, all leaf pixels from the column i were averaged.

2.3.2. Generation of the Dataset Samples

For each variety, the m mean leaf spectra were divided into 40 consecutive sets with a size of $m/40$ spectra. The average spectra from those sets were obtained and, thus, 40 leaf spectra per variety (four per plant) were finally generated, following previous methodologies by Gutiérrez et al. (2015, 2016). Having 30 varieties and two measurement days, a total of 2,400 samples (80 per variety) were generated, each one obtained from the averaging of approximately 21,500 spectra (86,000 leaf pixels per plant).

2.4. Spectral Pre-processing and Machine Learning Modeling

In the development of prediction models from spectral information, the raw absorbance data is seldom used directly as input. Spectral pre-processing is a common step that seeks to remove most of the noise that is inherent to many spectral acquisitions. As several algorithms and parameters can be applied, and they noticeably affect the spectral shape, the influence of two different pre-processing techniques were tested in the training of the varietal classification models:

- **Scatter correction.** Sometimes, it is usual for spectral signal to retain interferences of scatter. One of the techniques usually applied for this correction is the combination of standard normal variate (SNV) followed by a de-trending (Barnes et al., 1989; Dhanoa et al., 1995). Nevertheless, there are situations in which the application of scatter correction is not necessary, so for this study it was tested the use of SNV + de-trending and the complete omission of this scatter correction step.
- **Smoothing filtering.** Savitzky-Golay filtering along with a derivative function (Savitzky and Golay, 1964) is commonly used in spectroscopy, as they are able to remove noise from external sources and to emphasize certain parts from the original spectrum. The combination of two derivative orders (first and second) and three different Savitzky-Golay window sizes (5, 9, and 15) was tested.

Regarding machine learning modeling, two different classification algorithms were tested:

- **Support vector machines (SVM).** SVMs are algorithms based on kernels that transform the original data into high-dimensional feature spaces (Capparuccia et al., 1995). The parameters tested for SVM were: the penalty parameter C (six different values: 0.01, 0.1, 1, 10, 100, and 1,000) and three different kernels (*linear*, *polynomial*, and *radial basis function–RBF*). A total of 18 parameter combinations were thus generated. As SVM are binary classification algorithms, a one-*vs.*-one approach was followed in this work to perform multi-class classification Bishop (2006). This approach trains $n(n-1)/2$ binary models (where n is the number of classes), one for each one of the two-classes combinations that can be arranged. As in this case all the classes had the same number of samples, no bias was introduced in the models, hence avoiding over-estimation of a majority class.
- **Multilayer perceptrons (MLP).** MLPs are a kind of artificial neural networks (ANN) that consist of at least three layers

of neurons and make use of backpropagation in the training process (Hornik et al., 1989). The parameters tested for MLP were: number of neurons in the hidden layer (*t*: the sum of the number of attributes and classes. *a*: half the amount of *t*; *i*: the number of attributes), activation function for the hidden layer (*logistic*: logistic sigmoid function; *tanh*: hyperbolic tangent function; *relu*: rectif ed linear unit function) and using or not a warm start (reuse or reject previous solutions in the ANN training process). The total number of combinations were also 18.

Each developed model was evaluated using a stratif ed *k*-fold cross validation, with $k = 5$. In a *k*-fold cross validation, *k* models are trained with $k-1$ folds and tested with the remaining fold, rotating the latter until all of them have been used. The average performance of the *k* models is thus considered as the performance of the cross validation. Five replicates of 5-fold cross validation were also carried out, each one of them with random fold splits. In summary, having two options for scatter correction, six combinations for smoothing f ltering, two algorithms, 18 parameter combinations for each one and f ve cross validation replicates, a total of 2,160 classif cation models were developed.

The performance statistics used were the recall, F1 score, def ned as:

$$\text{recall} = \frac{tp}{tp + fn} = \frac{\text{number of correctly classif ed samples}}{\text{total number of testing samples}} \quad (2)$$

$$\text{F1 score} = 2 \times \frac{\text{precision} \times \text{recall}}{\text{precision} + \text{recall}} \quad (3)$$

where *tp* is *true positives* (number of samples correctly classif ed) and *fn* (number of samples incorrectly classif ed) is *false negatives*, and the area under the receiver operating characteristic curve (AUC) (Bradley, 1997), computed from the SVM and ANN class membership probability estimates. The performance statistics used were averaged among all the classes. An experimental modeling diagram is presented in **Figure 3**.

The evaluation of the models was developed using Python 3.6.1 and scikit-learn 0.18.1. The training of the MLP was performed using on scikit-learn multilayer perceptron implementation (Pedregosa et al., 2011). Statistical tests were

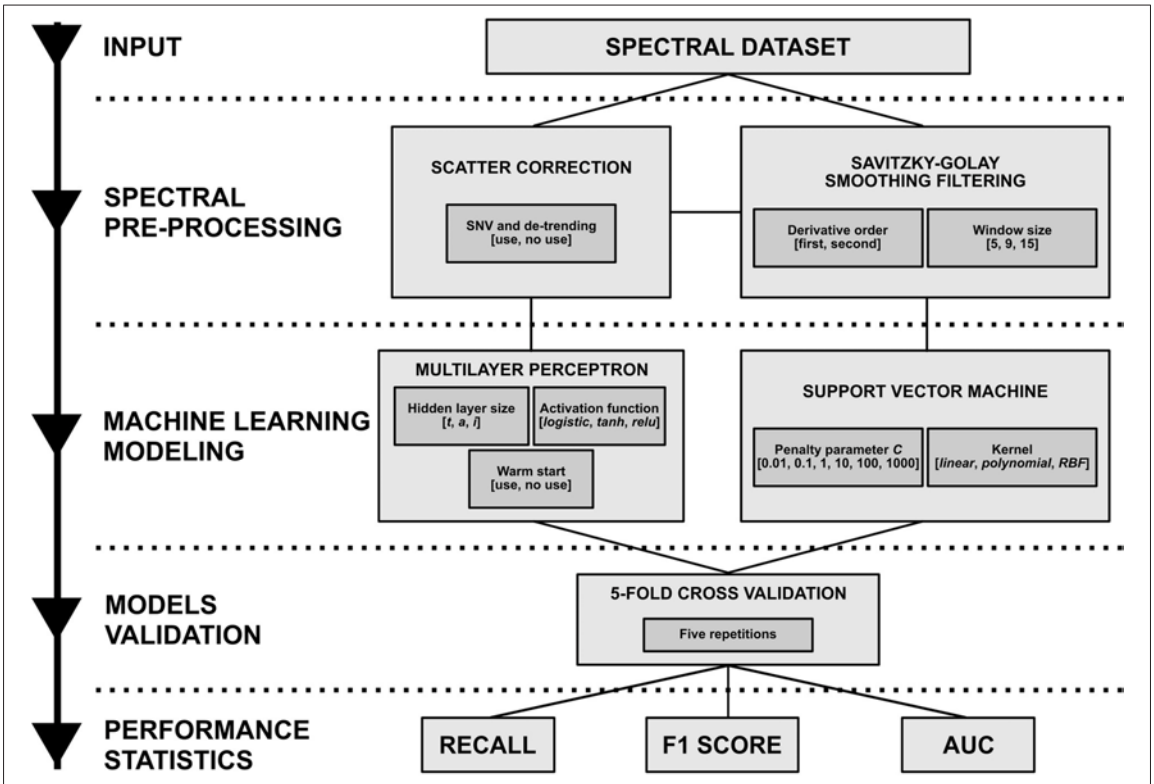

FIGURE 3 | Experimental modeling diagram summarizing the analyses performed. From the spectral dataset (input), different combinations of various pre-processing techniques were applied, modeled using two machine learning algorithms (with many parameters) and validated by several 5-fold cross validation replicates. Finally, three performance statistics were evaluated.

carried out using InfoStat software (Córdoba, Argentina), version 2017, using Tukey's range test at a signif cance level $p = 0.05$.

3. RESULTS

3.1. Influence of Scatter Correction and Derivative Order

The comparison of means of classif cation recall for scatter correction was performed for each algorithm. No statistically signif cant differences were found between the means from any statistic when using and omitting SNV followed by a de-trending (data not shown). Therefore, the successive statistical analyses were performed without splitting by scatter correction treatments. Besides, the inf uence of the f rst and second order derivatives was analyzed, and statistically signif cant differences were found between them for MLP ($p < 0.0001$ for the three performance statistics) and SVM (mean recall with $p < 0.05$ and F1 with $p < 0.01$) toward the second order derivative.

3.2. Influence of Smoothing Filtering

The statistical analyses for the recall results attending to the different Savitzky-Golay window size are gathered in **Table 1**.

In all cases, the classif cation outcomes from the MLP surpassed those from the SVM models.

SVM results did not yield statistically signif cant differences between window size for both derivative orders, with values that ranged from 0.84 to 0.90 for recall, from 0.84 to 0.91 for F1 score and 0.93 in all cases for AUC. The best scores came from the second derivative smoothing with the lower window size values (f ve and nine), and in all cases the f rst derivative casted equal or lower recall outcomes.

MLP showed strong and consistent statistically signif cant differences, at $p < 0.001$ for both derivative orders, across all the performance statistics, supporting that the best scores were obtained in general using the second order derivatives (regardless the window size). In both f rst and second order derivatives, there existed a trend in which the lower the value of the window size, the better the recall values.

3.3. Analysis of the Algorithm Parameters

The results for the statistical analyses per parameter value are gathered in **Tables 2**, **3**, for SVM and MLP respectively.

The models trained with SVM presented large differences depending on the specif c values selected (averages with high variability, from 0.65 up to 0.99 for recall, from 0.68 to 0.99 for F1 and from 0.60 to 0.99 for AUC), especially regarding the *C* parameter. In this case, a noticeable gap in terms of average recall can be found between *C* values equal or greater than one and 10 (that performed signif cantly better) and those that lied below that (whose scores casted worst results). For the different SVM kernel values, the three of them presented signif cant differences in all the statistics, being the linear *kernel* the one with the highest score. The *polynomial* kernel presented signif cantly lower average values.

The variability of the MLP results was considerably lower than that from SVM, with all values above the 0.95 mark and up to 0.99, for all the performance statistics. In terms of recall values, the number of neurons in the neural network models (hidden layer parameter) presented signif cant differences when selecting *i* or *t* over *a* (with slightly lower values for the latter), differences that were almost similar for both F1 and AUC. Nevertheless, the activation function responded differently depending on their selected values with the same behavior for the three statistics. In the f rst case, the *tanh* and *relu* functions worked signif cantly better than the *logistic* **one** (**Table 3**). The use of warm start exhibited no statistical signif cant differences in any case.

TABLE 1 | Comparison of means of classification recall, F1 score and AUC for each Savitzky-Golay window size by algorithm and derivative order.

			Window size			
Algorithm	**Performance statistic**	**Derivative order**	**5**	**9**	**15**	**Significance**
SVM	Recall	First	0.8839	0.8648	0.8351	*n.s.*
		Second	0.9024	0.8947	0.8842	*n.s.*
	F1 score	First	0.8934	0.8747	0.8450	*n.s.*
		Second	0.9142	0.9058	0.8938	*n.s.*
	AUC	First	0.9309	0.9305	0.9297	*n.s.*
		Second	0.9339	0.9328	0.9265	*n.s.*
MLP	Recall	First	0.9796 *a*	0.9678 *b*	0.9404 *c*	***
		Second	0.9905 *a*	0.9842 *b*	0.9804 *c*	***
	F1 score	First	0.9796 *a*	0.9687 *b*	0.9404 *c*	***
		Second	0.9905 *a*	0.9842 *b*	0.9804 *c*	***
	AUC	First	0.9998 *a*	0.9995 *b*	0.9986 *c*	***
		Second	0.9999 *a*	0.9998 *b*	0.9996 *c*	***

The values represent the average recall.
Dissimilar lowercase letters within rows represent statistically different means among different window sizes, using Tukey's range test at a significance level p = 0.05.
*AUC, area under the receiver operating characteristic curve; SVM, support vector machine; MLP, multilayer perceptron. n.s., not significant (p ≥ 0.05); *** p < 0.001.*

TABLE 2 | Comparison of means of classification recall, F1 score and AUC for the different parameters tested for support vector machine (SVM).

Parameter	Value	Average recall	Average F1 score	Average AUC
Penalty parameter (*C*)	1,000	0.99 *a*	0.99 *a*	0.99 *a*
	100	0.99 *a*	0.99 *a*	0.99 *a*
	10	0.98 *a*	0.98 *a*	0.99 *a*
	1	0.92 *b*	0.94 *b*	0.99 *a*
	0.1	0.73 *c*	0.75 *c*	0.98 *a*
	0.01	0.65 *d*	0.68 *d*	0.60 *b*
	Significance	***	***	***
Kernel	*Linear*	0.99 *a*	0.99 *a*	0.99 *a*
	Radial basis function	0.90 *b*	0.90 *b*	0.95 *b*
	Polynomial	0.74 *c*	0.77 *c*	0.84 *c*
	Significance	***	***	***

Dissimilar lowercase letters within the different parameter values represent statistically different means, using Tukey's range test at a significance level $p = 0.05$.
$^{***}p < 0.001$.

TABLE 3 | Comparison of means of classification recall, F1 score and AUC for the different parameters tested for multilayer perceptron (MLP).

Parameter	Value	Average recall	Average F1 score	Average AUC
Hidden layer	t	0.9746 *a*	0.9746 *ab*	0.9995 *ab*
	i	0.9757 *a*	0.9757 *a*	0.9996 *a*
	a	0.9717 *b*	0.9717 *b*	0.9994 *b*
	Significance	**	**	**
Activation function	*tanh*	0.9855 *a*	0.9855 *a*	0.9998 *a*
	relu	0.9837 *a*	0.9837 *a*	0.9998 *a*
	Logistic	0.9527 *b*	0.9527 *b*	0.9990 *b*
	Sign.	***	***	***
Warm start	True	0.9740	0.9739	0.9995
	False	0.9739	0.9739	0.9994
	Significance	*n.s.*	*n.s.*	*n.s.*

Dissimilar lowercase letters within the different parameter values represent statistically different means, using Tukey's range test at a significance level $p = 0.05$.
n.s., not significant ($p \geq 0.05$); $^{**}p < 0.01$. $^{***}p < 0.001$.
AUC, area under the receiver operating characteristic curve. t, the number of neurons is the sum of the number of attributes and classes. i, the number of neurons is the number of attributes. a, the number of neurons is half the amount of t. tanh, hyperbolic tangent function. relu, rectified linear unit function. logistic, logistic sigmoid function.

3.4. Prediction Capability per Variety

The average recall, F1 scores and AUC values, for each grapevine variety, were computed for SVM and MLP models. **Figure 4** displays bar plots of these averages for the 30 varieties. No clear correlation between the trends of both algorithms was found (the ranking for best classif ed classes was not the same between algorithms). For recall values, the difference between the best and the worst score for MLP was 0.04, presenting a low variability, while for SVM this difference swelled to 0.11. The plot shapes between both algorithms were similar for recall (**Figures 4A,B**) and F1 score (**Figures 4C,D**), but the AUC values for MLP showed a very small variability level (**Figure 4E**), unlike SVM (**Figure 4F**).

Attending to recall values per variety, representing the ratio of correctly classif ed samples, the varieties that showed the best recall values for MLP were Semillón, Perruno Fino and Blanca Cayetana, while Centurión was the one with the lowest value. All grapevine varieties, still, reached or surpassed the 0.94 mark. In the case of SVM, the best scores came from Semillón and Blanca Cayetana, as in the case of MLP, and Tempranillo, in third place, with recall values of greater than 0.92. All the varieties were on or above the 0.83 mark.

3.5. Execution Time Estimation

In the processing of the hyperspectral images, the segmentation and f ltering step (section 2.3.1) of the 60 images (30 varieties, two different days per variety) took approximately 27 h to complete on an Intel® Core™ i7-5820K CPU with 16 GB of RAM (with no thread optimization). This resulted in an average of 1.45 s per image column to be processed (i.e., the comparison of 900 spectra with a leaf signature and the average of the spectra marked as leaves). In the case of the prediction of an unknown spectrum by a previously MLP or SVM trained model, the time required was of 0.05 s. Therefore, the total time for obtaining an average spectra from the column of a hyperspectral image and the prediction of its variety would take 1.5 s.

4. DISCUSSION

The results from the present work reveal the actual capability of on-the-go hyperspectral imaging and machine learning for the classif cation of grapevine varieties growing under f eld conditions. Two main novelties have been addressed: the successful deployment of a hyperspectral camera in the f eld, under uncontrolled illumination conditions, and the prediction of a very large number of classes (30). This, supported by the wide evaluation of different machine learning classif ers and parameters, made possible to obtain classif cation results up to 0.99 for both SVM and MLP. The models were able to cast notable prediction results from data acquired in two different phenological stages, correctly classifying leaves of different degree of development.

To the best of our knowledge, no previous studies can be found on in-f eld plant varietal classif cation neither on-the-go nor using ground-based hyperspectral imaging. Nevertheless, recent works have displayed the use of in-f eld portable NIR spectroscopy for the classif cation of grapevine varieties (Gutiérrez et al., 2015, 2016), discriminating among 20 and 10 different varieties, respectively. The reported cross validation classif cation results went up to 87.25 and 88.7%, remarkable values considering the high number of classes employed in the training of the models. The present study improved both the number of varieties discriminated and the classif cation response. The different spectroscopic device used (hyperspectral imaging vs. spectral measurement of a very reduced area)

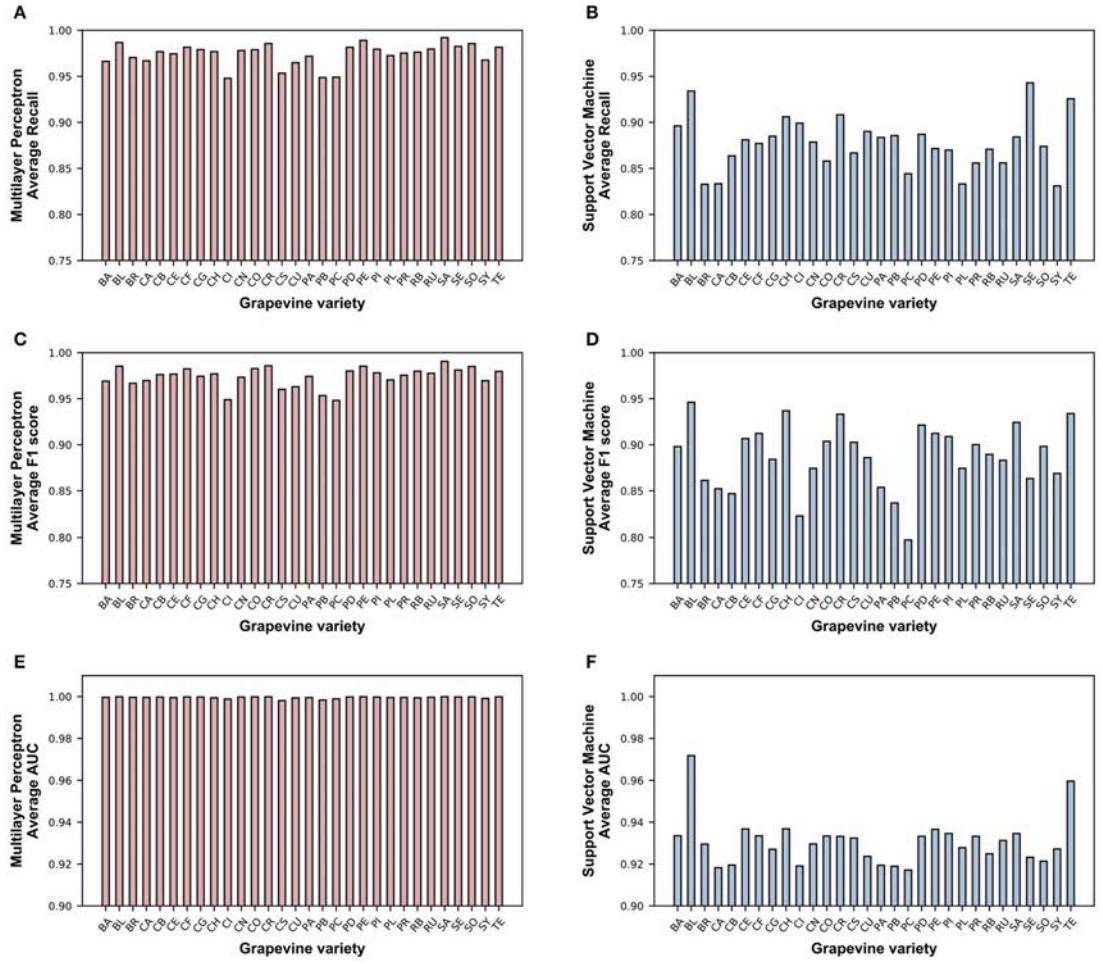

FIGURE 4 | Average recall **(A,B)**, F1 score **(C,D)** and area under the receiver operating characteristic curve, AUC, **(E,F)** per grapevine variety (n = 2160) for Multilayer Perceptron **(A,C,E)** and Support Vector Machine **(B,D,F)**. BA, Baladí; BL, Blanca Cayetana; BR, Brancellao; CA, Catalán Blanco; CB, Chenin Blanc; CE, Centurion; CF, Cabernet Sauvignon; CG, Calagraño; CH, Chardonnay; CI, Cigüente; CN, Calop Negro; CO, Concord; CR, Carnelian; CS, Cabernet Franc; CU, Crujidera; PA, Palomino; PB, Pinot Blanc; PC, Picapoll Blanco; PD, Pardina; PE, Pedro Ximénez; PI, Pinot Noir; PL, Parellada; PR, Perruno Fino; RB, Rubired; RU, Rufete; SA, Sauvignon; SE, Semillón; SO, Sousón; SY, Syrah; TE, Tempranillo.

could be the key factor of these enhancements. A portable spectrophotometer is only capable of acquiring spectral signals from a reduced portion of the target (grapevine leaves, in this case), hence a lot of information is lost if the whole canopy is not monitored by the device. On the other hand, adding two spatial dimensions to spectral data greatly increases the quantity of the information acquired from the canopy, as all the intervariability (among plants) and intra-variability (within plants) is considered. Hence the prediction capability of the machine learning algorithms is expected to be increased, as they are fed with more information. Hyperspectral imaging has been previously attempted for the varietal classif cation of grapevine leaves and clones by Diago et al. (2013) and Fernandes et al. (2015), respectively. In these studies, the authors demonstrated the ability of this technology for the discrimination of samples from three varieties and four clones. However, these approaches, unlike the present study, needed for specif c sample preparation. Moreover, imaging was conducted under laboratory conditions and only at harvest time, over leaves of different ages. Varietal classif cation by spectroscopy has been previously achieved in several agricultural and food applications. Maize seed discrimination attending to the variety was recently reported by Guo et al. (2017a) and Yang et al. (2017), with up to 14 varieties and using hyperspectral imaging and SVM.

Artif cial neural networks and SVM have also been used for this purpose in pummelo (Li et al., 2016), olive oil (Binetti et al., 2017), barley malt (Porker et al., 2017), or lotus seed (Guo et al., 2017b). All these studies had two common factors: the use of non-portable devices and the need of laboratory conditions. The present study tried to overcome these two major issues, by developing a methodology for varietal classif cation that is also able to be performed on-the-go, directly in the f eld, under uncontrolled illumination conditions, as on-the-go imaging brings the great advantage of covering large areas and thus acquiring a larger and richer amount of information from the crops.

The results obtained from the different spectral pre-processing steps allow to draw some interesting deductions. The fact that scatter correction had no inf uence in the results (no statistically signif cant differences were found when using and omitting SNV and de-trending) could suggest that the spectral information used as input for the classif cation algorithms suffered from no interferences of scatter. This might be explained by one of the main advantages of hyperspectral imaging: the huge amount of spectra that it provides. Each sample of the built dataset came from the average of approximately 43,000 leaf spectra, and this extreme averaging could have minimized the scatter inf uence. When it comes to smoothing f ltering, the different treatments showed no signif cant differences for SVM, but they were inf uential for MLP. The second order derivative casted the best performance statistics for this algorithm, making these results to be in line with those concluded by Gutiérrez et al. (2015), for the same purpose. Although, as mentioned, smoothing treatments had no inf uence for SVM (a fact that could be explained by the higher variability in classif cation results from this algorithm), the trend in terms of average values remained similar to those of MLP.

In general, the models trained with SVM and MLP were able to return very high statistical values of classif cation (for specif c parameters), highlighting that hyperspectral data (and the high amount of samples) retained enough information for both machine learning algorithms to successfully extract underlying classif cation rules, when providing a considerable amount of samples. The best results were found in those models that were trained with MLP (average performance values from 0.95 to 0.99), but SVM was also able to provide outcomes up to 0.99. Additionally AUC values per variety were much regular for MLP (**Figure 4E**) than for SVM (**Figure 4F**), implying that MLP had a higher capability to precisely classify from any class. As it can be concluded from **Table 2**, wider variability results came again from SVM, displaying high differences depending on the kernel selected and much larger gaps depending on the value of the *C* parameter. The inf uence of the kernel was statistically present, and the analyses promoted the *linear* kernel as clearly the best, setting aside more complex kernels. This enables to aÿ rm that spectral information was better exploited when, in the case of SVM, linear approaches were applied. Other studies have also reported good performance of hyperspectral imaging and SVM when using linear kernels in other crops and fruits (Baranowski et al., 2015; Schmitter et al., 2017; Siedliska et al., 2017), and Hsu et al. (2003) also suggested the use of linear kernels when the number of attributes is large (as in the case of spectral information). Another consideration that can be extracted from the obtained results is that the penalty parameter *C* should be set at or above 10. *C* determines the strength of regularization of the SVM (larger values imply lower regularization, i.e., correct classif cation of training data is more important, and vice versa), so in the present case, the best results came when the correct classif cation of the samples from the dataset was maximized. This situation could lead to an overf tting scenario, in which testing samples that did not participate in the training of the model yield bad predictions. Nevertheless, the fact that all the models were tested by f ve replicates of 5-fold cross validation could evidence that the generalization capability of SVM with larger *C* values remained present, as in each fold 20% of the samples were not used in the training, but correctly classif ed. Even so, a virtual performance plateau was present at a *C* value of 10, as increasing it above that amount did not improve the classif cation results. The different values that MLP parameters could take presented a lower variability, and not a mean lied below the 0.95 mark. In the case of the hidden layer size, the tested values had inf uence in the results when using larger sizes (as in *i* or *t*), implying that the artif cial neural networks were able to infer the rules for high classif cation reports on cross validation better with increased number of neurons in the hidden layer. The activation function parameter also showed statistical differences, making the rectif ed linear unit function or hyperbolic tangent function the candidates that best managed the input spectral data. On the other hand, the use warm start, attending to the outcomes, has no inf uence in the performance of the models. Regarding the classif cation performance by variety (**Figure 4**), it is noteworthy to mention that the average response of the algorithms did not exactly agree for each variety (except for the two varieties with greater recall values: Semillón and Blanca Cayetana). This would allow to aÿ rm that each one of the machine learning algorithms extracted concrete classif cation rules, and thus the specif c information carried by each variety's spectral data was addressed differently by each algorithm.

Based on the exposed results, plant phenotyping under f eld conditions using on-the-go hyperspectral imaging is an achievable goal in precision viticulture, and has a strong potential not only for the varietal classif cation task, but for the prediction of many useful parameters (e.g., water status, nutritional status, disease detection, fruit composition, etc.). The effective monitoring of the vineyard can be performed in real time and georeferenced, taking advantage of the integration between sensors and computing. Some other published works support the viability of on-the-go hyperspectral imaging (Underwood et al., 2017; Wendel and Underwood, 2017; Williams et al., 2017). The methodology exposed in the present work takes into consideration the works and machinery that are employed in the vineyard. Hyperspectral imaging was performed at 5 km/h, a speed commonly found in vineyard operations from agricultural vehicles, so the integration of a hyperspectral camera with a processing hardware could by translated into a vehicle (e.g., a tractor) to acquire and compute the spectral signals

in real time. The numbers exposed in section 3.5 that the segmentation, averaging and machine learning prediction of a whole hyperspectral line (column in the image) would take 1.5 s. Considering this, a hyperspectral camera could be set up for acquiring two spectra per plant, thus taking 30 s for each 10 plants to provide the predictive output (that can also be considerably reduced with hardware and software optimization). This real-time response could be in line with the way of working in current viticulture, as a fast, on-the-go varietal classif cation could be an useful phenotyping tool for commercial vineyards, nurseries, appellation boards, etc. Additionally, it would be possible for this integration, among many other instruments, to be deployed in agricultural robots, as demonstrated by many works found in the literature (Ruckelshausen et al., 2009; Weiss and Biber, 2011; Cheein and Carelli, 2013; Bargoti and Underwood, 2017; Underwood et al., 2017; Wendel and Underwood, 2017). The deployment of the application described in this study is also bolstered by the use of samples from different phenological states. This brings the advantage of performing on-the-go hyperspectral imaging for varietal classif cation at different times of the season, due to the fact that the developed models—trained with leaves from different ages—were able to notably modeling the different phenological features from the measured leaves.

As in-f eld varietal classif cation by on-the-go hyperspectral imaging and machine learning has been successfully proven within a vineyard, it is advisable to perform additional research covering supplementary aspects. The involvement of samples from the same varieties but from different locations or seasons could contribute to a richer dataset and a deeper understanding of the relationship between the spectral signal and the variety of the plant. Finally, dimensionality reduction is an interesting research topic that could focus on the future development of cheaper multispectral devices.

5. CONCLUSIONS

The present study displayed the actual capability of on-the-go hyperspectral imaging under f eld conditions for the classif cation of many grapevine varieties using machine learning. The results from the models obtained from testing different algorithm parameters and spectral pre-processing techniques demonstrate that a new way is opened for the task of plant phenotyping, as hyperspectral imaging has been usually performed under laboratory conditions and restricted to a selected, relatively small amount of samples. Both support vector machines and artif cial neural networks, when selecting the proper parameters, proved to be reliable modeling algorithms for the training of precise classif ers. This could let for a hyperspectral imaging system to be attached to an agricultural vehicle as a phenotyping tool for real time, on-the-go classif cation of grapevine varieties, bringing information very useful in the context of plant phenotyping and precision viticulture.

AUTHOR CONTRIBUTIONS

JT and SG: conceived and designed the experiments; SG and JF-N: performed the experiments: SG and JF-N: analyzed the data: JT and MD: contributed reagents, materials, analysis tools; SG, JT, JF-N, and MD: wrote the paper.

FUNDING

The work leading to these results has received funding from the European Union under grant agreement number 737669 (VINESCOUT project). SG would like to acknowledge the research funding FPI grant 299/2016 by Universidad de La Rioja, Gobierno de La Rioja. MD is funded by the Spanish Ministry of Economy, Industry and Competitiveness (MINECO) with a Ramon y Cajal grant RYC-2015-18429.

REFERENCES

Altube, H., F. Cabello, and J. M. Ortiz. (1991). Caracterización de variedades y portainjertos de vid mediante isoenzimas de los sarmientos. *Vitis* 30, 203–212.

Arab, M. M., Yadollahi, A., Ahmadi, H., Eftekhari, M., and Maleki, M. (2017). Mathematical modeling and optimizing of *in vitro* hormonal combination for G× N15 vegetative rootstock proliferation using Artif cial Neural Network-Genetic Algorithm (ANN-GA). *Front. Plant Sci.* 8:1853. doi: 10.3389/fpls.2017.01853

Baranowski, P., Jedryczka, M., Mazurek, W., Babula-Skowronska, D., Siedliska, A., and Kaczmarek, J. (2015). Hyperspectral and thermal imaging of oilseed rape (*Brassica napus*) response to fungal species of the genus Alternaria. *PLoS ONE* 10:e0122913. doi: 10.1371/journal.pone.0122913

Bargoti, S., and Underwood, J. P. (2017). Image segmentation for fruit detection and yield estimation in apple orchards. *J. Field Robot.* 34, 1039–1060. doi: 10.1002/rob.21699

Barnes, R., Dhanoa, M. S., and Lister, S. J. (1989). Standard normal variate transformation and de-trending of near-infrared diffuse ref ectance spectra. *Appl. Spectrosc.* 43, 772–777. doi: 10.1366/0003702894202201

Binetti, G., Del Coco, L., Ragone, R., Zelasco, S., Perri, E., Montemurro, C., et al. (2017). Cultivar classif cation of Apulian olive oils: use of artif cial neural networks for comparing NMR, NIR and merceological data. *Food Chem.* 219, 131–138. doi: 10.1016/j.foodchem.2016.09.041

Bishop, C. (2006). *Pattern Recognition and Machine Learning*. New York, NY: Springer-Verlag.

Borrego, J., De Andrés, M., Gómez, J., and Ibáñez, J. (2002). Genetic study of Malvasia and Torrontes groups through molecular markers. *Am. J. Enol. Viticult.* 53, 125–130.

Bradley, A. P. (1997). The use of the area under the ROC curve in the evaluation of machine learning algorithms. *Patt. Recogn.* 30, 1145–1159. doi: 10.1016/S0031-3203(96)00142-2

Capparuccia, R., De Leone, R., and Marchitto, E. (1995). Support-vector networks. *Mach. Learn.* 20, 273–297. doi: 10.1007/BF00994018

Cheein, F. A. A., and Carelli, R. (2013). Agricultural robotics: unmanned robotic service units in agricultural tasks. *IEEE Indust. Electr. Mag.* 7, 48–58. doi: 10.1109/MIE.2013.2252957

Clarke, O., and Rand, M. (2015). *Grapes & Wines: A Comprehensive Guide to Varieties and Flavours*. London: Pavilion Books.

Coombe, B. (1995). Growth stages of the grapevine: adoption of a system for identifying grapevine growth stages. *Aust. J. Grape Wine Res.* 1, 104–110. doi: 10.1111/j.1755-0238.1995.tb00086.x

Dhanoa, M., Lister, S., and Barnes, R. (1995). On the scales associated with near-infrared ref ectance difference spectra. *Appl. Spectrosc.* 49, 765–772. doi: 10.1366/0003702953964615

Diago, M. P., Fernandes, A., Millan, B., Tardaguila, J., and Melo-Pinto, P. (2013). Identif cation of grapevine varieties using leaf spectroscopy and partial least squares. *Comput. Electr. Agricult.* 99, 7–13. doi: 10.1016/j.compag.2013.08.021

Dronova, I., Spotswood, E. N., and Suding, K. N. (2017). Opportunities and constraints in characterizing landscape distribution of an invasive grass from very high resolution multi-spectral imagery. *Front. Plant Sci.* 8:890. doi: 10.3389/fpls.2017.00890

Fernandes, A., Melo-Pinto, P., Millan, B., Tardaguila, J., and Diago, M. (2015). Automatic discrimination of grapevine (*Vitis vinifera* L.) clones using leaf hyperspectral imaging and partial least squares. *J. Agricult. Sci.* 153, 455–465. doi: 10.1017/S0021859614000252

Galet, P. (1979). *A Practical Ampelography.* Ithaca, NY: Cornell University Press.

Gao, L., Zhu, X., Li, C., and Cheng, L. (2017). Evaluation of the nitrogen content during the new-shoot-growing stage in apple leaves using two-dimensional correlation spectroscopy. *PLoS ONE* 12:e0186751. doi: 10.1371/journal.pone.0186751

Guo, D., Zhu, Q., Huang, M., Guo, Y., and Qin, J. (2017a). Model updating for the classif cation of different varieties of maize seeds from different years by hyperspectral imaging coupled with a pre-labeling method. *Comput. Electr. Agricult.* 142, 1–8. doi: 10.1016/j.compag.2017.08.015

Guo, Y., Ding, X., and Ni, Y. (2017b). The combination of NIR spectroscopy and HPLC chromatography for differentiating lotus seed cultivars and quantitative prediction of four main constituents in lotus with the aid of chemometrics. *Anal. Methods* 9, 6420–6429. doi: 10.1039/C7AY02021J

Gutiérrez, S., Tardaguila, J., Fernández-Novales, J., and Diago, M. P. (2015). Support vector machine and artif cial neural network models for the classif cation of grapevine varieties using a portable NIR spectrophotometer. *PLoS ONE* 10:e0143197. doi: 10.1371/journal.pone.0143197

Gutiérrez, S., Tardaguila, J., Fernández-Novales, J., and Diago, M. P. (2016). Data mining and NIR spectroscopy in viticulture: applications for plant phenotyping under f eld conditions. *Sensors* 16:236. doi: 10.3390/s16020236

Han, J., Pei, J., and Kamber, M. (2011). *Data Mining: Concepts and Techniques.* Burlington: Elsevier.

Hornik, K., Stinchcombe, M., and White, H. (1989). Multilayer feedforward networks are universal approximators. *Neural Netw.* 2, 359–366. doi: 10.1016/0893-6080(89)90020-8

Hsu, C.-W., Chang, C.-C., and Lin, C.-J. (2003). *A Practical Guide to Support Vector Classif cation.* Technical report. National Taiwan University.

Li, X.-L., Yi, S.-L., He, S.-L., Lv, Q., Xie, R.-J., Zheng, Y.-Q., et al. (2016). Identif cation of pummelo cultivars by using Vis/NIR spectra and pattern recognition methods. *Precis. Agricult.* 17, 365–374. doi: 10.1007/s11119-015-9426-5

McCulloch, W. S., and Pitts, W. (1943). A logical calculus of the ideas immanent in nervous activity. *Bull. Math. Biophys.* 5, 115–133. doi: 10.1007/BF02478259

Nelissen, H., Moloney, M., and Inzé, D. (2014). Translational research: from pot to plot. *Plant Biotechnol. J.* 12, 277–285. doi: 10.1111/pbi.12176

Ni, Y., Aghamirzaie, D., Elmarakeby, H., Collakova, E., Li, S., Grene, R., et al. (2016). A machine learning approach to predict gene regulatory networks in seed development in Arabidopsis. *Front. Plant Sci.* 7:1936. doi: 10.3389/fpls.2016.01936

Pedregosa, F., Varoquaux, G., Gramfort, A., Michel, V., Thirion, B., Grisel, O., et al. (2011). Scikit-learn: machine learning in Python. *J. Mach. Learn. Res.* 12, 2825–2830.

Pelsy, F., Hocquigny, S., Moncada, X., Barbeau, G., Forget, D., Hinrichsen, P., et al. (2010). An extensive study of the genetic diversity within seven French wine grape variety collections. *Theor. Appl. Genet.* 120, 1219–1231. doi: 10.1007/s00122-009-1250-8

Pérez-Bueno, M. L., Pineda, M., Cabeza, F. M., and Barón, M. (2016). Multicolor f uorescence imaging as a candidate for disease detection in plant phenotyping. *Front. Plant Sci.* 7:1790. doi: 10.3389/fpls.2016.01790

Poorter, H., Fiorani, F., Pieruschka, R., Wojciechowski, T., Putten, W. H., Kleyer, M., et al. (2016). Pampered inside, pestered outside? Differences and similarities between plants growing in controlled conditions and in the f eld. *New Phytol.* 212, 838–855. doi: 10.1111/nph.14243

Porker, K., Zerner, M., and Cozzolino, D. (2017). Classif cation and authentication of barley (Hordeum vulgare) malt varieties: combining attenuated total ref ectance mid-infrared spectroscopy with chemometrics. *Food Anal. Methods* 10, 675–682. doi: 10.1007/s12161-016-0627-y

Ruckelshausen, A., Biber, P., Dorna, M., Gremmes, H., Klose, R., Linz, A., et al. (2009). BoniRob–an autonomous f eld robot platform for individual plant phenotyping. *Precis. Agricult.* 9, 841–847. doi: 10.3920/978-90-8686-664-9

Rumelhart, D. E., Hinton, G. E., and Williams, R. J. (1986). Learning representations by back-propagating errors. *Nature* 323:533. doi: 10.1038/323533a0

Sánchez, M.-T., De la Haba, M. J., Benítez-López, M., Fernández-Novales, J., Garrido-Varo, A., and Pérez-Marín, D. (2012). Non-destructive characterization and quality control of intact strawberries based on NIR spectral data. *J. Food Eng.* 110, 102–108. doi: 10.1016/j.jfoodeng.2011.12.003

Savitzky, A., and Golay, M. J. (1964). Smoothing and differentiation of data by simplif ed least squares procedures. *Anal. Chem.* 36, 1627–1639. doi: 10.1021/ac60214a047

Schmitter, P., Steinruecken, J., Roemer, C., Ballvora, A., Leon, J., Rascher, U., et al. (2017). Unsupervised domain adaptation for early detection of drought stress in hyperspectral images. *ISPRS J. Photogram. Remote Sens.* 131, 65–76. doi: 10.1016/j.isprsjprs.2017.07.003

Sefc, K., Lefort, F., Grando, M., Scott, K., Steinkellner, H., and Thomas, M. (2001). "Microsatellite markers for grapevine: a state of the art," in *Molecular Biology and Biotechnology of the Grapevine*, ed K. A. Roubelakis-Angelakis (Dordrecht: Springer), 433–463.

Siedliska, A., Baranowski, P., Zubik, M., and Mazurek, W. (2017). Detection of pits in fresh and frozen cherries using a hyperspectral system in transmittance mode. *J. Food Eng.* 215, 61–71. doi: 10.1016/j.jfoodeng.2017.07.028

Underwood, J., Wendel, A., Schof eld, B., McMurray, L., and Kimber, R. (2017). Eÿ cient in-f eld plant phenomics for row-crops with an autonomous ground vehicle. *J. Field Robot.* 34, 1061–1083. doi: 10.1002/rob.21728

Walter, A., Liebisch, F., and Hund, A. (2015). Plant phenotyping: from bean weighing to image analysis. *Plant Methods* 11:14. doi: 10.1186/s13007-015-0056-8

Weiss, U., and Biber, P. (2011). Plant detection and mapping for agricultural robots using a 3D LIDAR sensor. *Robot. Auton. Syst.* 59, 265–273. doi: 10.1016/j.robot.2011.02.011

Wendel, A., and Underwood, J. (2017). Illumination compensation in ground based hyperspectral imaging. *ISPRS J. Photogram. Remote Sens.* 129, 162–178. doi: 10.1016/j.isprsjprs.2017.04.010

Werbos, P. (1974). *New Tools for Prediction and Analysis in the Behavioral Science.* Ph. D. Dissertation, Harvard University.

Williams, D., Britten, A., McCallum, S., Jones, H., Aitkenhead, M., Karley, A., et al. (2017). A method for automatic segmentation and splitting of hyperspectral images of raspberry plants collected in f eld conditions. *Plant Methods* 13:74. doi: 10.1186/s13007-017-0226-y

Witten, I. H., Frank, E., Hall, M. A., and Pal, C. J. (2016). *Data Mining: Practical Machine Learning Tools and Techniques.* Burlington: Morgan Kaufmann.

Yang, S., Zhu, Q.-B., Huang, M., and Qin, J.-W. (2017). Hyperspectral image-based variety discrimination of maize seeds by using a multi-model strategy coupled with unsupervised joint skewness-based wavelength selection algorithm. *Food Anal. Methods* 10, 424–433. doi: 10.1007/s12161-016-0597-0

Yuan, H., Yang, G., Li, C., Wang, Y., Liu, J., Yu, H., et al. (2017). Retrieving soybean leaf area index from unmanned aerial vehicle hyperspectral remote sensing: analysis of RF, ANN, and SVM regression models. *Remote Sens.* 9:309. doi: 10.3390/rs9040309

Conf ict of Interest Statement: The authors declare that the research was conducted in the absence of any commercial or f nancial relationships that could be construed as a potential conf ict of interest.

5.2 Monitoring of grape composition in a vineyard under field conditions

Wine quality is directly related with the compounds present in grapes. The evaluation of grape quality and ripeness is frequently done by analysis of two important composition parameters: soluble solid content and anthocyanin content. Having knowledge about the spatial distribution of these parameters in the vineyard would make easier the decision-making process at harvest, as different strategy could be designed. Nevertheless, the assessment of these parameters has always been costly and labour-demanding, also requiring expert personnel. These features greatly limits the sampling within a vineyard. The objective of the following published paper was to use a hyperspectral camera for the on-the-go estimation of grape composition in the field. The prediction of soluble solid content anthocyanin concentrations were successfully modelled using ML techniques, and spatial-temporal maps of the vineyard were also developed for both parameters. These results are great advance for the precise monitoring of two important vineyard parameters, also presenting new methodologies that combine in-field HSI and modelling with ML.

Overcome challenges

- The fast, on-the-go prediction of two grape composition parameters under field conditions.
- To achieve the precise identification of pixels (spectra) belonging to grape under natural illumination conditions.
- To train prediction models using data from different dates within the same campaign.

Datos del artículo

- **Title of the paper**: On-the-go hyperspectral imaging for the in-field estimation of grape composition
- **Authors:** Salvador Gutiérrez, Javier Tardáguila, Juan Fernández-Novales, María P. Diago
- **Published in:** Australian Journal of Grape and Wine Research 25 (1), 127-133.
- **DOI:** 10.1111/ajgw.12376

Contributions of the PhD Thesis' author: Salvador Gutiérrez contributed to the experimental design, data acquisition in the field, and laboratory analyses. He also performed data pre-processing, analysis and machine learning modelling. Salvador Gutiérrez wrote the full text of the paper during all review stages.

5.3 Extensive fruit yield prediction under field conditions from an automatic platform

Yield estimation is a key element in crop management and production control in any agricultural business. Classic practices on fruit yield estimation involve visual inspections, inaccurate and subjective, or manual sampling, that limits the capability of representation in large areas, also being time-consuming. A review of the literature in the last years on yield estimation, many novelties are present making use of non-invasive sensing technologies and deep learning, virtually all of them using computer vision based on RGB imaging. Nevertheless, the prediction of many other important crop features would be very useful to the farmer. Some works have demonstrated that the prediction of these features can be achieved using promising sensors other than RGB, like HSI. There are no works on the use of line scan hyperspectral cameras for yield estimation so far. If it is possible to demonstrate that this technology is capable of performing this task, HSI alone would thus be very useful for the prediction of several parameters from a single measurement. The objective of the following paper, result of an internship in the Australian Centre for Field Robotics, The University of Sydney, was the evaluation of the use of HSI and ML for the extensive mango yield estimation in hundreds of trees from a whole plot. The optimisation of the parameters in the prediction algorithm, performed using GAs, resulted in accurate yield estimation models. The results show that, although computer vision with RGB cameras still are a reliable technique for yield estimation, this task can be accomplished at satisfactory levels only using a line scan camera, like a hyperspectral one. The development of the techniques explained in this publication entails an important novelty in DA. Moreover, its implementation in other crops like vineyards, that shares common features with mango trees (*e.g.*, the possibility of performing measurements from lateral points of views), is practically direct.

Overcome challenges

- To use a line scan hyperspectral camera for yield estimation.
- The design of a methodology for parameter optimisation in a yield prediction system.
- To validate a methodology extensively in hundred of trees from a whole commercial plot.

Paper information

- **Title of the publication**: Ground based hyperspectral imaging for extensive mango yield estimation

- **Authors:** Salvador Gutiérrez, Alexander Wendel, James Underwood
- **Published in:** Computers and Electronics in Agriculture 157, 126-135.
- **DOI:** 10.1016/j.compag.2018.12.041

Contributions of the PhD Thesis' author: During his internship at The University of Sydney, Salvador Gutiérrez contributed to data pre-processing, analysis and machine learning modelling. He also wrote the full text of the paper during all review stages.

Chapter 6

Conclusions

Main conclusion: The work that lead to this PhD Thesis established the potential of the combination of machine learning and non-invasive sensing technologies for the assessment of relevant agronomical, physiological and qualitative traits in digital agriculture and viticulture.

The specific conclusions of this PhD Thesis are:

Machine learning and spectroscopy for in-field grapevine phenotyping and monitoring

1. Machine learning methodologies are able to model vine spectral data for the characterisation of key grapevine traits, such as varietal classification or the plant water status assessment. This can be of utmost importance in viticulture as new portable tools can be designed to be easily used under field conditions.

2. The combination of artificial intelligence and handheld sensors can be readily deployed in industrial applications in viticulture, becoming effective tools for grapegrowers and wineries.

Machine learning and thermal imaging for vineyard water status assessment

4. Ensemble data analysis techniques applied to thermal data acquired from the plants are capable of developing models for the assessment of vineyard water status during the growing season.

5. On-the-go thermal imaging permits a fast coverage of plant water status in a vineyard plot and, with the ability of georeferencing at data acquisition, the individual characterisation of each vine.

6. Thermal imaging, along with data analysis from machine learning, allow this combination to be applied in viticulture, to become a feasible

alternative to existing solutions for vineyard water status assessments along the season, and to drive better irrigation scheduling decisions.

In-field, on-the-go hyperspectral imaging and machine learning for crop monitoring

7. Advanced techniques of machine learning algorithms perform with high efficiency dealing with grapevine data from hyperspectral imaging.

8. It is possible to perform hyperspectral imaging under field conditions, under uncontrolled light conditions, and from a moving vehicle.

9. On-the-go hyperspectral imaging, under uncontrolled light conditions, has many applications for crop monitoring, such as varietal classification, grape composition assessment or fruit yield estimation, either from manned or autonomous platforms.

10. Hyperspectral imaging along with artificial intelligence makes this combination a new, promising tool in digital agriculture.

Bibliography

Agati, G., Pinelli, P., Cortés Ebner, S., Romani, A., Cartelat, A. and Cerovic, Z. G. 2005. Nondestructive evaluation of anthocyanins in olive (Olea europaea) fruits by in situ chlorophyll fluorescence spectroscopy. *Journal of Agricultural and Food Chemistry*, vol. 53(5), pages 1354–1363.

Al-Saddik, H., Simon, J. and Cointault, F. 2018. Assessment of the optimal spectral bands for designing a sensor for vineyard disease detection: The case of 'Flavescence dorée'. *Precision Agriculture*, pages 1–25.

Alpaydin, E. 2009. *Introduction to Machine Learning*. MIT press. ISBN 9780262012430.

Amara, J., Bouaziz, B., Algergawy, A. et al. 2017. A deep learning-based approach for banana leaf diseases classification. In *BTW (Workshops)*, pages 79–88.

Appenzeller, T. 2017. The AI revolution in science. *Science*, vol. 357, pages 16–17.

Aquino, A., Diago, M. P., Millán, B. and Tardáguila, J. 2017. A new methodology for estimating the grapevine-berry number per cluster using image analysis. *Biosystems Engineering*, vol. 156, pages 80–95.

Arkeman, Y., Buono, A., Hermadi, I. et al. 2017. Satellite image processing for precision agriculture and agroindustry using convolutional neural network and genetic algorithm. In *IOP Conference Series: Earth and Environmental Science*, vol. 54, page 012102. IOP Publishing.

Arnó Satorra, J., Martínez Casasnovas, J. A., Ribes Dasi, M. and Rosell Polo, J. R. 2009. Precision viticulture. Research topics, challenges and opportunities in site-specific vineyard management. *Spanish Journal of Agricultural Research*, vol. 7(4), pages 779–790.

Asseng, S. and Asche, F. 2019. Future farms without farmers. *Science Robotics*, vol. 4(27), page eaaw1875.

BALUJA, J., DIAGO, M. P., BALDA, P., ZORER, R., MEGGIO, F., MORALES, F. and TARDAGUILA, J. 2012. Assessment of vineyard water status variability by thermal and multispectral imagery using an unmanned aerial vehicle (UAV). *Irrigation Science*, vol. 30(6), pages 511–522.

BARGOTI, S. and UNDERWOOD, J. P. 2017. Image segmentation for fruit detection and yield estimation in apple orchards. *Journal of Field Robotics*, vol. 34(6), pages 1039–1060.

BARNES, A., SOTO, I., EORY, V., BECK, B., BALAFOUTIS, A., SÁNCHEZ, B., VANGEYTE, J., FOUNTAS, S., VAN DER WAL, T. and GÓMEZ-BARBERO, M. 2019. Exploring the adoption of precision agricultural technologies: A cross regional study of EU farmers. *Land Use Policy*, vol. 80, pages 163–174.

BEHMANN, J., ACEBRON, K., EMIN, D., BENNERTZ, S., MATSUBARA, S., THOMAS, S., BOHNENKAMP, D., KUSKA, M., JUSSILA, J., SALO, H. ET AL. 2018. Specim IQ: evaluation of a new, miniaturized handheld hyperspectral camera and its application for plant phenotyping and disease detection. *Sensors*, vol. 18(2), page 441.

BEHROOZI-KHAZAEI, N. and MALEKI, M. R. 2017. A robust algorithm based on color features for grape cluster segmentation. *Computers and Electronics in Agriculture*, vol. 142, pages 41–49.

BELLVERT, J., ZARCO-TEJADA, P. J., GIRONA, J. and FERERES, E. 2014. Mapping crop water stress index in a 'Pinot-noir' vineyard: comparing ground measurements with thermal remote sensing imagery from an unmanned aerial vehicle. *Precision Agriculture*, vol. 15(4), pages 361–376.

BENGIO, Y., COURVILLE, A. and VINCENT, P. 2013. Representation learning: A review and new perspectives. *IEEE transactions on pattern analysis and machine intelligence*, vol. 35(8), pages 1798–1828.

BERGERMAN, M., BILLINGSLEY, J., REID, J. and VAN HENTEN, E. 2016. Robotics in agriculture and forestry. In *Springer Handbook of Robotics*, pages 1463–1492. Springer.

BILGER, W., VEIT, M., SCHREIBER, L. and SCHREIBER, U. 1997. Measurement of leaf epidermal transmittance of UV radiation by chlorophyll fluorescence. *Physiologia Plantarum*, vol. 101(4), pages 754–763.

BISHOP, C. M. 2006. *Pattern Recognition and Machine Learning (Information Science and Statistics)*. Springer-Verlag, Berlin, Heidelberg. ISBN 0387310738.

BOJARSKI, M., DEL TESTA, D., DWORAKOWSKI, D., FIRNER, B., FLEPP, B., GOYAL, P., JACKEL, L. D., MONFORT, M., MULLER, U., ZHANG, J. ET AL. 2016. End to end learning for self-driving cars. *arXiv preprint arXiv:1604.07316*.

BOTTACI, L., DREW, P. J., HARTLEY, J. E., HADFIELD, M. B., FAROUK, R., LEE, P. W., MACINTYRE, I. M., DUTHIE, G. S. and MONSON, J. R. 1997. Artificial neural networks applied to outcome prediction for colorectal cancer patients in separate institutions. *The Lancet*, vol. 350(9076), pages 469–472.

BRAMLEY, R. 2001. Progress in the development of precision viticulture-variation in yield, quality and soil properties in contrasting Australian vineyards.

BRAMLEY, R. 2010. Precision Viticulture: Managing vineyard variability for improved quality outcomes. In *Managing Wine Quality: Viticulture and Wine Quality*, pages 445–480. Elsevier.

BRAMLEY, R. and HAMILTON, R. 2004. Understanding variability in wine-grape production systems: 1. Within vineyard variation in yield over several vintages. *Australian Journal of Grape and Wine Research*, vol. 10(1), pages 32–45.

BRAMLEY, R., PEARSE, B. and CHAMBERLAIN, P. 2003. Being profitable precisely-a case study of precision viticulture from Margaret River. *Australian and New Zealand Grapegrower and Winemaker*, pages 84–87.

BRAMLEY, R. and PROFFITT, A. 1999. Managing variability in viticultural production. *Grapegrower and Winemaker*, vol. 427, pages 11–16.

BUCH, V. H., AHMED, I. and MARUTHAPPU, M. 2018. Artificial intelligence in medicine: current trends and future possibilities. *Br J Gen Pract*, vol. 68(668), pages 143–144.

CARLEO, G. and TROYER, M. 2017. Solving the quantum many-body problem with artificial neural networks. *Science*, vol. 355(6325), pages 602–606.

CEROVIC, Z., OUNIS, A., CARTELAT, A., LATOUCHE, G., GOULAS, Y., MEYER, S. and MOYA, I. 2002. The use of chlorophyll fluorescence excitation spectra for the non-destructive in situ assessment of UV-absorbing compounds in leaves. *Plant, Cell & Environment*, vol. 25(12), pages 1663–1676.

CEROVIC, Z. G., MASDOUMIER, G., GHOZLEN, N. B. and LATOUCHE, G. 2012. A new optical leaf-clip meter for simultaneous non-destructive

assessment of leaf chlorophyll and epidermal flavonoids. *Physiologia Plantarum*, vol. 146(3), pages 251–260.

CHUVIECO SALINERO, E. 2006. *Teledetección ambiental: la observación de la Tierra desde el espacio*. Ariel. ISBN 8434434989.

CORTES, C. and VAPNIK, V. 1995. Support-vector networks. *Machine Learning*, vol. 20(3), pages 273–297.

COSTA, J. M., GRANT, O. and CHAVES, M. 2010. Use of thermal imaging in viticulture: current application and future prospects. In *Methodologies and Results in Grapevine Research*, pages 135–150. Springer.

CRISTIANINI, N., SHAWE-TAYLOR, J. ET AL. 2000. *An introduction to support vector machines and other kernel-based learning methods*. Cambridge university press. ISBN 9780511801389.

CROSBY, J. L. 1973. *Computer simulation in genetics*. John Wiley & Sons. ISBN 9780471188803.

DEERY, D., JIMENEZ-BERNI, J., JONES, H., SIRAULT, X. and FURBANK, R. 2014. Proximal remote sensing buggies and potential applications for field-based phenotyping. *Agronomy*, vol. 4(3), pages 349–379.

DENG, J., DONG, W., SOCHER, R., LI, L.-J., LI, K. and FEI-FEI, L. 2009. Imagenet: A large-scale hierarchical image database. In *Computer Vision and Pattern Recognition, 2009. CVPR 2009. IEEE Conference on*, pages 248–255. IEEE.

DIAGO, M. P., FERNANDES, A. M., MILLAN, B., TARDÁGUILA, J. and MELO-PINTO, P. 2013. Identification of grapevine varieties using leaf spectroscopy and partial least squares. *Computers and Electronics in Agriculture*, vol. 99, pages 7–13.

DIAGO, M. P., FERNÁNDEZ-NOVALES, J., FERNANDES, A. M., MELO-PINTO, P. and TARDAGUILA, J. 2016a. Use of visible and short-wave near-infrared hyperspectral imaging to fingerprint anthocyanins in intact grape berries. *Journal of Agricultural and Food Chemistry*, vol. 64(40), pages 7658–7666.

DIAGO, M. P., FERNÁNDEZ-NOVALES, J., GUTIÉRREZ, S., MARAÑÓN, M. and TARDAGUILA, J. 2018. Development and validation of a new methodology to assess the vineyard water status by on-the-go near infrared spectroscopy. *Frontiers in Plant Science*, vol. 9, page 59.

DIAGO, M. P., REY-CARAMES, C., LE MOIGNE, M., FADAILI, E., TARDAGUILA, J. and CEROVIC, Z. 2016b. Calibration of non-invasive fluorescence-based sensors for the manual and on-the-go assessment of

grapevine vegetative status in the field. *Australian Journal of Grape and Wine Research*, vol. 22(3), pages 438–449.

DÍAZ, C. A., PÉREZ, D. S., MIATELLO, H. and BROMBERG, F. 2018. Grapevine buds detection and localization in 3D space based on Structure from Motion and 2D image classification. *Computers in Industry*, vol. 99, pages 303–312.

DOMINGOS, P. 2002. Machine Learning. In *Handbook of Data Mining and Knowledge Discovery* (edited by W. Klösgen and J. M. Zytkow), pages 660–670. Oxford University Press, Inc., New York, NY, USA.

DRUCKER, H., BURGES, C. J., KAUFMAN, L., SMOLA, A. J. and VAPNIK, V. 1997. Support vector regression machines. In *Advances in Neural Information Processing Systems*, pages 155–161.

ERICKSON, B., LOWENBERG-DEBOER, J. and BRADFORD, J. 2017. 2017 Precision Agriculture Dealership Survey. *Departments of Agricultural Economics and Agronomy, Purdue University*.

ESCALONA, J., BOTA, J., MEDRANO, H. ET AL. 2015. Distribution of leaf photosynthesis and transpiration within grapevine canopies under different drought conditions. *VITIS-Journal of Grapevine Research*, vol. 42(2), page 57.

ESTEVA, A., KUPREL, B., NOVOA, R. A., KO, J., SWETTER, S. M., BLAU, H. M. and THRUN, S. 2017. Dermatologist-level classification of skin cancer with deep neural networks. *Nature*, vol. 542(7639), page 115.

EUROPEAN SPACE AGENCY. Sentinel Program. `https://sentinel.esa.int/web/sentinel/home`, 2019. Accessed: 2018-01-11.

EUROSTAT. Structure of vineyards in 2015. `https://ec.europa.eu/eurostat/documents/2995521/7964277/5-04042017-BP-EN.pdf/149e5e9a-4ae6-466b-baec-0273fe0c08a4`, 2017. Accessed: 2018-02-13.

FERNANDES, A. M., MELO-PINTO, P., MILLAN, B., TARDÁGUILA, J. and DIAGO, M. P. 2015. Automatic discrimination of grapevine (Vitis vinifera L.) clones using leaf hyperspectral imaging and partial least squares. *The Journal of Agricultural Science*, vol. 153(3), pages 455–465.

FERNÁNDEZ-NOVALES, J., TARDAGUILA, J., GUTIÉRREZ, S., MARAÑÓN, M. and DIAGO, M. P. 2018. In field quantification and discrimination of different vineyard water regimes by on-the-go NIR spectroscopy. *Biosystems Engineering*, vol. 165, pages 47–58.

FOUNTAS, S., BLACKMORE, S., ESS, D., HAWKINS, S., BLUMHOFF, G., LOWENBERG-DEBOER, J. and SORENSEN, C. 2005. Farmer experience

with precision agriculture in Denmark and the US Eastern Corn Belt. *Precision Agriculture*, vol. 6(2), pages 121–141.

FRASER, A., BURNELL, D. ET AL. 1970. Computer models in genetics. *Computer Models in Genetics.*.

FUENTES, S., HERNÁNDEZ-MONTES, E., ESCALONA, J., BOTA, J., VIEJO, C. G., POBLETE-ECHEVERRÍA, C., TONGSON, E. and MEDRANO, H. 2018. Automated grapevine cultivar classification based on machine learning using leaf morpho-colorimetry, fractal dimension and near-infrared spectroscopy parameters. *Computers and Electronics in Agriculture*, vol. 151, pages 311–318.

FUSSELL, J., RUNDQUIST, D. and HARRINGTON, J. 1986. On defining remote sensing. *Photogrammetric Engineering and Remote Sensing*, vol. 52(9), pages 1507–1511.

GANESAN, N., VENKATESH, K., RAMA, M. and PALANI, A. M. 2010. Application of neural networks in diagnosing cancer disease using demographic data. *International Journal of Computer Applications*, vol. 1(26), pages 76–85.

GARCÍA, S., LUENGO, J. and HERRERA, F. 2015. *Data Preprocessing in Data Mining*. Springer. ISBN 9783319102474.

GARCÍA, S., LUENGO, J. and HERRERA, F. 2016. Tutorial on practical tips of the most influential data preprocessing algorithms in data mining. *Knowledge-Based Systems*, vol. 98, pages 1–29.

GLADSTONES, J. 1992. *Viticulture and environment*. Winetitles. ISBN 9781875130122.

GOMES, V. M., FERNANDES, A. M., FAIA, A. and MELO-PINTO, P. 2017. Comparison of different approaches for the prediction of sugar content in new vintages of whole Port wine grape berries using hyperspectral imaging. *Computers and Electronics in Agriculture*, vol. 140, pages 244–254.

GOVERNMENT OF SPAIN. Estrategia Española de I+D+I en Inteligencia Artificial. `http://www.ciencia.gob.es/stfls/MICINN/Ciencia/Ficheros/Estrategia_Inteligencia_Artificial-IDI.pdf`, 2019. Accessed: 2018-03-21.

GOWARD, S. N., MARKHAM, B., DYE, D. G., DULANEY, W. and YANG, J. 1991. Normalized difference vegetation index measurements from the Advanced Very High Resolution Radiometer. *Remote Sensing of Environment*, vol. 35(2-3), pages 257–277.

GRANT, O. M., OCHAGAVÍA, H., BALUJA, J., DIAGO, M. P. and TARDÁGUILA, J. 2016. Thermal imaging to detect spatial and temporal variation in the water status of grapevine (Vitis vinifera L.). *The Journal of Horticultural Science and Biotechnology*, vol. 91(1), pages 43–54.

HAGEN, N. A. and KUDENOV, M. W. 2013. Review of snapshot spectral imaging technologies. *Optical Engineering*, vol. 52(9), page 090901.

HALL, A., LAMB, D., HOLZAPFEL, B. and LOUIS, J. 2002. Optical remote sensing applications in viticulture-A review. *Australian Journal of Grape and Wine Research*, vol. 8(1), pages 36–47.

HERRERA, F., CHARTE, F., RIVERA, A. J. and DEL JESUS, M. J. 2016. *Multilabel classification. Problem analysis, metrics and techniques*. Springer International Publishing. ISBN 9783319411101.

HERRERA, F., LOZANO, M. and VERDEGAY, J. L. 1998. Tackling real-coded genetic algorithms: Operators and tools for behavioural analysis. *Artificial intelligence review*, vol. 12(4), pages 265–319.

HERRMANN, R. and ONKELINX, C. 1986. Quantities and units in clinical chemistry: Nebulizer and flame properties in flame emission and absorption spectrometry (Recommendations 1986). *Pure and Applied Chemistry*, vol. 58(12), pages 1737–1742.

HIRSCHBERG, J. and MANNING, C. D. 2015. Advances in natural language processing. *Science*, vol. 349(6245), pages 261–266.

HORNIK, K., STINCHCOMBE, M. and WHITE, H. 1989. Multilayer feedforward networks are universal approximators. *Neural Networks*, vol. 2(5), pages 359–366.

HSU, C.-W. and LIN, C.-J. 2002. A comparison of methods for multiclass support vector machines. *IEEE Transactions on Neural Networks*, vol. 13(2), pages 415–425.

HU, S., WANG, H., SHE, C. and WANG, J. 2010. A semantic middleware of grain storage internet. In *International Conference on Computer and Computing Technologies in Agriculture*, pages 71–77. Springer.

HUANG, L., ZHOU, Y., MENG, L., WU, D. and HE, Y. 2017. Comparison of different CCD detectors and chemometrics for predicting total anthocyanin content and antioxidant activity of mulberry fruit using visible and near infrared hyperspectral imaging technique. *Food Chemistry*, vol. 224, pages 1–10.

HUNTER, M. C., SMITH, R. G., SCHIPANSKI, M. E., ATWOOD, L. W. and MORTENSEN, D. A. 2017. Agriculture in 2050: Recalibrating targets for sustainable intensification. *Bioscience*, vol. 67(4), pages 386–391.

IDSO, S. B. 1982. Non-water-stressed baselines: a key to measuring and interpreting plant water stress. *Agricultural Meteorology*, vol. 27(1-2), pages 59–70.

ISHIMWE, R., ABUTALEB, K. and AHMED, F. 2014. Applications of thermal imaging in agriculture-A review. *Advances in remote Sensing*, vol. 3(03), page 128.

JAYARAMAN, P. P., PALMER, D., ZASLAVSKY, A., SALEHI, A. and GEORGAKOPOULOS, D. 2015. Addressing information processing needs of digital agriculture with openiot platform. In *Interoperability and Open-Source Solutions for the Internet of Things*, pages 137–152. Springer.

JONES, H. 1992. Plants and Microclimate. *Cambridge University Press, New York*.

JONES, H. G. and VAUGHAN, R. A. 2010. *Remote sensing of vegetation: principles, techniques, and applications*. Oxford university press. ISBN 9780199207794.

JORDAN, M. I. and MITCHELL, T. M. 2015. Machine learning: Trends, perspectives, and prospects. *Science*, vol. 349(6245), pages 255–260.

KING, B. and SHELLIE, K. 2016. Evaluation of neural network modeling to predict non-water-stressed leaf temperature in wine grape for calculation of crop water stress index. *Agricultural Water Management*, vol. 167, pages 38–52.

KOHAVI, R. ET AL. 1995. A study of cross-validation and bootstrap for accuracy estimation and model selection. In *International Joint Conference on Articial Intelligence*, vol. 14, pages 1137–1145. Montreal, Canada.

KRIZHEVSKY, A., SUTSKEVER, I. and HINTON, G. E. 2012. Imagenet classification with deep convolutional neural networks. In *Advances in Neural Information Processing Systems*, pages 1097–1105.

KRUSE, P. W. 2001. *Uncooled thermal imaging: arrays, systems, and applications*, vol. 2003. SPIE press Bellingham, WA. ISBN 9780819441225.

LAKHANI, P. and SUNDARAM, B. 2017. Deep learning at chest radiography: automated classification of pulmonary tuberculosis by using convolutional neural networks. *Radiology*, vol. 284(2), pages 574–582.

LAUDIEN, R., BARETH, G. and DOLUSCHITZ, R. 2003. Analysis of hyperspectral field data for detection of sugar beet diseases. In *Proceedings of the EFITA Conference, Debrecen, Hungary*, vol. 59, pages 375–381.

LECUN, Y., BENGIO, Y. and HINTON, G. 2015. Deep learning. *Nature*, vol. 521(7553), page 436.

LeCun, Y., Boser, B. E., Denker, J. S., Henderson, D., Howard, R. E., Hubbard, W. E. and Jackel, L. D. 1990. Handwritten digit recognition with a back-propagation network. In *Advances in Neural Information Processing Systems*, pages 396–404.

Lee, W., Alchanatis, V., Yang, C., Hirafuji, M., Moshou, D. and Li, C. 2010. Sensing technologies for precision specialty crop production. *Computers and Electronics in Agriculture*, vol. 74(1), pages 2–33.

van Leeuwen, C. and Darriet, P. 2016. The impact of climate change on viticulture and wine quality. *Journal of Wine Economics*, vol. 11(1), pages 150–167.

Li, J. and Chen, L. 2017. Comparative analysis of models for robust and accurate evaluation of soluble solids content in 'Pinggu' peaches by hyperspectral imaging. *Computers and Electronics in Agriculture*, vol. 142, pages 524–535.

Liu, S. and Whitty, M. 2015. Automatic grape bunch detection in vineyards with an SVM classifier. *Journal of Applied Logic*, vol. 13(4), pages 643–653.

Lloyd, J. M. 2013. *Thermal imaging systems*. Springer Science & Business Media. ISBN 9781489911827.

Lowe, A., Harrison, N. and French, A. P. 2017. Hyperspectral image analysis techniques for the detection and classification of the early onset of plant disease and stress. *Plant Methods*, vol. 13(1), page 80.

Ma, T., Li, X., Inagaki, T., Yang, H. and Tsuchikawa, S. 2018. Noncontact evaluation of soluble solids content in apples by near-infrared hyperspectral imaging. *Journal of Food Engineering*, vol. 224, pages 53–61.

Mancuso, S., Pisani, P., Bandinelli, R. and Rinaldelli, E. 1998. Application of an artificial neural network (ANN) for the identification of grapevine genotypes. *Vitis*, vol. 37, pages 27–32.

Martínez-Sandoval, J. R., Nogales-Bueno, J., Rodríguez-Pulido, F. J., Hernández-Hierro, J. M., Segovia-Quintero, M. A., Martínez-Rosas, M. E. and Heredia, F. J. 2016. Screening of anthocyanins in single red grapes using a non-destructive method based on the near infrared hyperspectral technology and chemometrics. *Journal of the Science of Food and Agriculture*, vol. 96(5), pages 1643–1647.

Matese, A. and Di Gennaro, S. F. 2015. Technology in precision viticulture: A state of the art review. *International Journal of Wine Research*, vol. 7, pages 69–81.

MATESE, A., TOSCANO, P., DI GENNARO, S. F., GENESIO, L., VACCARI, F. P., PRIMICERIO, J., BELLI, C., ZALDEI, A., BIANCONI, R. and GIOLI, B. 2015. Intercomparison of UAV, aircraft and satellite remote sensing platforms for precision viticulture. *Remote Sensing*, vol. 7(3), pages 2971–2990.

MCCULLOCH, W. S. and PITTS, W. 1943. A logical calculus of the ideas immanent in nervous activity. *The Bulletin of Mathematical Biophysics*, vol. 5(4), pages 115–133.

MOGHADAM, P., WARD, D., GOAN, E., JAYAWARDENA, S., SIKKA, P. and HERNANDEZ, E. 2017. Plant disease detection using hyperspectral imaging. In *2017 International Conference on Digital Image Computing: Techniques and Applications (DICTA)*, pages 1–8. IEEE.

MOHANTY, S. P., HUGHES, D. P. and SALATHÉ, M. 2016. Using deep learning for image-based plant disease detection. *Frontiers in plant science*, vol. 7, page 1419.

MUÑOZ-ORDÓÑEZ, J., COBOS, C., MENDOZA, M., HERRERA-VIEDMA, E., HERRERA, F. and TABIK, S. 2018. Framework for the training of deep neural networks in tensorflow using metaheuristics. In *International Conference on Intelligent Data Engineering and Automated Learning*, pages 801–811. Springer.

NINFA, A. J., BALLOU, D. P. and PARSONS, M. B. P. 2010. *Fundamental laboratory approaches for biochemistry and biotechnology*. Wiley. ISBN 9780470087664.

PARKES, D. C. and WELLMAN, M. P. 2015. Economic reasoning and artificial intelligence. *Science*, vol. 349(6245), pages 267–272.

PATRÍCIO, D. I. and RIEDER, R. 2018. Computer vision and artificial intelligence in precision agriculture for grain crops: a systematic review. *Computers and Electronics in Agriculture*, vol. 153, pages 69–81.

PEDERSEN, S. M. 2003. *Precision farming–Technology assessment of site-specific input application in cereals*. PhD Thesis, IPL.

PÉREZ, D. S., BROMBERG, F. and DIAZ, C. A. 2017. Image classification for detection of winter grapevine buds in natural conditions using scale-invariant features transform, bag of features and support vector machines. *Computers and Electronics in Agriculture*, vol. 135, pages 81–95.

PÉREZ-MARÍN, D., PAZ, P., GUERRERO, J.-E., GARRIDO-VARO, A. and SÁNCHEZ, M.-T. 2010. Miniature handheld NIR sensor for the on-site non-destructive assessment of post-harvest quality and refrigerated storage behavior in plums. *Journal of Food Engineering*, vol. 99(3), pages 294–302.

Piazzolla, F., Amodio, M. L. and Colelli, G. 2017. Spectra evolution over on-vine holding of Italia table grapes: prediction of maturity and discrimination for harvest times using a Vis-NIR hyperspectral device. *Journal of Agricultural Engineering*, vol. 48(2), pages 109–116.

Pou, A., Diago, M. P., Medrano, H., Baluja, J. and Tardaguila, J. 2014. Validation of thermal indices for water status identification in grapevine. *Agricultural Water Management*, vol. 134, pages 60–72.

Proffitt, A. P. B., Bramley, R., Lamb, D. and Winter, E. 2006. *Precision viticulture: a new era in vineyard management and wine production*. Ashford, Winetitles. ISBN 0975685044.

Pu, Y.-Y., Sun, D.-W., Riccioli, C., Buccheri, M., Grassi, M., Cattaneo, T. M. and Gowen, A. 2018. Calibration transfer from micro NIR spectrometer to hyperspectral imaging: a case study on predicting soluble solids content of bananito fruit (Musa acuminata). *Food Analytical Methods*, vol. 11(4), pages 1021–1033.

Rahman, A., Kandpal, L., Lohumi, S., Kim, M., Lee, H., Mo, C. and Cho, B.-K. 2017. Nondestructive estimation of moisture content, pH and soluble solid contents in intact tomatoes using hyperspectral imaging. *Applied Sciences*, vol. 7(1), page 109.

Ray, S., Jain, N., Miglani, A., Singh, J., Singh, A., Panigrahy, S. and Parihar, J. 2010. Defining optimum spectral narrow bands and bandwidths for agricultural applications. *Current Science*, pages 1365–1369.

Reis, M. J., Morais, R., Peres, E., Pereira, C., Contente, O., Soares, S., Valente, A., Baptista, J., Ferreira, P. J. S. and Cruz, J. B. 2012. Automatic detection of bunches of grapes in natural environment from color images. *Journal of Applied Logic*, vol. 10(4), pages 285–290.

Rey-Caramés, C., Diago, M. P., Martín, M. P., Lobo, A. and Tardaguila, J. 2015. Using RPAS multi-spectral imagery to characterise vigour, leaf development, yield components and berry composition variability within a vineyard. *Remote Sensing*, vol. 7(11), pages 14458–14481.

Rey-Caramés, C., Tardaguila, J., Sanz-Garcia, A., Chica-Olmo, M. and Diago, M. P. 2016. Quantifying spatio-temporal variation of leaf chlorophyll and nitrogen contents in vineyards. *Biosystems Engineering*, vol. 150, pages 201–213.

Robbins, H. and Monro, S. 1985. A stochastic approximation method. In *Herbert Robbins Selected Papers*, pages 102–109. Springer.

RODRÍGUEZ-PÉREZ, J. R., RIAÑO, D., CARLISLE, E., USTIN, S. and SMART, D. R. 2007. Evaluation of hyperspectral reflectance indexes to detect grapevine water status in vineyards. *American Journal of Enology and Viticulture*, vol. 58(3), pages 302–317.

RODRÍGUEZ-PULIDO, F. J., GIL-VICENTE, M., GORDILLO, B., HEREDIA, F. J. and GONZÁLEZ-MIRET, M. L. 2017. Measurement of ripening of raspberries (Rubus idaeus L) by near infrared and colorimetric imaging techniques. *Journal of Food Science and Technology*, vol. 54(9), pages 2797–2803.

ROMERO, M., LUO, Y., SU, B. and FUENTES, S. 2018. Vineyard water status estimation using multispectral imagery from an UAV platform and machine learning algorithms for irrigation scheduling management. *Computers and Electronics in Agriculture*, vol. 147, pages 109–117.

ROSALES-PÉREZ, A., GARCÍA, S., GONZALEZ, J. A., COELLO, C. A. C. and HERRERA, F. 2017. An evolutionary multiobjective model and instance selection for support vector machines with pareto-based ensembles. *IEEE Transactions on Evolutionary Computation*, vol. 21(6), pages 863–877.

ROSENBLATT, F. 1958. The perceptron: a probabilistic model for information storage and organization in the brain. *Psychological Review*, vol. 65(6), page 386.

RUMELHART, D. E., HINTON, G. E. and WILLIAMS, R. J. 1986. Learning representations by back-propagating errors. *Nature*, vol. 323(6088), pages 533–536.

RUNGPICHAYAPICHET, P., NAGLE, M., YUWANBUN, P., KHUWIJITJARU, P., MAHAYOTHEE, B. and MÜLLER, J. 2017. Prediction mapping of physicochemical properties in mango by hyperspectral imaging. *Biosystems Engineering*, vol. 159, pages 109–120.

SA, I., GE, Z., DAYOUB, F., UPCROFT, B., PEREZ, T. and MCCOOL, C. 2016. Deepfruits: A fruit detection system using deep neural networks. *Sensors*, vol. 16(8), page 1222.

SAMUEL, A. L. 1959. Some studies in machine learning using the game of checkers. *IBM Journal of Research and Development*, vol. 3(3), pages 210–229.

SÁNCHEZ, M.-T., DE LA HABA, M. J., BENÍTEZ-LÓPEZ, M., FERNÁNDEZ-NOVALES, J., GARRIDO-VARO, A. and PÉREZ-MARÍN, D. 2012. Non-destructive characterization and quality control of intact strawberries based on NIR spectral data. *Journal of Food Engineering*, vol. 110(1), pages 102–108.

Schrijver, R., Poppe, K. and Daheim, C. 2016. Precision agriculture and the future of farming in Europe: Scientific Foresight Study. *Brussels: European Parliament Research Service*.

Sejnowski, T. J. 2018. *The deep learning revolution*. MIT Press. ISBN 9780262038034.

Silver, D., Huang, A., Maddison, C. J., Guez, A., Sifre, L., Van Den Driessche, G., Schrittwieser, J., Antonoglou, I., Panneershelvam, V., Lanctot, M. et al. 2016. Mastering the game of Go with deep neural networks and tree search. *Nature*, vol. 529(7587), page 484.

Skoog, D. A., Holler, F. J. and Crouch, S. R. 2017. *Principles of instrumental analysis*. Cengage Learning. ISBN 0495012017.

Soar, C., Sadras, V. O. and Petrie, P. R. 2008. Climate drivers of red wine quality in four contrasting Australian wine regions. *Australian Journal of Grape and Wine Research*, vol. 14(2), pages 78–90.

Stajic, J., Stone, R., Chin, G. and Wible, B. 2015. Rise of the machines. *Science*, vol. 349(6245), pages 248–249.

Sun, D.-W. 2009. *Infrared spectroscopy for food quality analysis and control*. Academic Press. ISBN 9780123741363.

Sun, J., Ma, B., Dong, J., Zhu, R., Zhang, R. and Jiang, W. 2017a. Detection of internal qualities of hami melons using hyperspectral imaging technology based on variable selection algorithms. *Journal of Food Process Engineering*, vol. 40(3), page e12496.

Sun, M., Zhang, D., Liu, L. and Wang, Z. 2017b. How to predict the sugariness and hardness of melons: A near-infrared hyperspectral imaging method. *Food Chemistry*, vol. 218, pages 413–421.

Taylor, J., Tisseyre, B. and Praat, J.-P. 2005. Bottling good information: mixing tradition and technology in vineyards. *Proceedings of FRUTIC 05: Information and Technology for Sustainable Fruit and Vegetable Production*, pages 12–16.

Thomas, S., Behmann, J., Steier, A., Kraska, T., Muller, O., Rascher, U. and Mahlein, A.-K. 2018a. Quantitative assessment of disease severity and rating of barley cultivars based on hyperspectral imaging in a non-invasive, automated phenotyping platform. *Plant Methods*, vol. 14(1), page 45.

THOMAS, S., KUSKA, M. T., BOHNENKAMP, D., BRUGGER, A., ALISAAC, E., WAHABZADA, M., BEHMANN, J. and MAHLEIN, A.-K. 2018b. Benefits of hyperspectral imaging for plant disease detection and plant protection: A technical perspective. *Journal of Plant Diseases and Protection*, vol. 125(1), pages 5–20.

TIAN, X., LI, J., WANG, Q., FAN, S. and HUANG, W. 2018. A bi-layer model for nondestructive prediction of soluble solids content in apple based on reflectance spectra and peel pigments. *Food chemistry*, vol. 239, pages 1055–1063.

TISSEYRE, B., MAZZONI, C. and FONTA, H. 2008. Whithin-field temporal stability of some parameters in viticulture: Potential toward a site specific management. *OENO One*, vol. 42(1), pages 27–39.

TISSEYRE, B., OJEDA, H. and TAYLOR, J. 2007. New technologies and methodologies for site-specific viticulture. *Journal International des Sciences de la Vigne et du Vin*, vol. 41(2), pages 63–76.

TOLEDO-MARTÍN, E. M., GARCÍA-GARCÍA, M. C., FONT, R., MORENO-ROJAS, J. M., GÓMEZ, P., SALINAS-NAVARRO, M. and DEL RÍO-CELESTINO, M. 2016. Application of visible/near-infrared reflectance spectroscopy for predicting internal and external quality in pepper. *Journal of the Science of Food and Agriculture*, vol. 96(9), pages 3114–3125.

TUCKER, C. J. 1979. Red and photographic infrared linear combinations for monitoring vegetation. *Remote Sensing of Environment*, vol. 8(2), pages 127–150.

UDIAS, A., PASTORI, M., MALAGO, A., VIGIAK, O., NIKOLAIDIS, N. P. and BOURAOUI, F. 2018. Identifying efficient agricultural irrigation strategies in Crete. *Science of the Total Environment*, vol. 633, pages 271–284.

UNDERWOOD, J., WENDEL, A., SCHOFIELD, B., MCMURRAY, L. and KIMBER, R. 2017. Efficient in-field plant phenomics for row-crops with an autonomous ground vehicle. *Journal of Field Robotics*, vol. 34(6), pages 1061–1083.

UNITED STATES GEOLOGICAL SURVEY. Landsat Program. `https://www.usgs.gov/land-resources/nli/landsat`, 2019. Accessed: 2018-01-11.

VAPNIK, V. and CHERVONENKIS, A. 1964. A note on class of perceptron. *Automation and Remote Control*, vol. 24.

WEBB, L., WHETTON, P. and BARLOW, E. 2008. Climate change and winegrape quality in Australia. *Climate Research*, vol. 36(2), pages 99–111.

WENDEL, A. 2018. *Hyperspectral Imaging from Ground Based Mobile Platforms and applications in Precision Agriculture*. PhD Thesis, Australian Centre for Field Robotics, School of Aerospace, Mechanical and Mechatronic Engineering, The University of Sydney.

WENDEL, A. and UNDERWOOD, J. 2017a. Extrinsic Parameter Calibration for Line Scanning Cameras on Ground Vehicles with Navigation Systems Using a Calibration Pattern. *Sensors*, vol. 17(11), page 2491.

WENDEL, A. and UNDERWOOD, J. 2017b. Illumination compensation in ground based hyperspectral imaging. *ISPRS Journal of Photogrammetry and Remote Sensing*, vol. 129, pages 162–178.

WERBOS, P. 1974. *New tools for Prediction and Analysis in the Behavioral Sciences*. PhD Thesis, Harvard University.

WILLIAMS, D., BRITTEN, A., MCCALLUM, S., JONES, H., AITKENHEAD, M., KARLEY, A., LOADES, K., PRASHAR, A. and GRAHAM, J. 2017. A method for automatic segmentation and splitting of hyperspectral images of raspberry plants collected in field conditions. *Plant Methods*, vol. 13(1), page 74.

WINDRIM, L. 2018. *Illumination invariant deep learning for hyperspectral data*. PhD Thesis, Australian Centre for Field Robotics, School of Aerospace, Mechanical and Mechatronic Engineering, The University of Sydney.

WOLPERT, D. H. 1992. Stacked generalization. *Neural Networks*, vol. 5(2), pages 241–259.

WU, D. and SUN, D.-W. 2013. Advanced applications of hyperspectral imaging technology for food quality and safety analysis and assessment: A review–Part I: Fundamentals. *Innovative Food Science & Emerging Technologies*, vol. 19, pages 1–14.

YOSINSKI, J., CLUNE, J., BENGIO, Y. and LIPSON, H. 2014. How transferable are features in deep neural networks? In *Advances in Neural Information Processing Systems*, pages 3320–3328.

YUAN, Y., ZENG, W. and ZHANG, Z. 2013. A semantic technology supported precision agriculture system: a case study for citrus fertilizing. In *International Conference on Knowledge Science, Engineering and Management*, pages 104–111. Springer.

ZARCO-TEJADA, P., HUBBARD, N. and LOUDJANI, P. 2014. Precision Agriculture: An Opportunity for EU Farmers–Potential Support with the CAP 2014-2020. *Joint Research Centre (JRC) of the European Commission*.

ZEILER, M. D. and FERGUS, R. 2014. Visualizing and understanding convolutional networks. In *European Conference on Computer Vision*, pages 818–833. Springer.

ZHANG, N., LIU, X., JIN, X., LI, C., WU, X., YANG, S., NING, J. and YANNE, P. 2017. Determination of total iron-reactive phenolics, anthocyanins and tannins in wine grapes of skins and seeds based on near-infrared hyperspectral imaging. *Food Chemistry*, vol. 237, pages 811–817.

ZHANG, N., WANG, M. and WANG, N. 2002. Precision agriculture–a worldwide overview. *Computers and Electronics in Agriculture*, vol. 36(2-3), pages 113–132.

ZHU, H., CHU, B., FAN, Y., TAO, X., YIN, W. and HE, Y. 2017. Hyperspectral imaging for predicting the internal quality of kiwifruits based on variable selection algorithms and chemometric models. *Scientific Reports*, vol. 7(1), page 7845.

ZISSIS, D., XIDIAS, E. K. and LEKKAS, D. 2015. A cloud based architecture capable of perceiving and predicting multiple vessel behaviour. *Applied Soft Computing*, vol. 35, pages 652–661.